

Supporting Information

Neutral tetrathia[22]annulene[2.1.2.1] based field-effect transistors. improved *on/off* ratio defies ring puckering†

Kamaljit Singh,* Tarunpreet Singh Virk, Jing Zhang, Wei Xu and Daoben Zhu*

Table of Contents

General Information	S2
Experimental Section	S3
Copies of ^1H, ^{13}C NMR, IR and Mass Spectra	S6
Theoretical Calculations	S34
UV-Visible Spectra	S51
Cyclic Voltamogram	S52
TGA graphs	S53
X-Rays	S54
Experimental details for OFET Device fabrication	S57
Cif files of 11a	S59

General Information

¹H (400 MHz), ¹³C (100 MHz) NMR spectra were recorded on a BRUKER AVANCE II 400 NMR Spectrometer and JEOL-FT NMR-AL Spectrometer at 300MHz. Tetramethylsilane (TMS) served as the internal standard (0 ppm for ¹H and 77.0 ppm for ¹³C) and CDCl₃ was used as solvent. The following abbreviations were used to express the multiplicities: s = singlet; d = doublet; t = triplet; q = quartet; m = multiplet; br = broad. Data are reported as follows: chemical shifts in ppm (δ), integration, coupling constant J (Hz) and assignment. Mass spectra were recorded on Bruker Daltonics esquire3000_00037 mass spectrometer. Elemental analyses were performed with a Thermoelectron FLASH EA1112 CHNS analyzer and were within $\pm 0.4\%$ of the theoretical values. IR spectrum was recorded on VARIAN 660-IR Fourier-Transform Spectrophotometer in range 400-4000 cm⁻¹ using KBr as medium. UV-Vis spectra were recorded on a SHIMADZU 1601 PC spectrophotometer, with a quartz cuvette (path length, 1 cm) and studies were performed in AR grade DCM. TGA were performed on a TA instrument with a DTG-60 detector with a temp. rise of 10 °C/minute under nitrogen atmosphere. Electrochemical studies were carried out on CHI 660C Electrochemical Workstation with a conventional three-electrode configuration consisting of platinum working electrode (2 mm diameter), counter electrode and Ag/AgCl as reference electrode. The experiments were carried out on 10⁻⁴ M solutions of samples in DCM containing 0.1 M tetrabutylammonium hexafluorophosphate (TBAPF₆) as supporting electrolyte at room temperature. Deoxygenation of the solutions was achieved by bubbling nitrogen for 30 min and the working electrode was cleaned after each run. The cyclic voltammograms were recorded with a scan rate of 100 mVs⁻¹. All reactions were monitored by thin-layer chromatography carried out on Merck pre-coated TLC plates (silica gel 60 F₂₅₄, 0.25 mm), visualization by using UV (254 nm). Melting points were determined in open capillaries and are uncorrected. Reactions that required anhydrous conditions were carried out under the blanket of deoxygenated (BASF catalyst) anhydrous nitrogen gas in oven/flame dried glassware. The products were purified by flash column chromatography on silica gel 60-120 mesh. All reagents and chemicals were purchased from Sigma-Aldrich. DMF, Diethyl ether, TiCl₄, Pyridine and DCM were purchased locally, dried and distilled prior to use. n-Buli was prepared and stored under a blanket of dry nitrogen gas. THF and toluene were distilled from sodium/benzophenone (benzophenone ketyl). Anhydrous DCM was stored over fused CaCl₂ and distilled before use. Zinc dust was activated prior to use using standard (2M

HCl and subsequent water washing) methods. DDQ and hydrazine hydrate were purchased from Sigma-Aldrich, and were used as received. All theoretical studies were performed with a GAUSSIAN 09 software package.

Experimental Section

General procedure for the synthesis of *meso*-substituted dithienyl methane dialdehydes (**9a,b**):

To a solution of *meso-p*-florophenyl dithienyl methane 1g (3.65 mmol) in dry diethyl ether (33ml) was added dropwise, n-Buli (8.2 mmol) at r.t.. to the deep red solution so obtained was added dropwise, anhydrous DMF (8 mmol) in diethyl ether. After 1 hour stirring, the mixture was washed sucessively with water, dil. HCl, water and sodium bicarbonate. The organic phase was then dried and vaccum evaporated. The residue was chromatographed on silica to give (1) as a deep red oil (750 mg) 62.3%.

The characteristic data for **8a**, **8b**, **9a** and **9b** is presented below.

m-Chlorophenyl-di(thien-2yl)methane, **8a**

(Yield = 16%), ^1H NMR (400 MHz, CDCl_3): δ (ppm) 7.27 (1H, m), 7.15-7.22 (5H, m), 6.90-6.93 (2H, m), 6.79-6.80 (2H, m), 5.81 (1H, s); ^{13}C NMR (100 MHz, CDCl_3): δ (ppm) 146.5, 145.5, 134.3, 129.7, 128.4, 127.3, 126.6, 126.4, 126.2, 124.9, 46.9; m/z 290.5, colourless oil.

p-Florophenyl-di(thien-2yl)methane, **8b**

(Yield = 15%), ^1H NMR (400 MHz, CDCl_3): δ (ppm) 7.27 (2H, m), 7.19-7.22 (4H, m), 6.93 (2H, t, $J=4.22$ Hz), 6.79 (2H, d, $J=4$ Hz), 5.82 (1H, s); ^{13}C NMR (100 MHz, CDCl_3): δ (ppm) 147, 142.2, 133, 129.7, 128.7, 126.7, 126.2, 124.9, 46.8; m/z 274.2, colourless oil.

m-Chlorophenyl-di(5-formylthien-2yl)methane, **9a**

(Yield = 64%), ^1H NMR (400 MHz, CDCl_3) 9.86 (2H, s), 7.65 (2H, d, $J=3.6$ Hz), 7.30-7.32 (2H, m), 7.26 (1H, s), 7.16-7.18 (1H, m), 6.98 (2H, dd, $J=2.8$ Hz), 5.87 (1H, s); ^{13}C NMR (100 MHz, CDCl_3) 182.7, 155.5, 143.5, 142.8, 136.3, 135, 130.4, 128.5, 128.4, 127.9, 126.4, 48.1; m/z 347 (M, 100%).

p-Florophenyl-di(5-formylthien-2yl)methane, 9b

(Yield = 62.3%), ^1H NMR (400 MHz, CDCl_3) 9.83 (2H, s), 7.63-7.65 (2H, m), 7.23-7.27 (2H, m), 7.01-7.06 (2H, m), 6.95-6.96 (2H, m), 5.89 (1H, s); ^{13}C NMR (100 MHz, CDCl_3) 182.7, 156.2, 143.2, 136.2, 129.9, 129.8, 127.7, 116.1, 115.8, 47.7; m/z 331 (M⁺, 100%).

General procedure for the synthesis of the *meso*-substituted dihydrotetrathia annulenes 10a and 10b:

To a stirring suspension of zinc dust (38 mmol) in 200 ml of THF maintained under nitrogen atmosphere, a solution of 19.6 ml of 1.0 M TiCl_4 (in CH_2Cl_2) was added over 20 minutes. The reaction mixture was refluxed for 1 hour, and treated with a solution of appropriate dialdehyde (1.78 mmol) and pyridine (35.6 mmol) dissolved in 200 ml of THF. The addition was made using a hypodermic syringe over 40 minutes to the gently refluxing suspension. After refluxing under nitrogen for 18 hours, the reaction was carefully quenched with a solution of aqueous K_2CO_3 (10%, 100 ml). The reaction mixture was filtered, and the filtrate was concentrated under reduced pressure and the residue extracted with 300 ml methylene chloride. The extract was washed with water (2 x 50 ml) and dried over anhydrous sodium sulfate. The solvent was evaporated under reduced pressure and the residue was chromatographed (over silica) to isolate the **10a,b** as light green solids (25%), (**10a,b**, m.pt. >280 °C).

Meso-m-chlorophenyldihydrotetrathia[22]annulene[2,1,2,1] 10a, (Yield = 13%), ^1H NMR (400 MHz, CDCl_3) 7.31 (2H, s), 7.20-7.27 (6H, m), 6.82-6.83 (4H, m), 6.65 (1H, dd, J = 4 Hz), 6.61 (3H, dd, J = 2.72 Hz), 6.51 (4H, s), 5.71 (2 H, m); ^{13}C NMR (100 MHz, CDCl_3) 148.2, 144.7, 138.7, 134.3, 129.8, 128.6, 128.5, 127.3, 126.7, 125.8, 123.6, 47.8; IR (KBr): 687, 763, 807, 889, 953, 1025, 1254, 1427, 1473, 1570, 1590, 2961, 3014, 3060, 3433 cm^{-1} ; (M+K) 668.

Meso-p-florophenyldihydrotetrathia[22]annulene[2,1,2,1] 10b, (Yield = 15%), ^1H NMR (400 MHz, CDCl_3) 7.26-7.30 (4H, m), 6.99-7.03 (4H, m), 6.80-6.82 (4H, m), 6.63 (2H, dd, J = 4 Hz), 6.60 (2H, dd, J = 4 Hz), 6.5 (4H, m), 5.73-5.75 (2H, m); ^{13}C NMR (100 MHz, CDCl_3) 148.9, 138.6, 130, 128.6, 125.6, 123.6, 123.4, 115.5, 115.2, 47.4; IR (KBr): 724, 793, 810, 860, 1025, 1158, 1222, 1389, 1506, 1600, 1621, 1892, 2970, 3020, 3065, 3401 cm^{-1} ; (M + K) 635.

General procedure for the synthesis of the *meso*-substituted tetrathia[22]annulenes **11a and **11b**:**

To a solution of **10a** (0.2 mmol) in 5 ml toluene, was added under nitrogen with stirring, a solution of DDQ (0.5 mmol) in 5 ml toluene. Shortly after mixing the two solutions, purple precipitates formed and the reaction mixture was stirred for additional 3 h. The purple precipitates were filtered and added to 3 ml of hydrazine hydrate (98%). After boiling for 10 minutes, the solid was filtered, washed with water, and dried. The resulting product was dissolved in methylene chloride and chromatographed on silica (DCM). Evaporation of the purple solution gave **11a** (50%) as shining metallic purple solid (**11a,b**, m.pt. >280 °C).

Meso-*m*-chlorophenyltetrathia[22]annulene[2,1,2,1] **11a,** (Yield = 50%), ¹H NMR (400 MHz, CDCl₃) 11.09 (4H, s), 10.41 (4H, d, J= 4 Hz), 9.98 (4H, d, J= 4.4 Hz), 8.47 (2H, s), 8.33-8.35 (2H, m), 7.91-7.97 (4H, m); IR (KBr): 776, 810, 1069, 1168, 1359, 1464, 1588, 1632, 2923, 3398 cm⁻¹; Anal. Calcd. (%) for C₃₄H₂₀S₄Cl₂: C, 65.07; H, 3.19; S, 20.41; Found: C, 65.09; H, 3.19; S, 20.40; *m/z* 627.9 (100%).

Meso-*p*-fluorophenyltetrathia[22]annulene[2,1,2,1] **11b,** (Yield = 45%), ¹H NMR (400 MHz, CDCl₃) 11.10 (4H, s), 10.41 (4H, d, J= 4.8 Hz), 9.98 (4H, d, J= 4.8 Hz), 8.41-8.44 (4H, m), 7.67-7.72 (4H, m); IR (KBr): 809, 1154, 1217, 1504, 3055 cm⁻¹; Anal. Calcd. (%) for C₃₄H₂₀S₄F₂ : C, 68.68; H, 3.36; S, 21.54 ; Found: C, 68.66; H, 3.35; S, 21.53; *m/z* 594 (100%).

Copies of ^1H , ^{13}C NMR, IR and Mass Spectra:

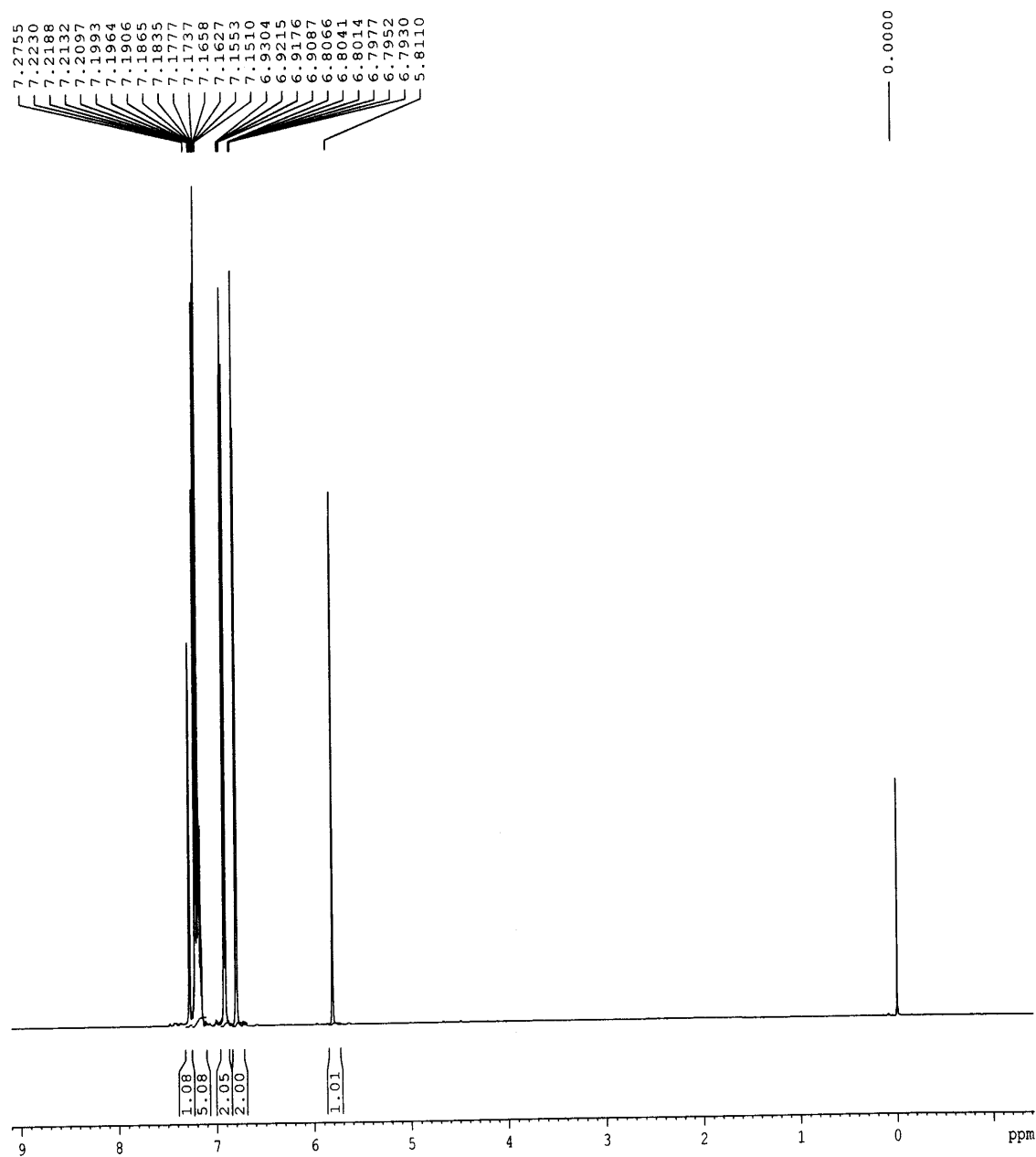


Figure S1: ^1H NMR spectrum of 8a.

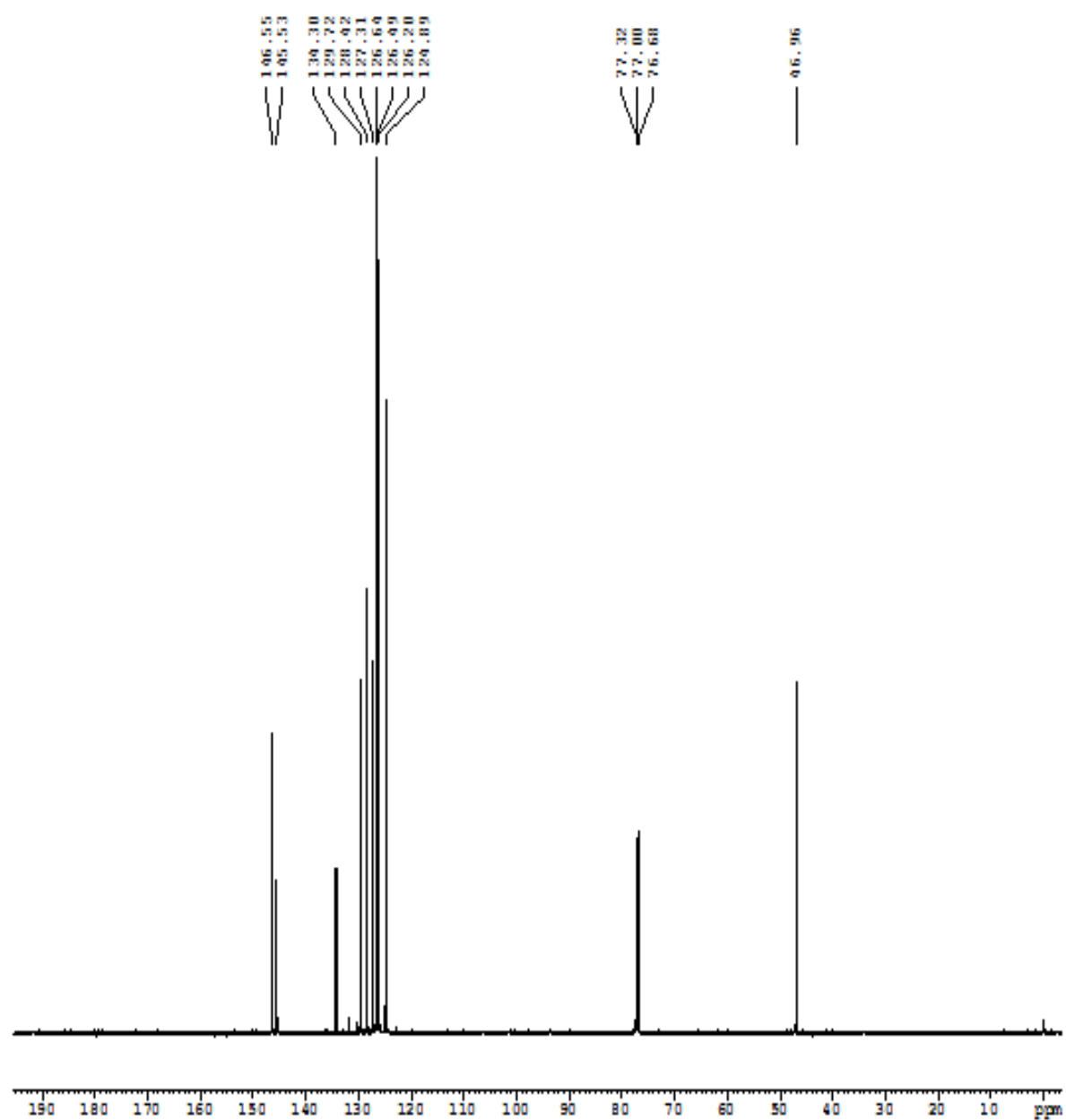


Figure S2: ¹³C NMR spectrum of 8a.

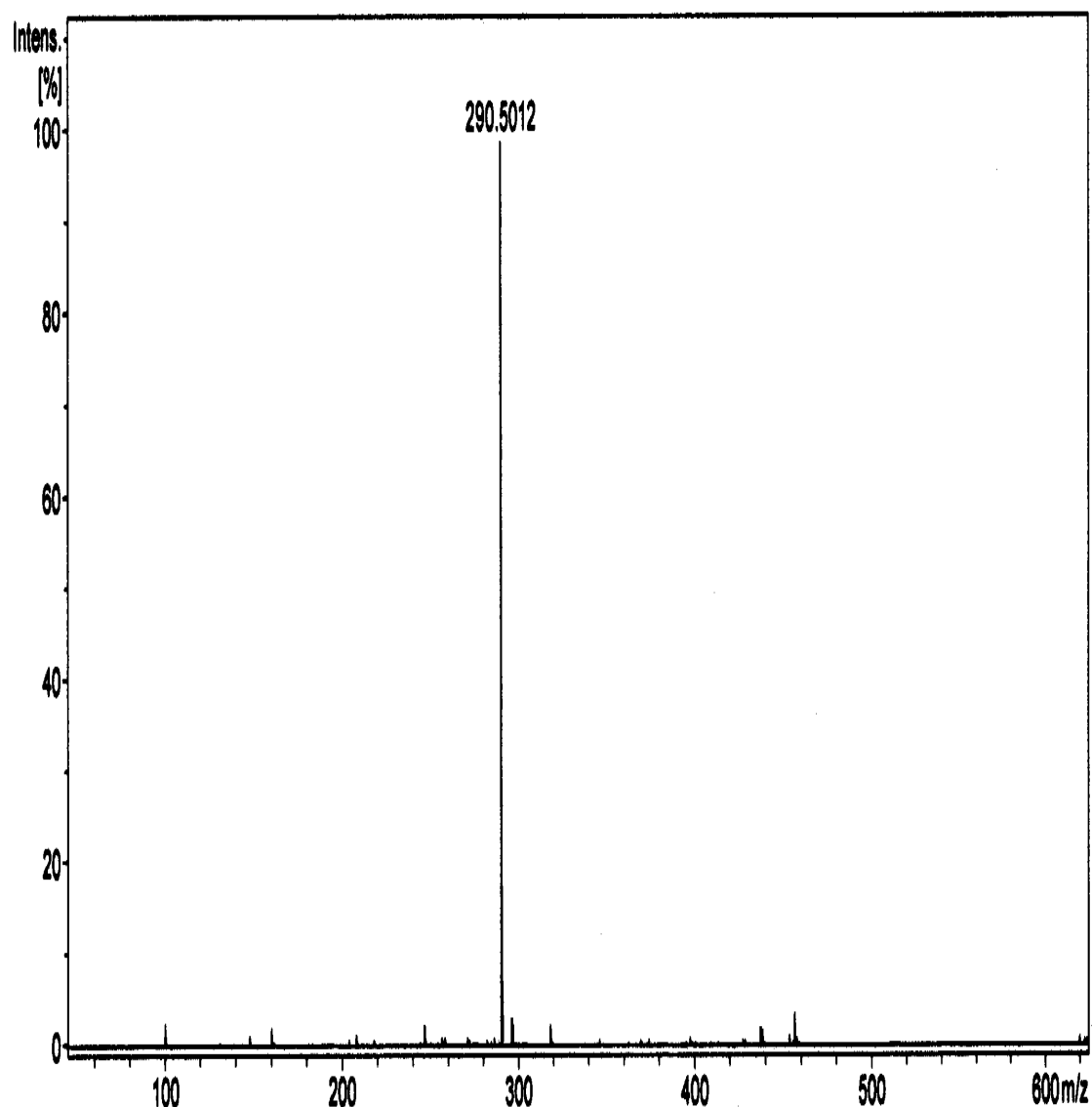


Figure S3: Mass spectrum of **8a**.

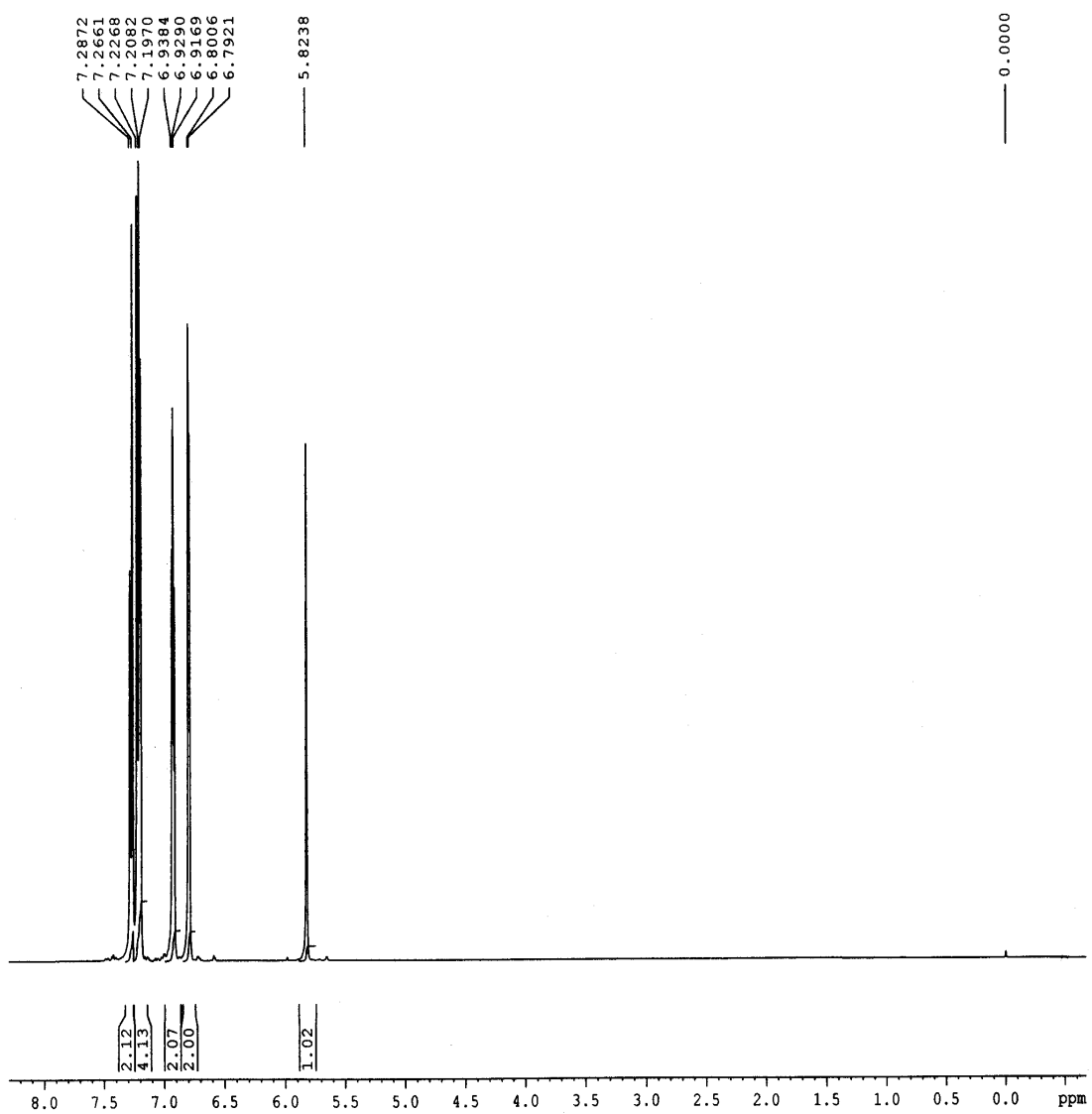


Figure S4: ^1H NMR spectrum of **8b**.

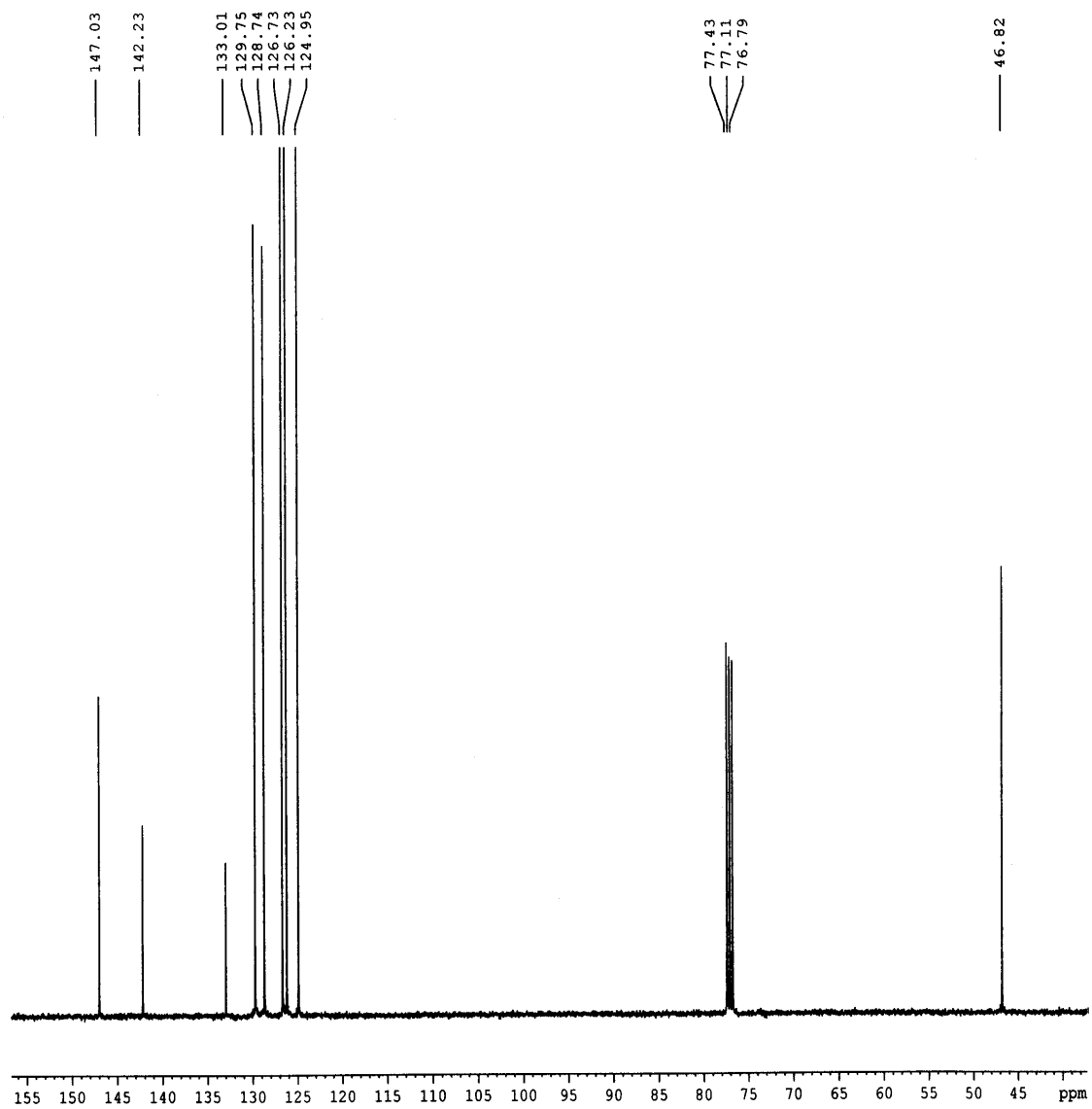


Figure S5: ¹³C NMR spectrum of **8b**.

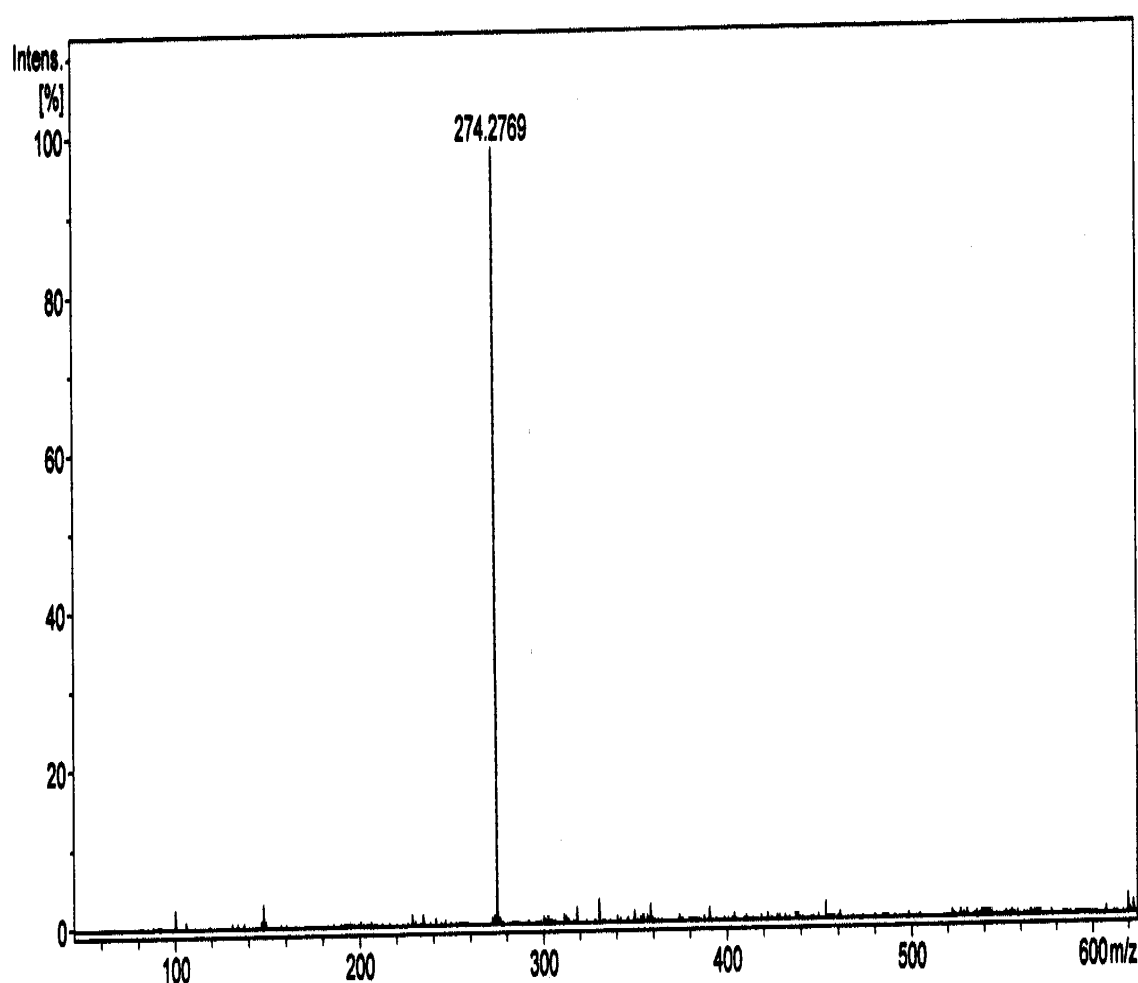


Figure S6: Mass spectrum of **8b**.

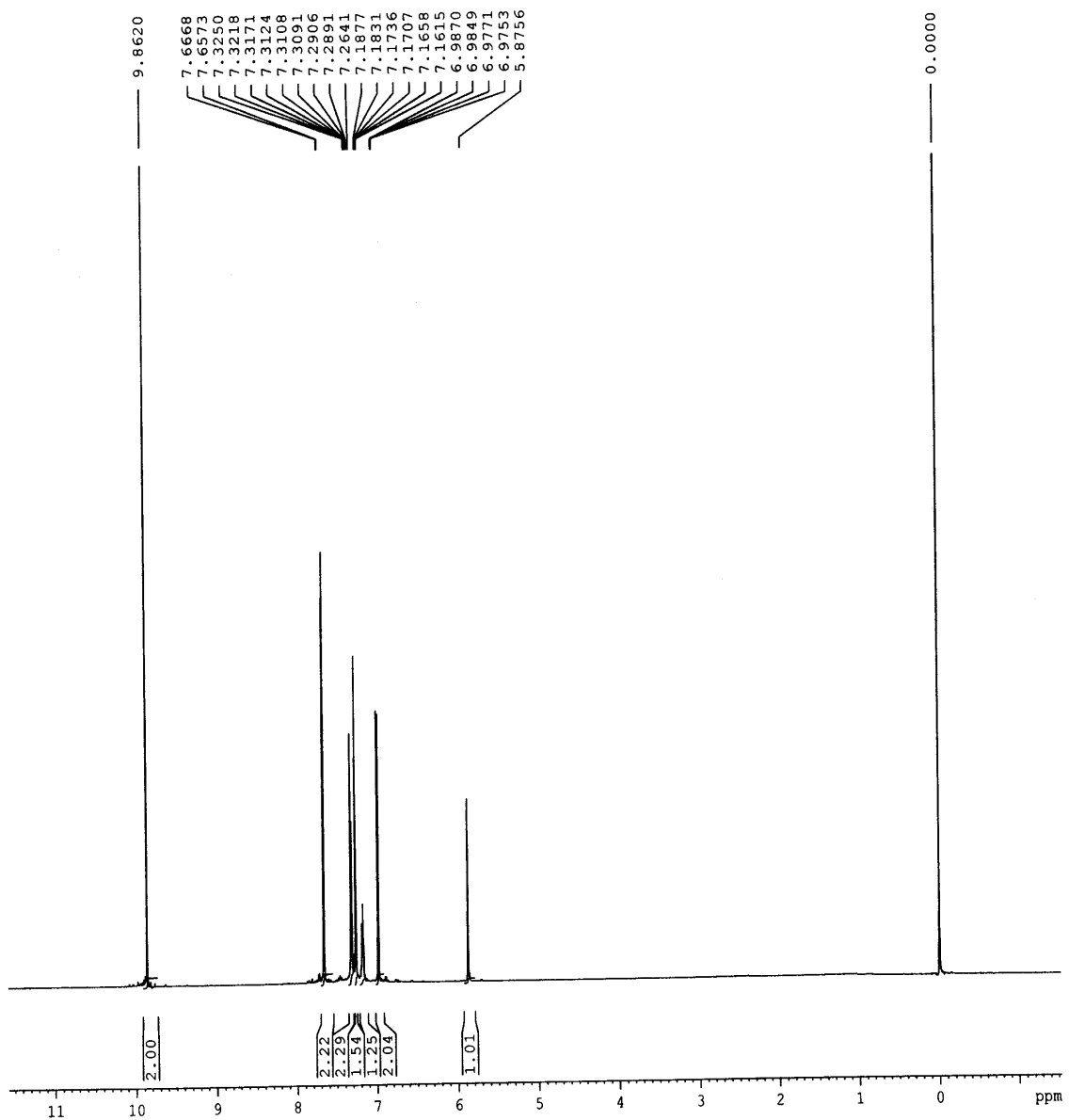


Figure S7: ^1H NMR spectrum of **9a**.

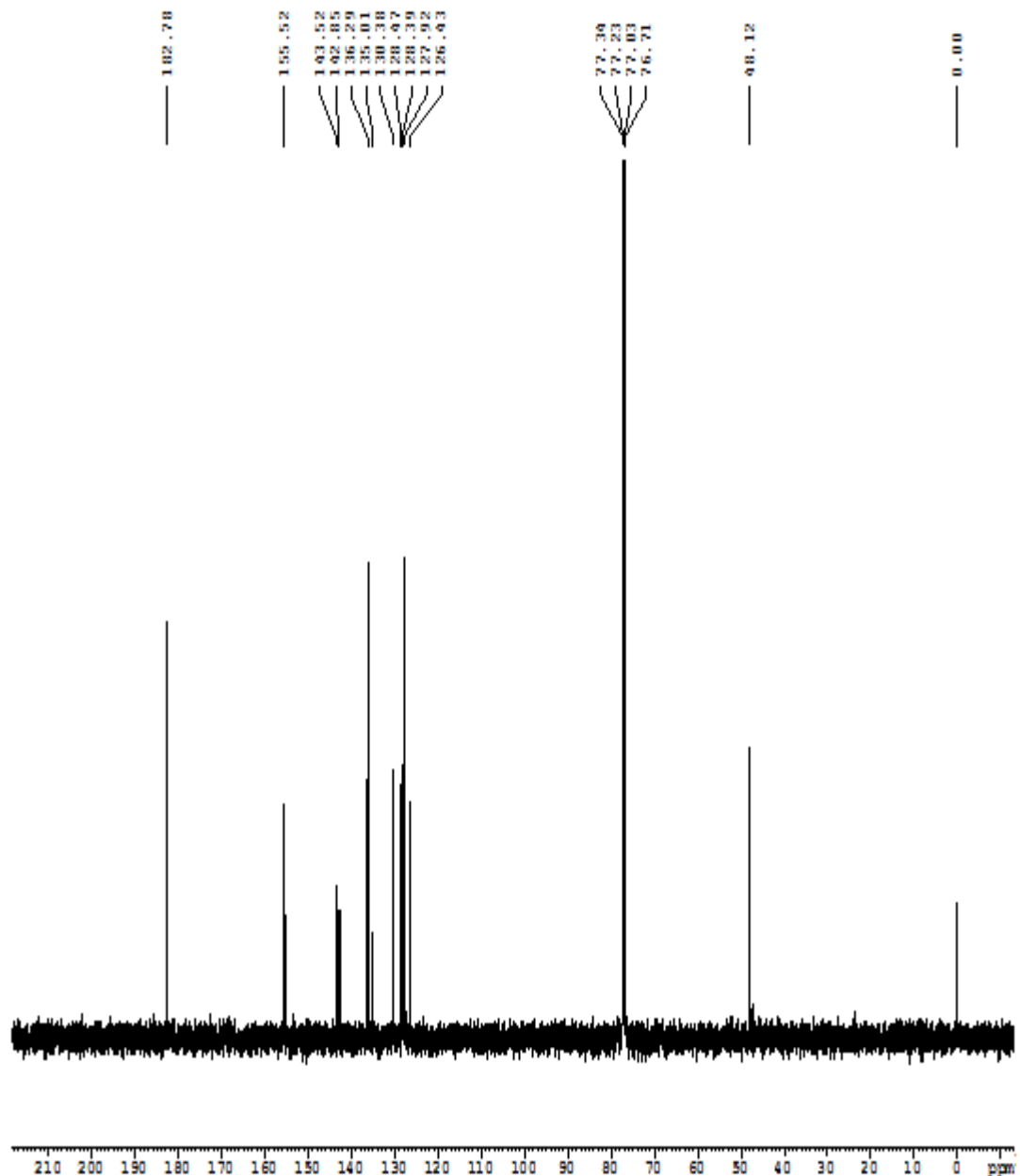


Figure S8: ^{13}C NMR spectrum of 9a.

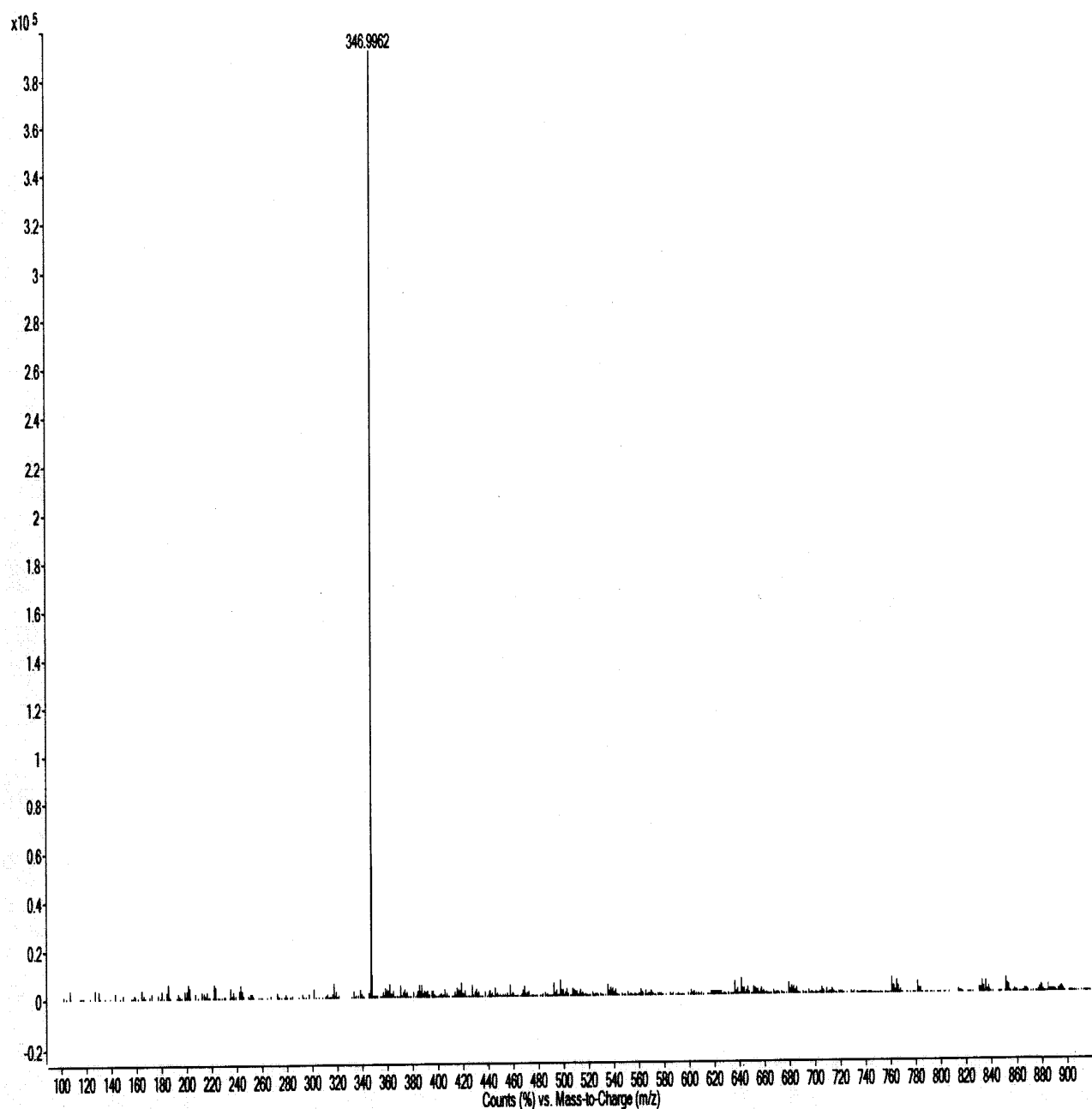


Figure S9: Mass spectrum spectrum of **9a**.

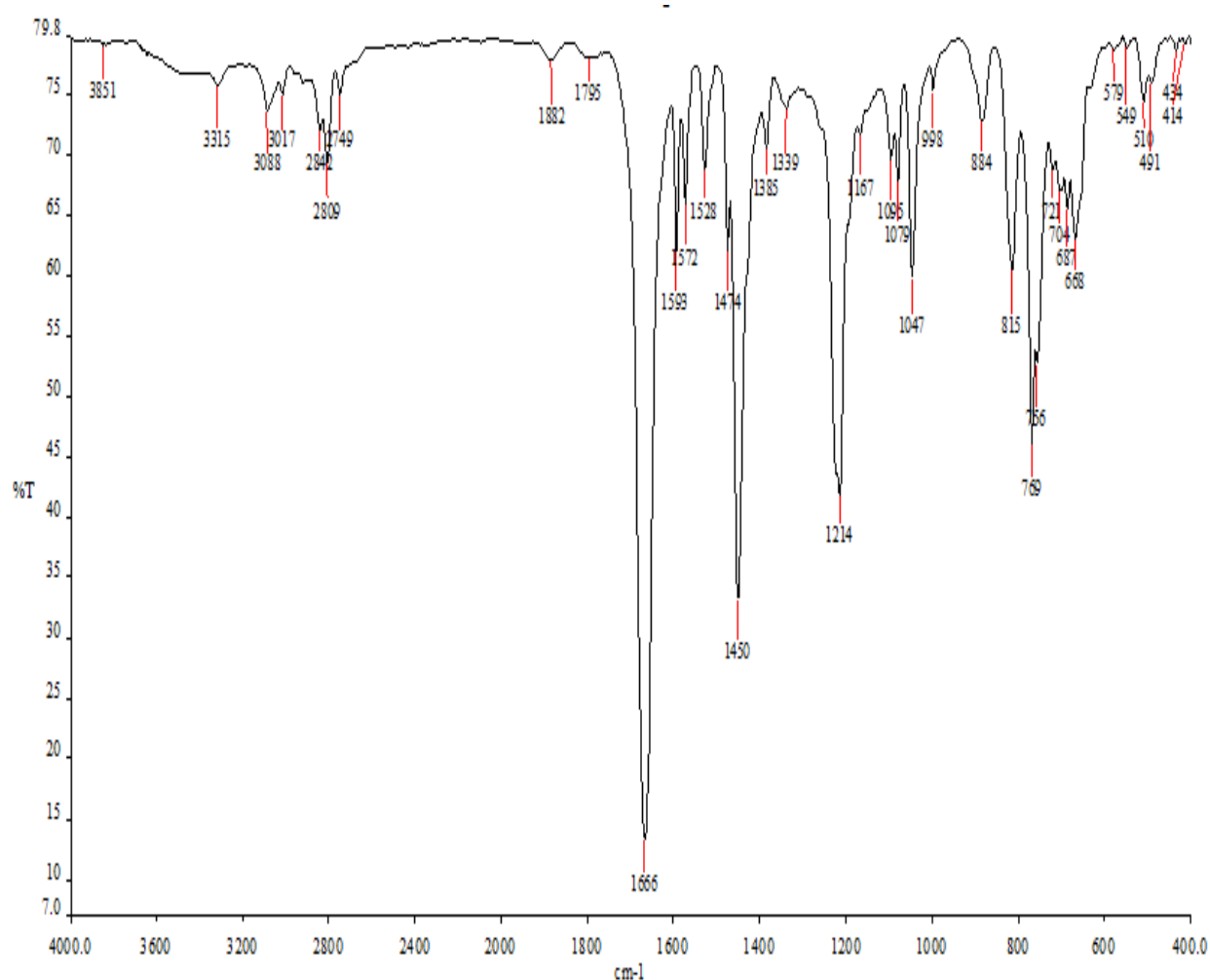


Figure S10: IR Spectrum of **9a**.

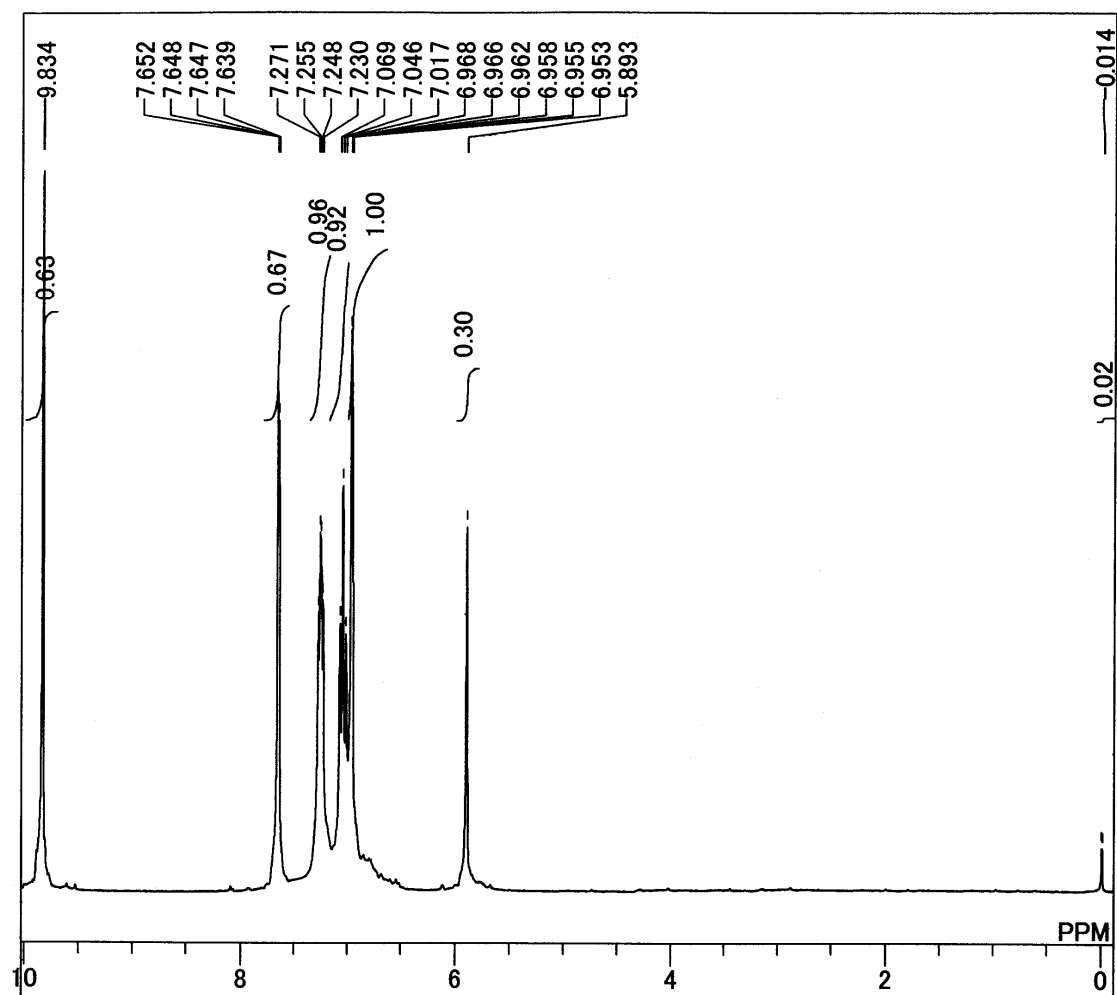


Figure S11: ¹H NMR spectrum of **9b**.

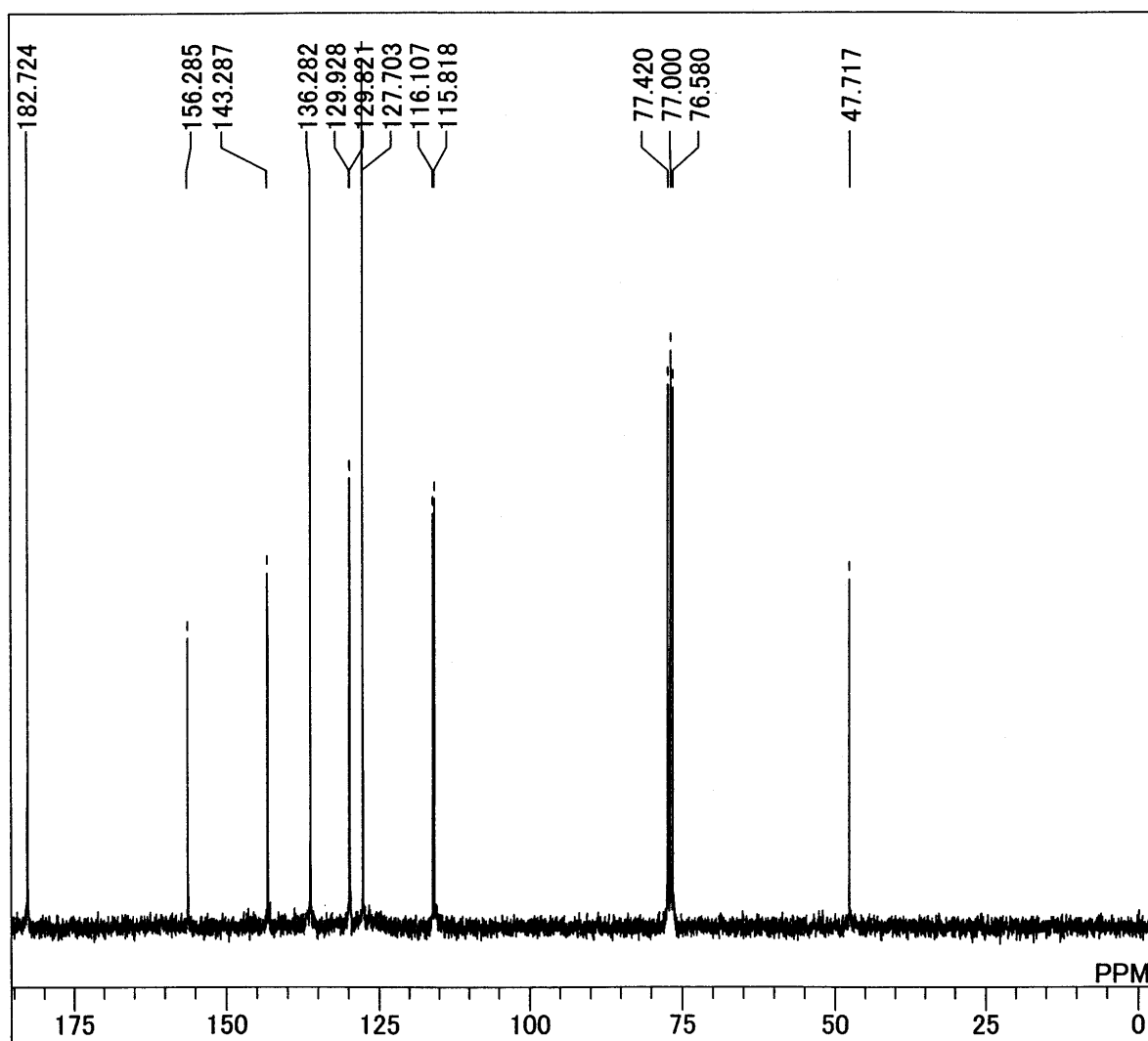


Figure S12: ^{13}C NMR spectrum of 9b.

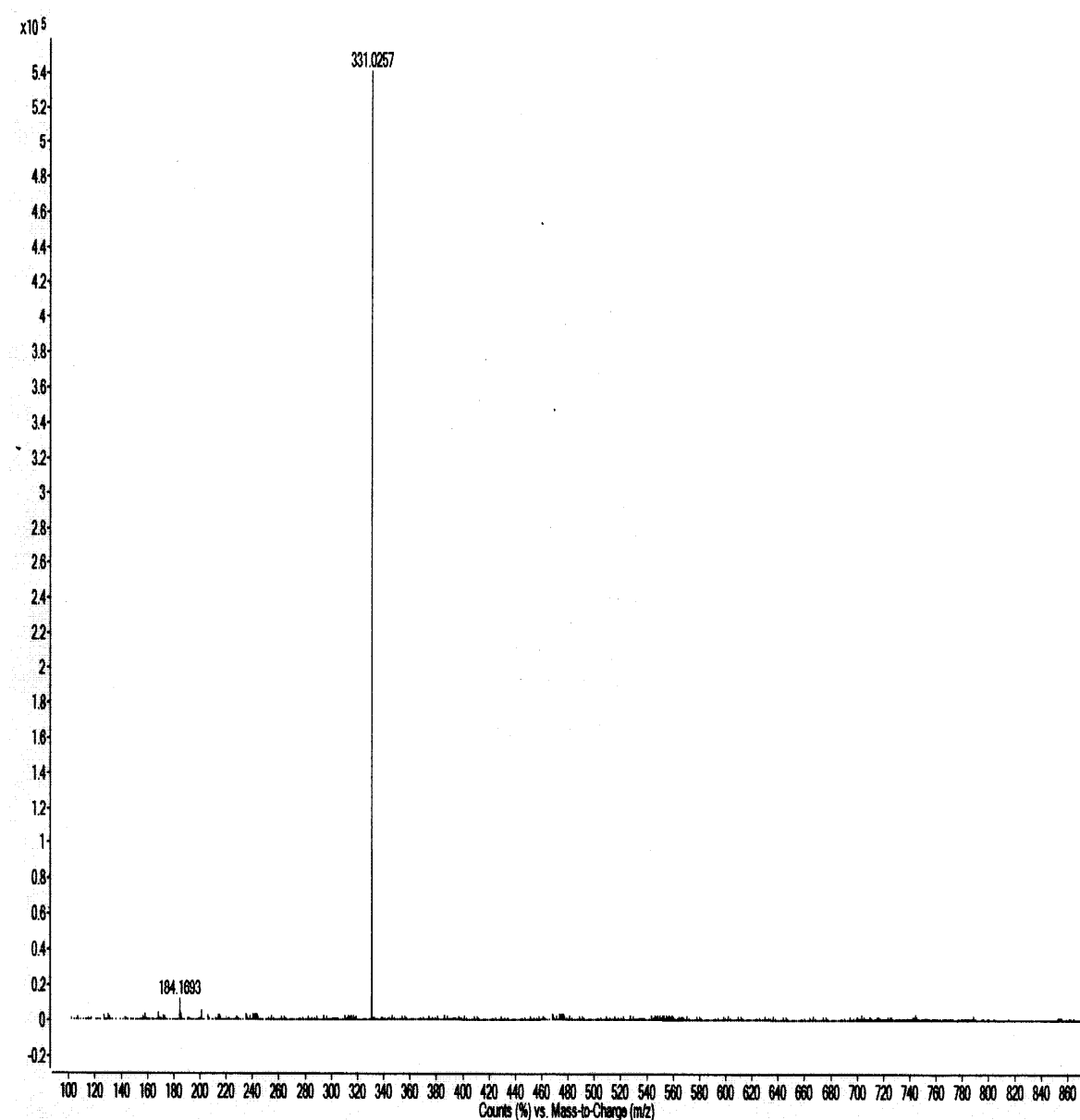


Figure S13: Mass spectrum of **9b**.

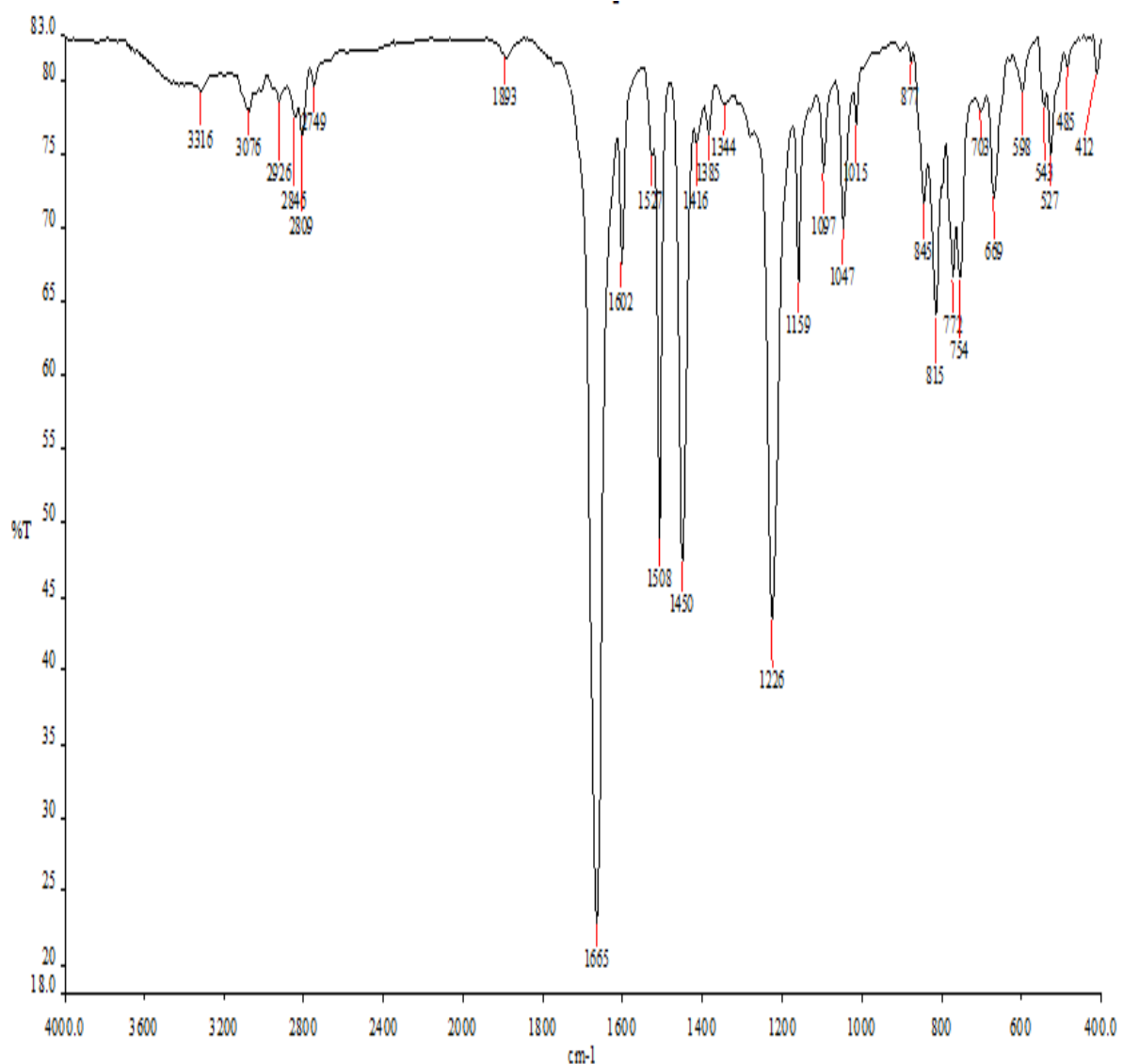


Figure S14: IR Spectrum of **9b**.

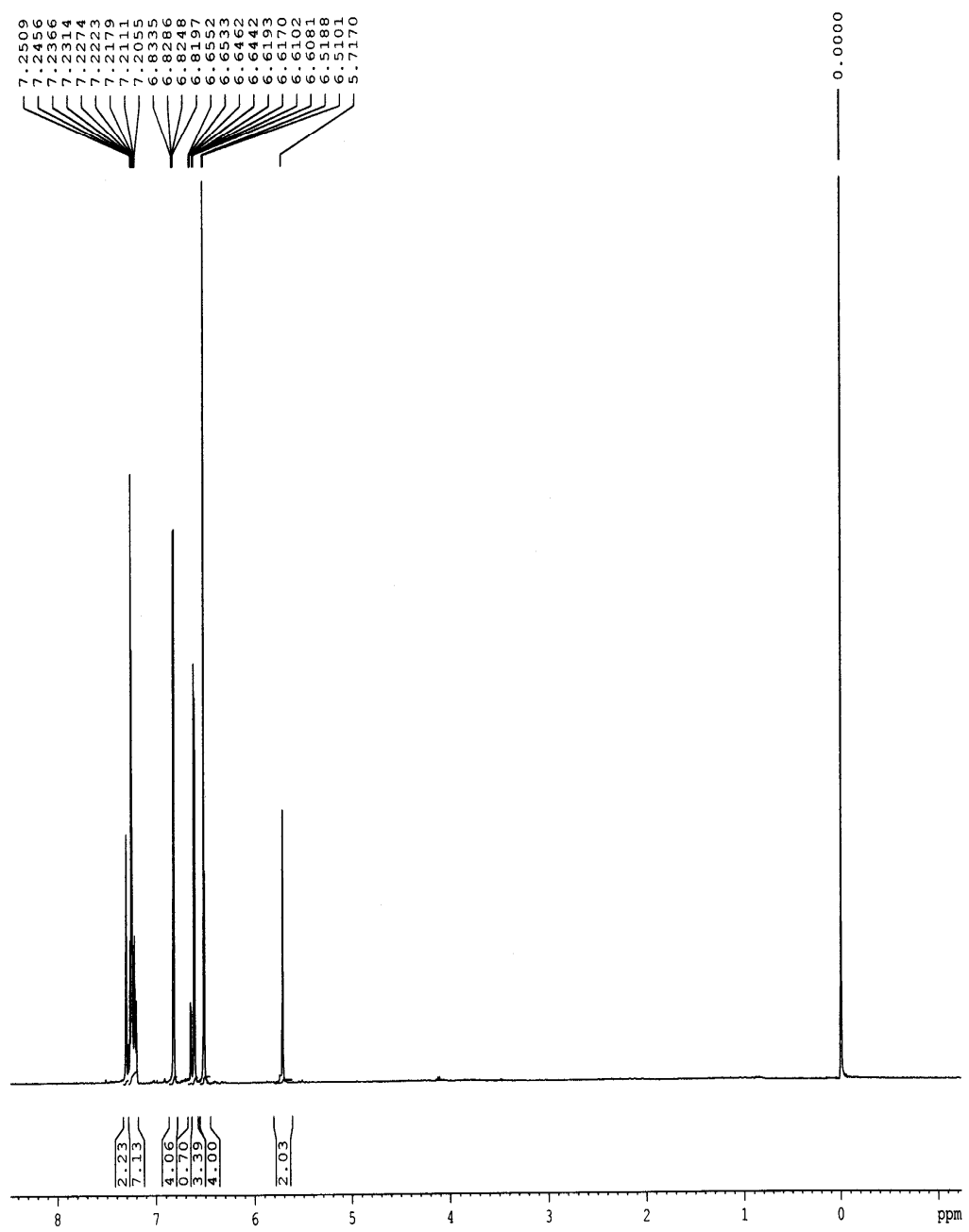


Figure S15: ^1H NMR Spectrum of **10a**.

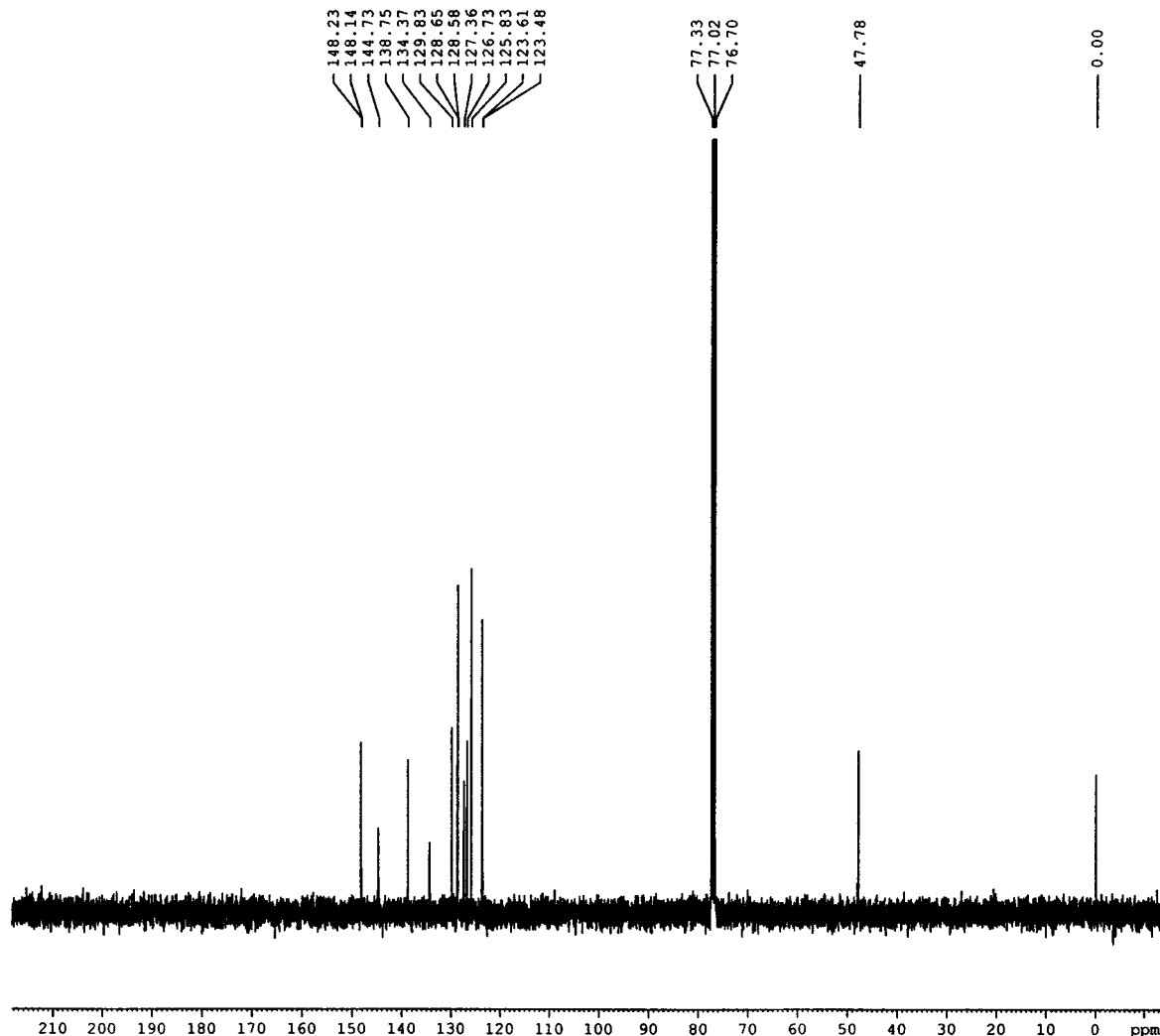


Figure S16: ^{13}C NMR spectrum of **10a**.

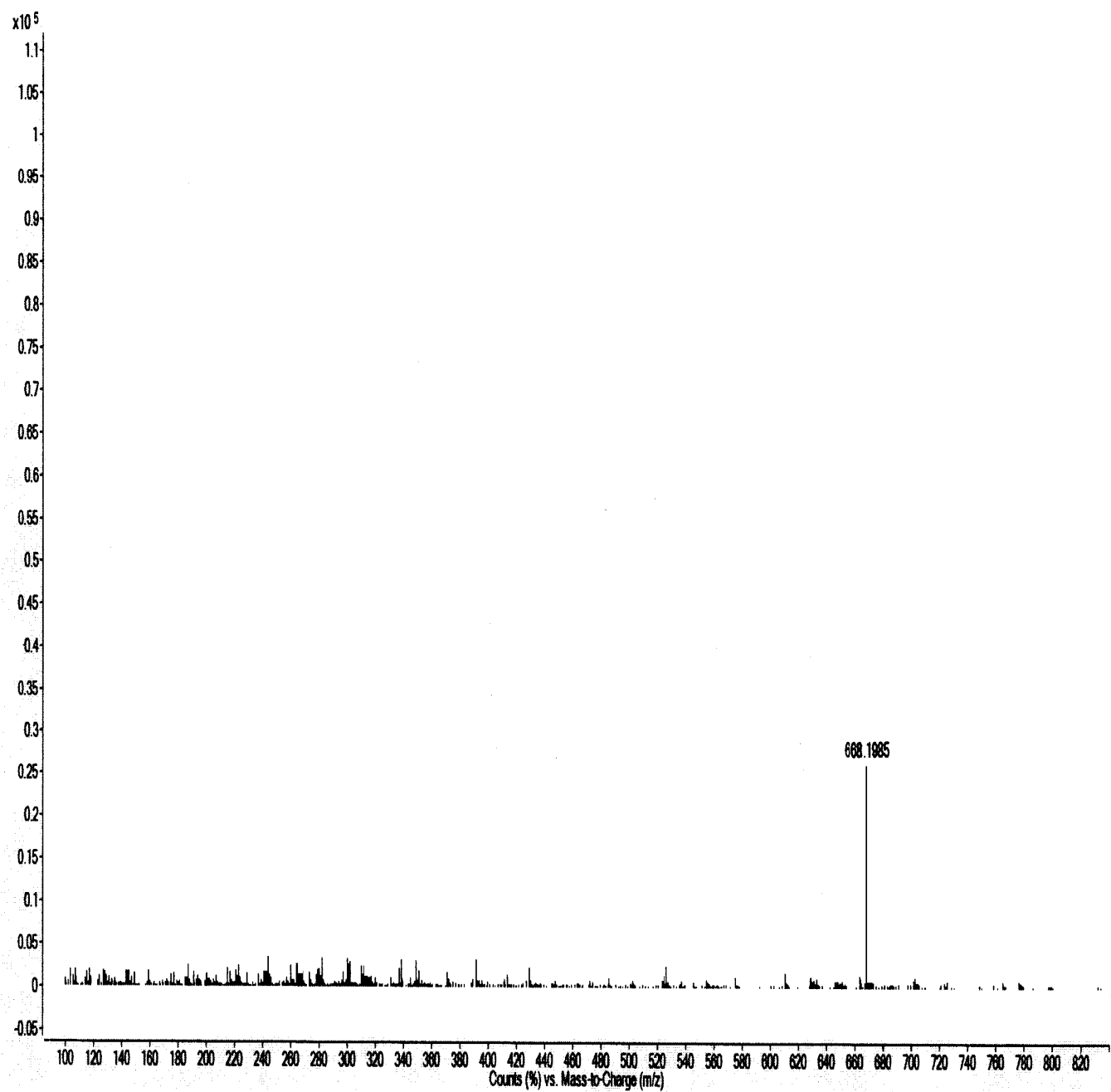


Figure S17: Mass spectrum of **10a**.

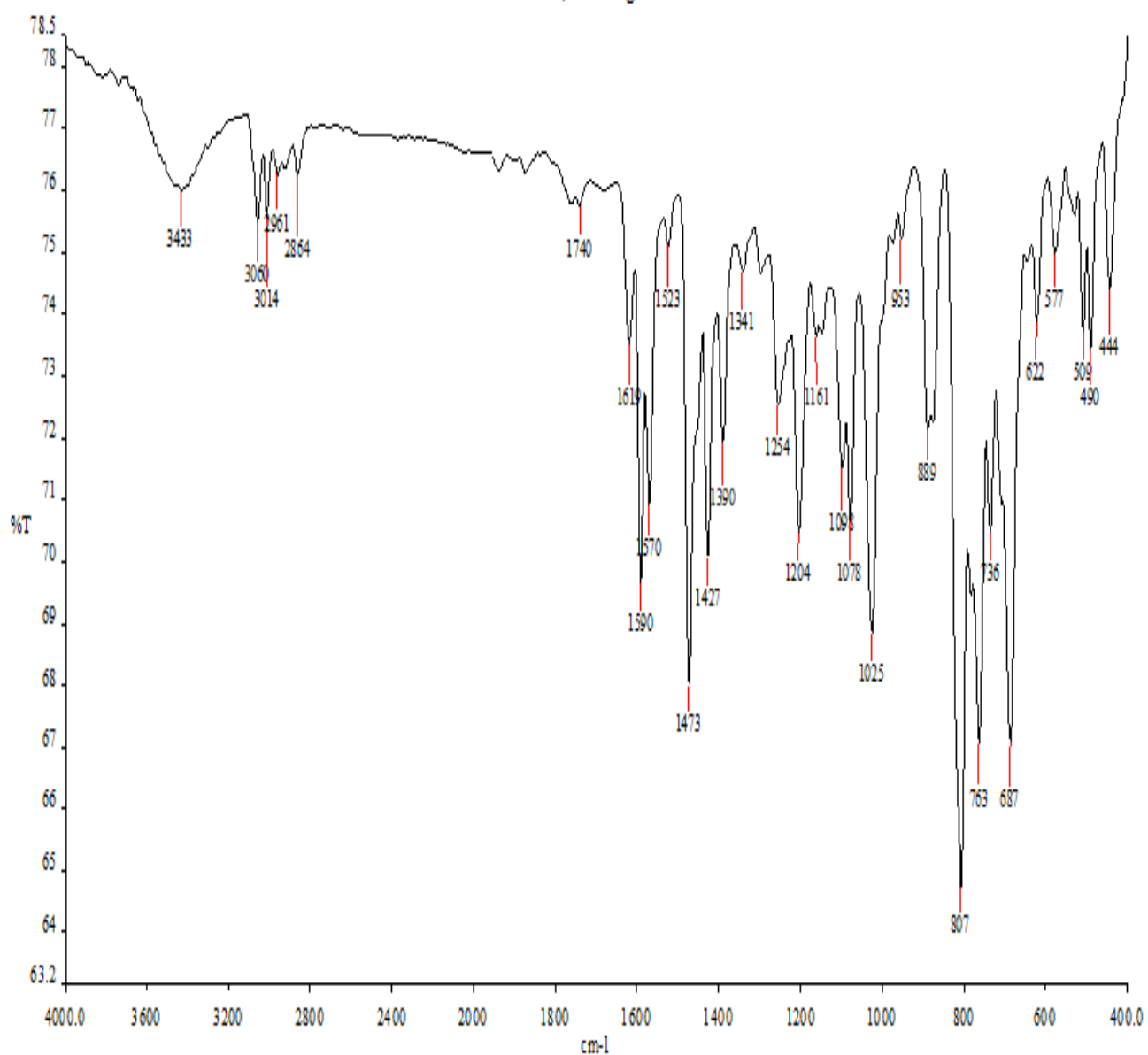


Figure S18: IR Spectrum of **10a**.

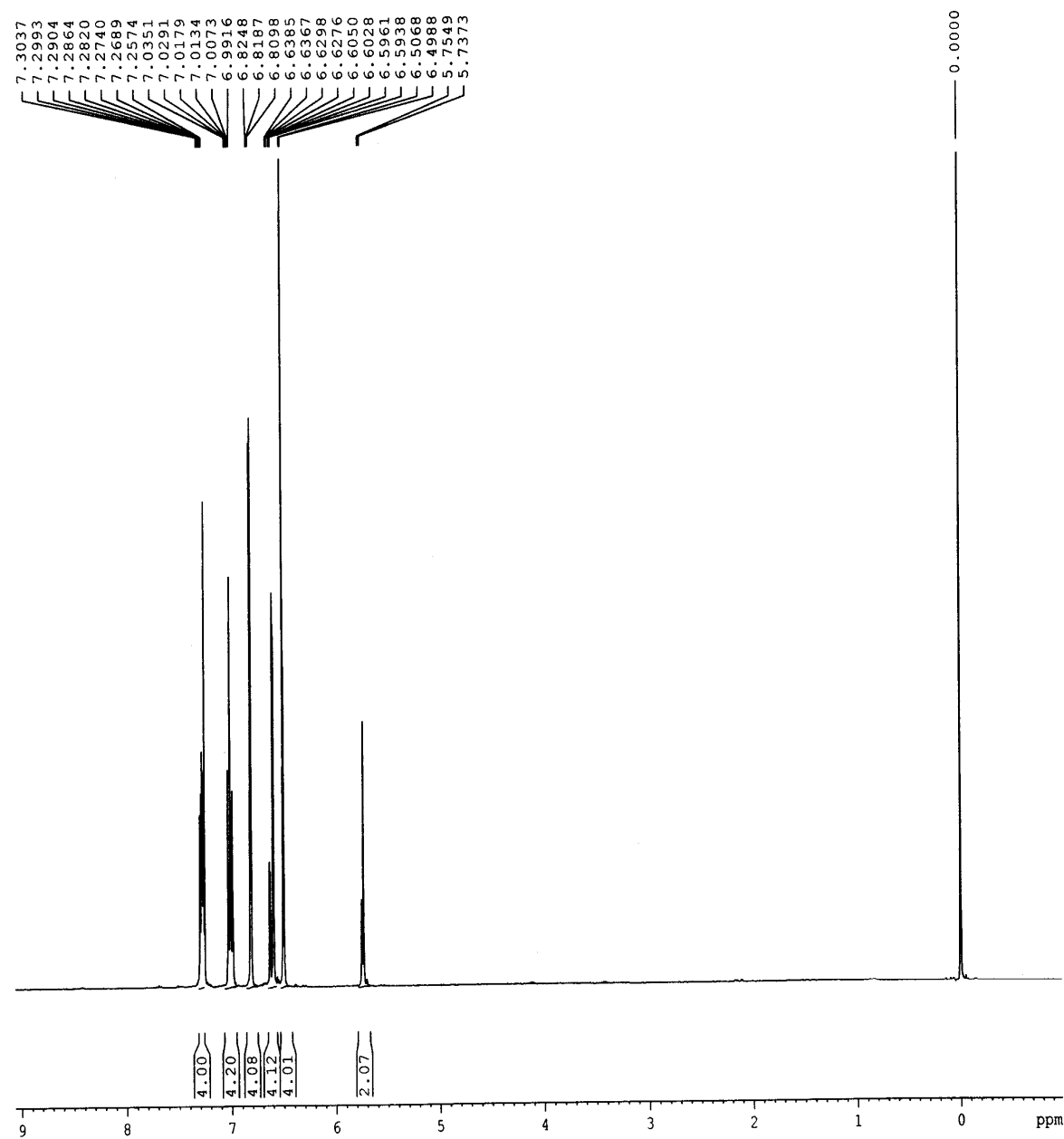


Figure S19: ^1H NMR Spectrum of **10b**.

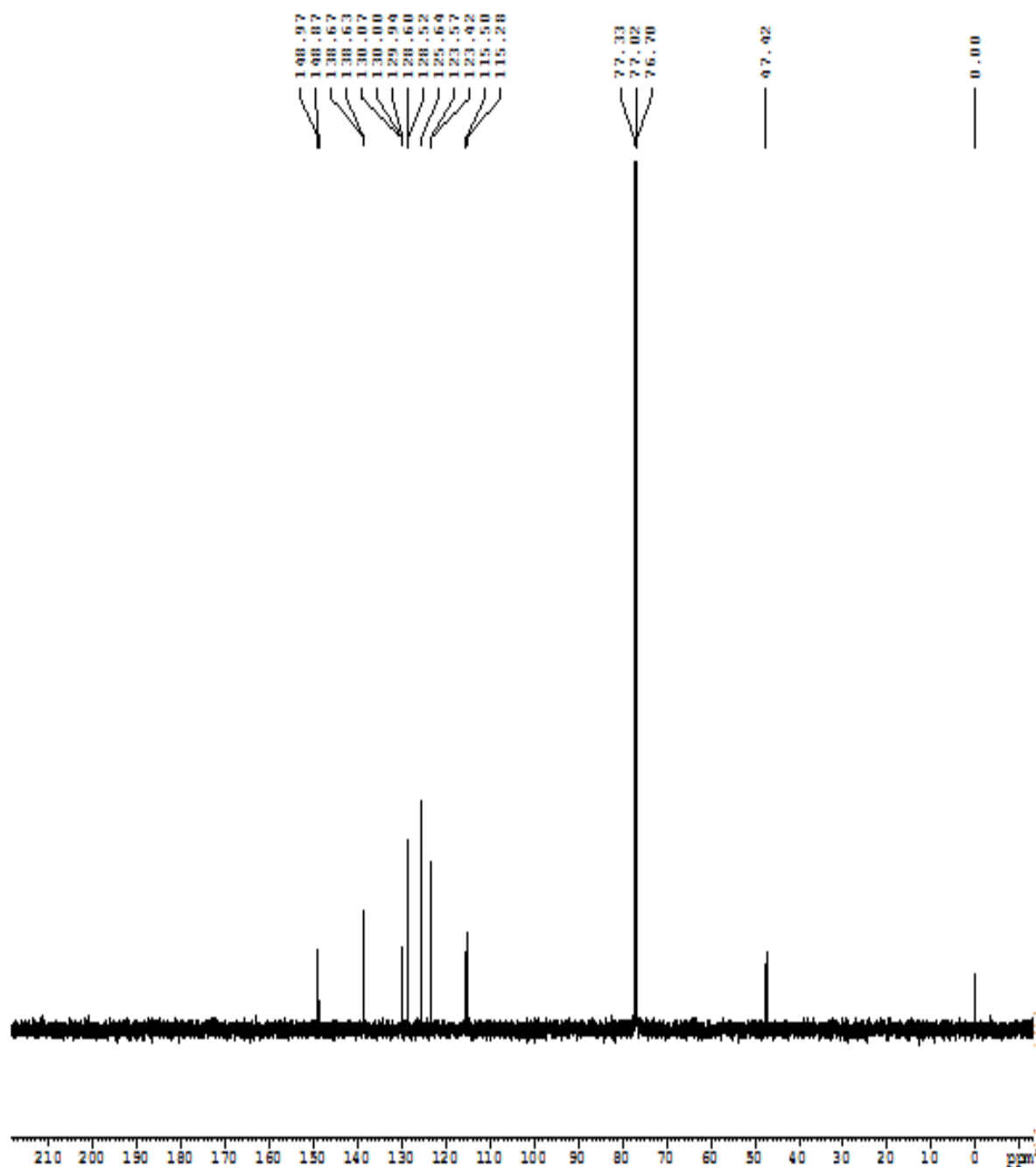


Figure S20: ¹³C NMR Spectrum of **10b**.

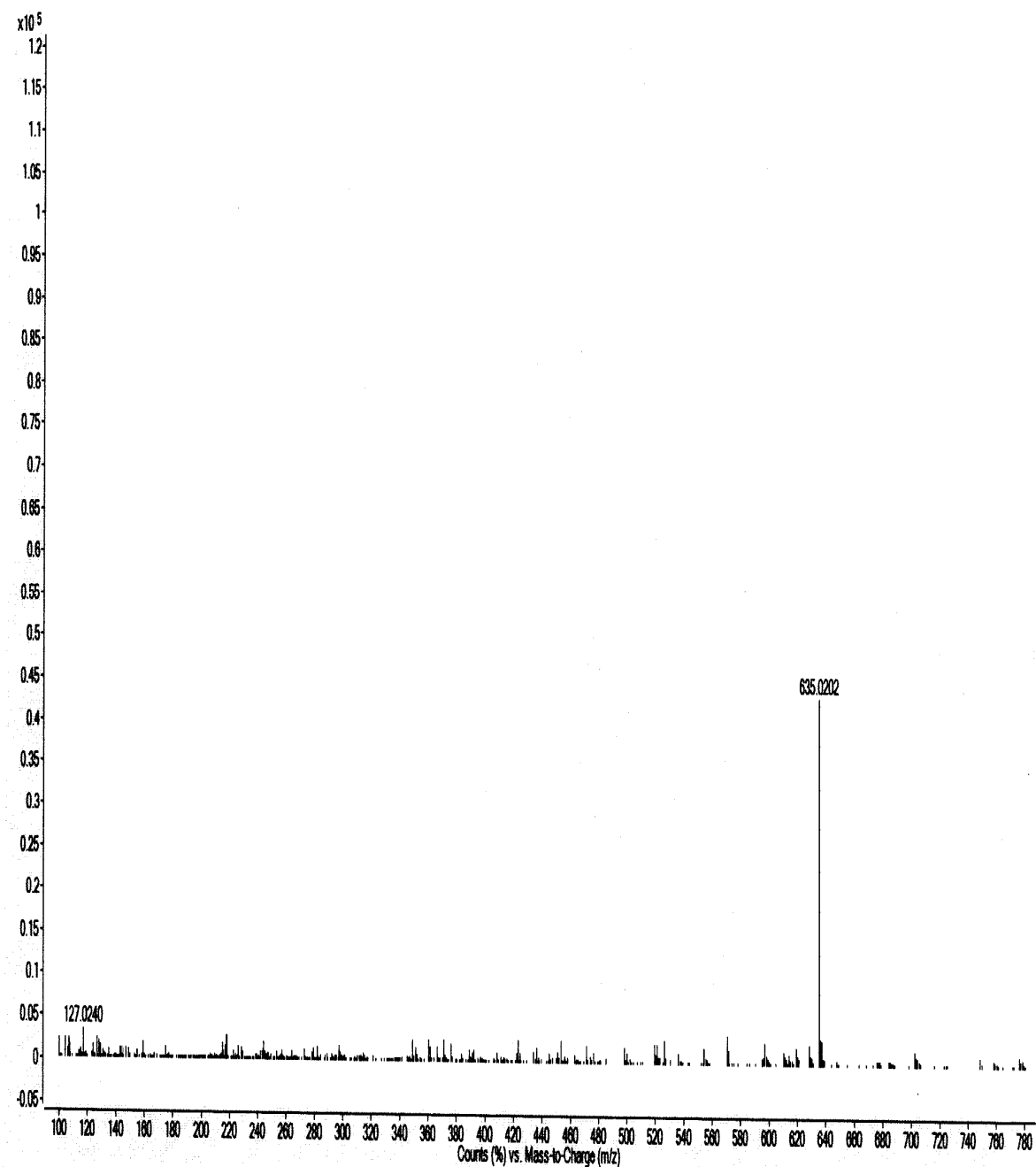


Figure S21: Mass spectrum of **10b**.

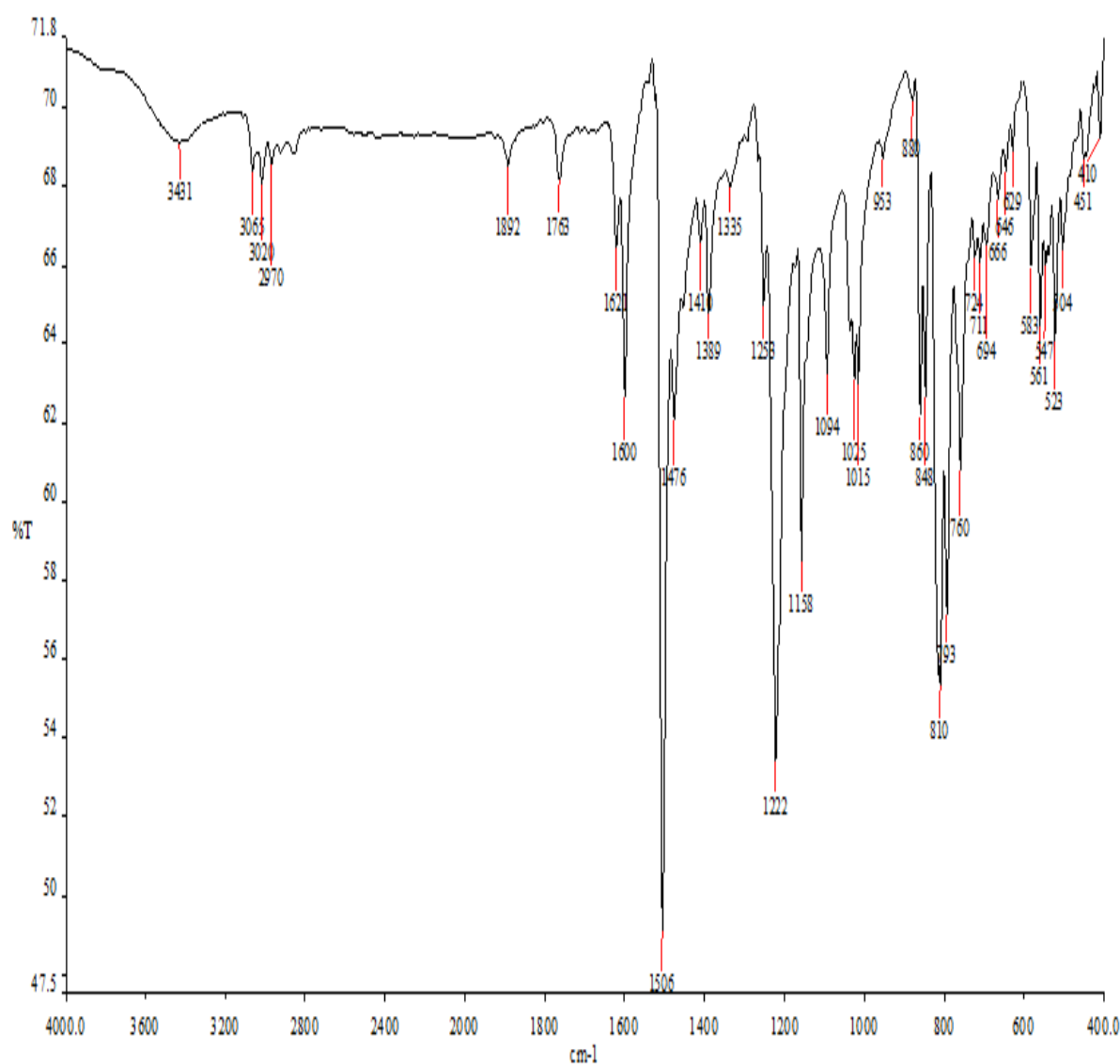


Figure S22: IR Spectrum of **10b**.

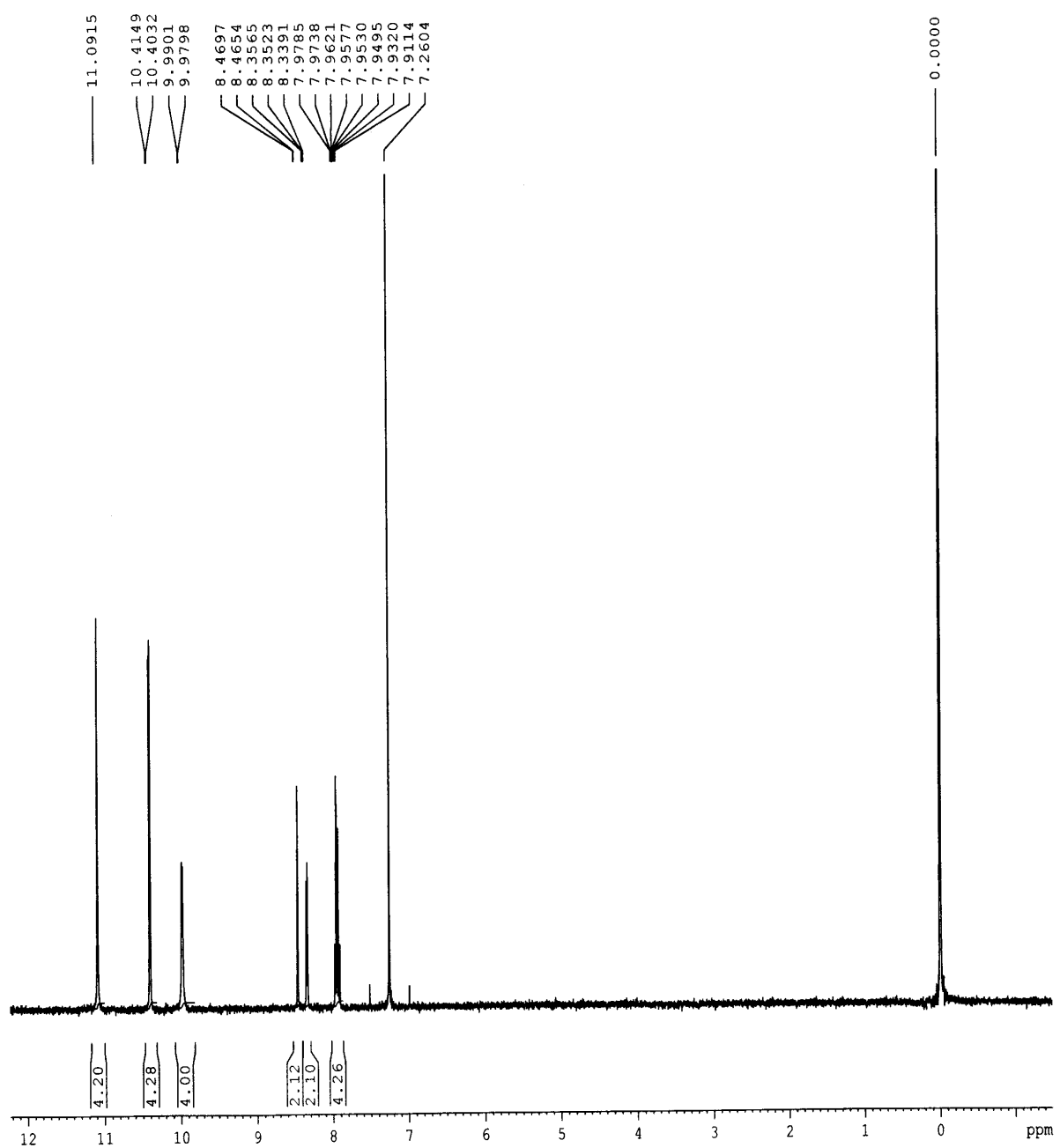


Figure S23: ^1H NMR Spectrum of **11a**.

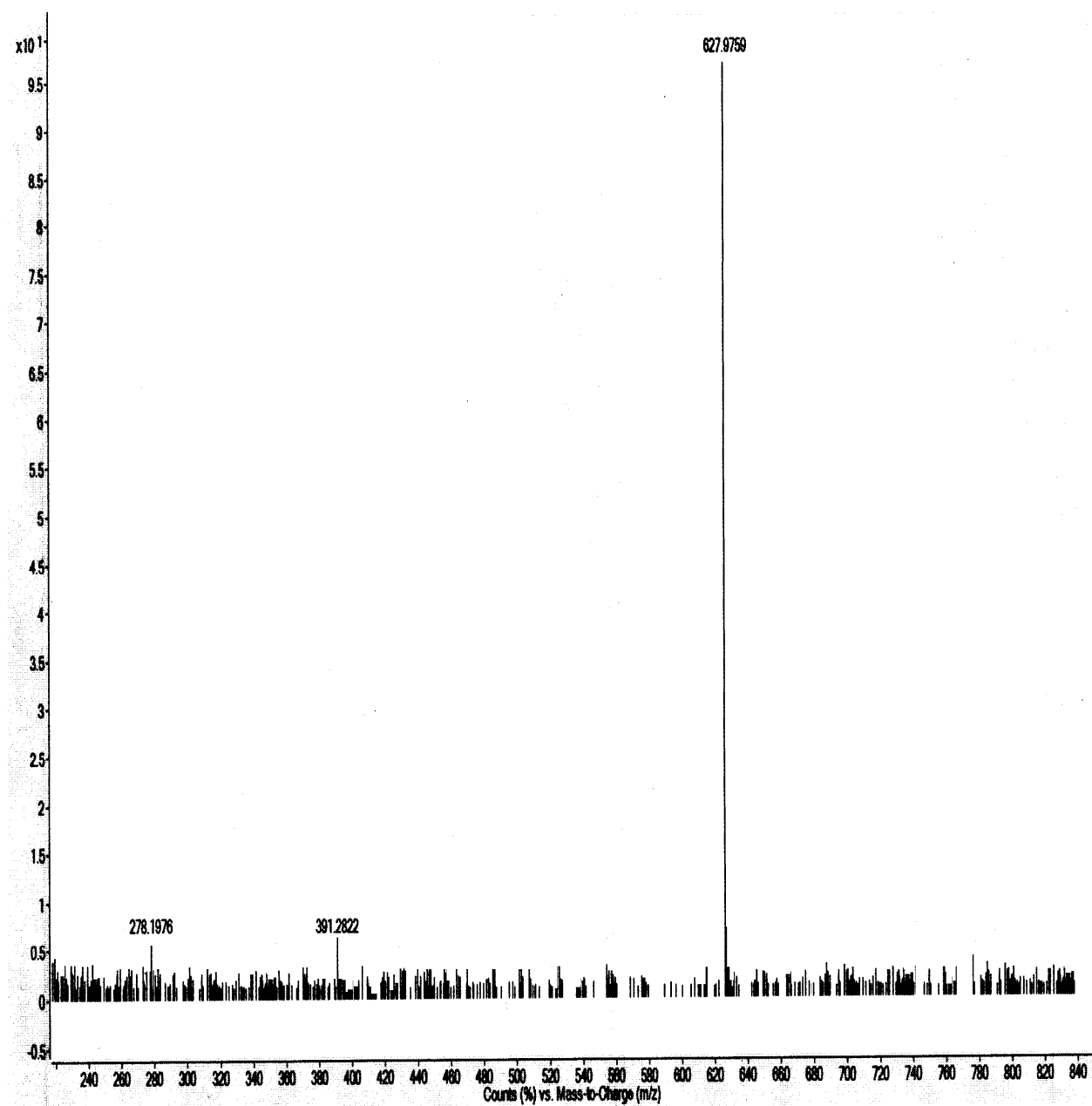


Figure S24: Mass spectrum of **11a**.

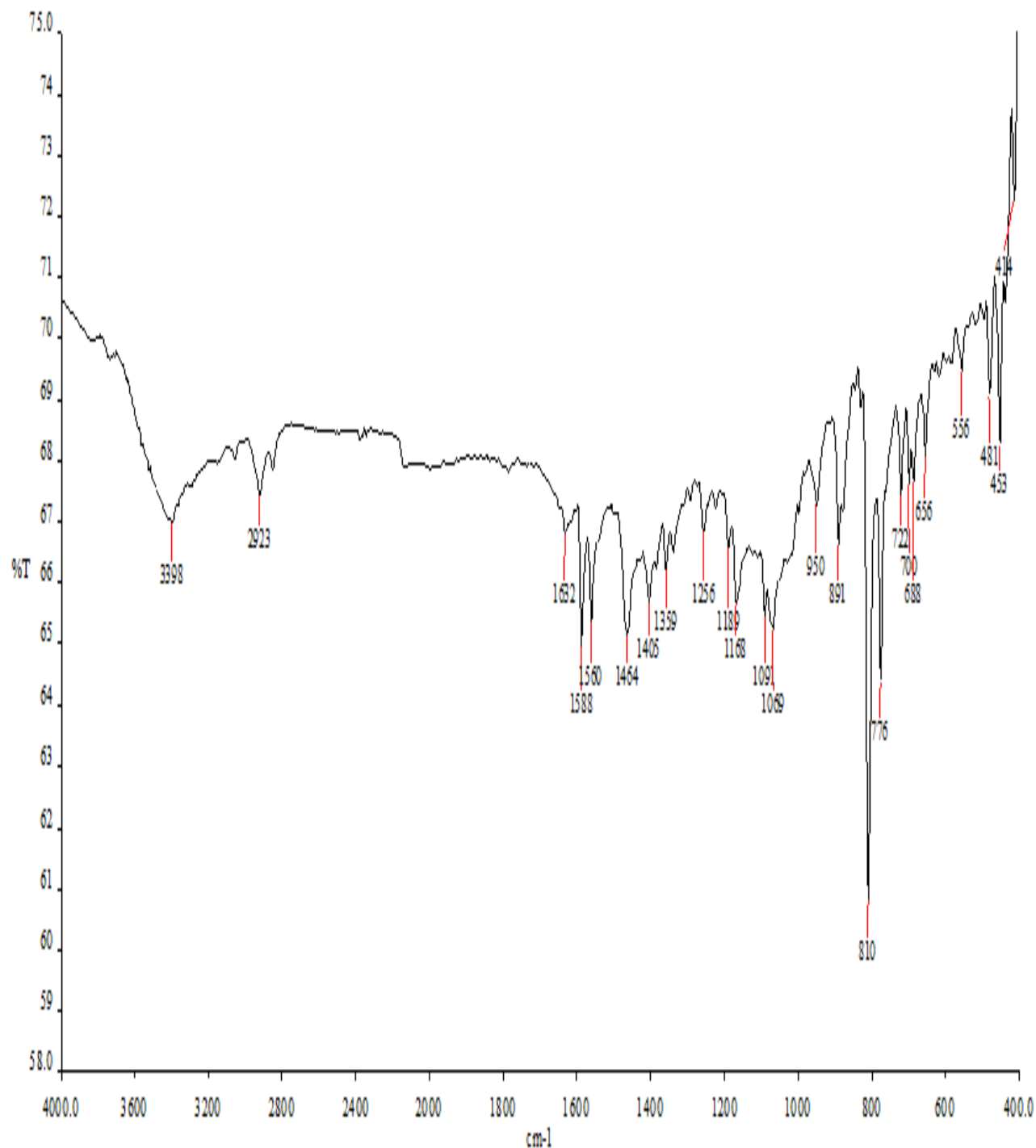


Figure S25: IR Spectrum of **11a**.

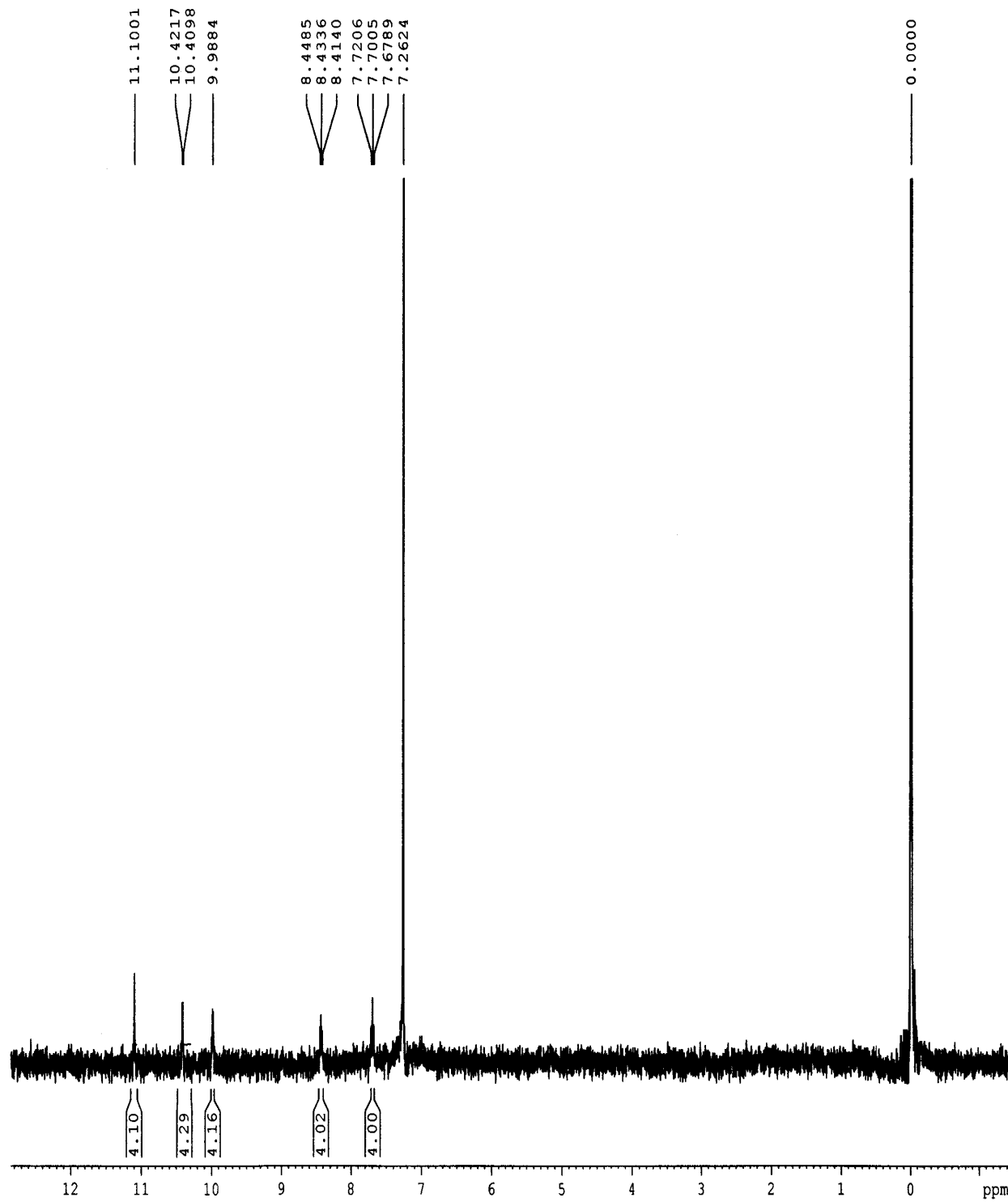


Figure S26: ¹H NMR Spectrum of **11b**.

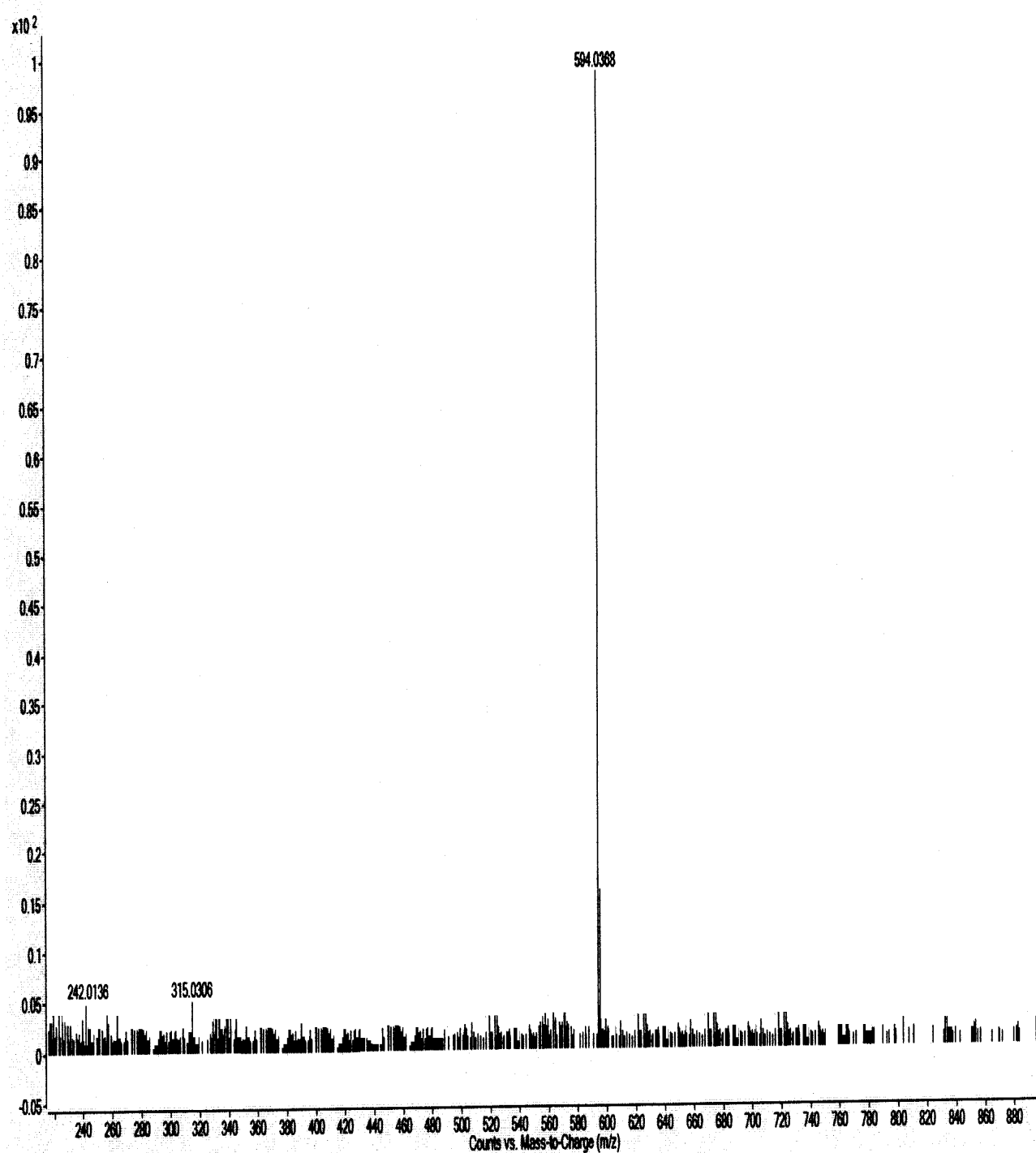


Figure S27: Mass spectrum of **11b**.

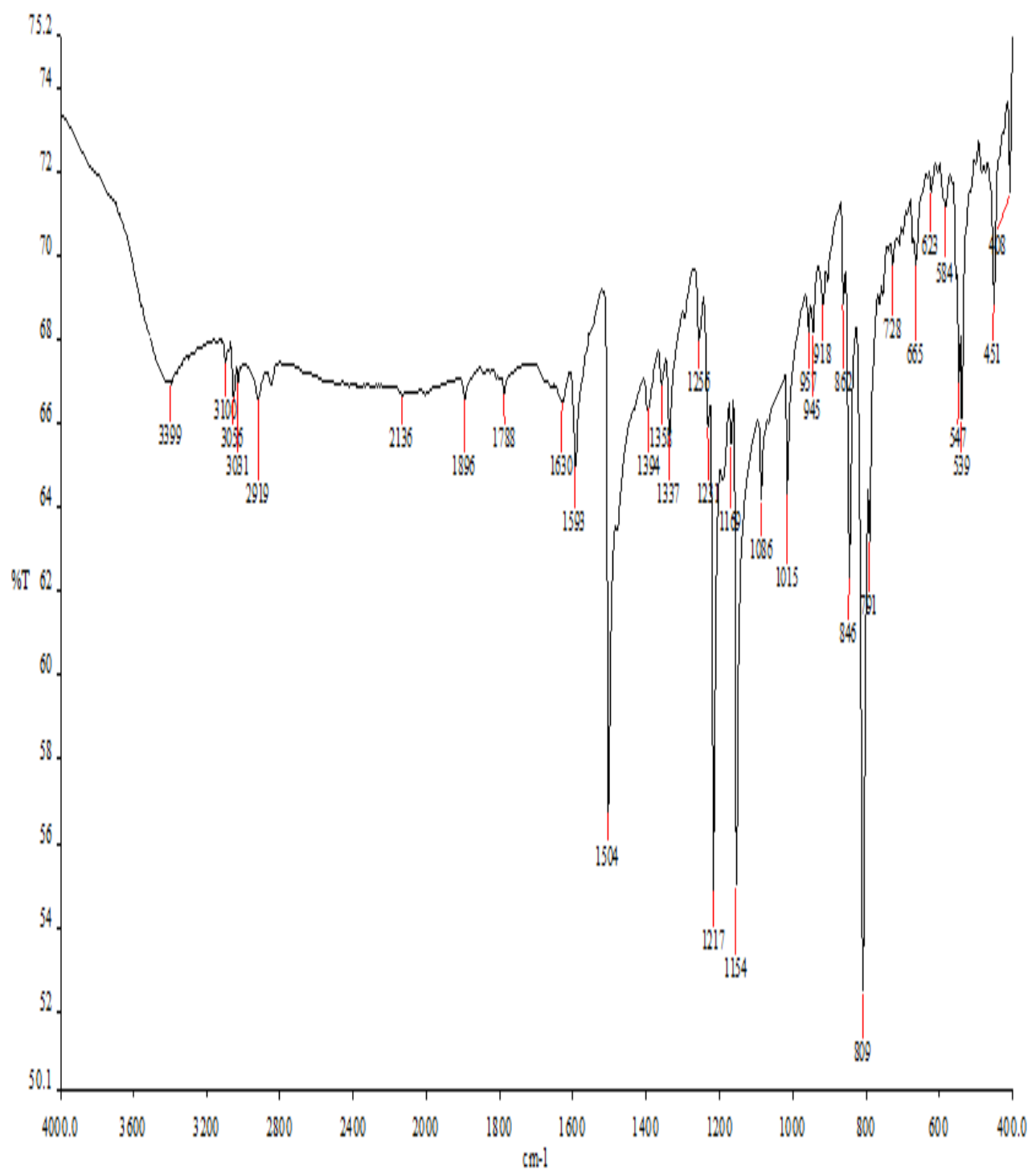


Figure S28: IR Spectrum of **11b**.

Theoretical Calculations

Computational methods

All the calculations were performed at the density functional theory (DFT) level with the B3LYP functional, the gradient correction of the exchange functional by Becke and the correlation functional by Lee, Yang and Parr. The 6-311G(d) split valence plus polarization basis set was used in Gaussian 09 program.^{[1],[2]} The results were analyzed and visualized on Gauss View 5.0.9.

^[1] Gaussian 09, Revision B.01, Frisch, M. J.; Trucks, G. W.; Schlegel, H. B.; Scuseria, W. H. G. E.; Robb, M. A.; Cheeseman, J. R.; Scalmani, G.; Barone, V.; Mennucci, B.; Petersson, G. A.; Nakatsuji, H.; Caricato, M.; Li, X.; Hratchian, H. P.; Izmaylov, A. F.; Bloino, J.; Zheng, G.; Sonnenberg, J. L.; Hada, M.; Ehara, M.; Toyota, K.; Fukuda, R.; Hasegawa, J.; Ishida, M.; Nakajima, T.; Honda, Y.; Kitao, O.; Nakai, H.; Vreven, T.; Montgomery, J. A.; Peralta, Jr., J. E.; Ogliaro, F.; Bearpark, M.; Heyd, J. J.; Brothers, E.; Kudin, K. N.; Staroverov, V. N.; Keith, T.; Kobayashi, R.; Normand, J.; Raghavachari, K.; Rendell, A.; Burant, J. C.; Iyengar, S. S.; Tomasi, J.; Cossi, M.; Rega, N.; Millam, J. M.; Klene, M.; Knox, J. E.; Cross, J. B.; Bakken, V.; Adamo, C.; Jaramillo, J.; Gomperts, R.; Stratmann, R. E.; Yazayev, O.; Austin, A. J.; Cammi, R.; Pomelli, C.; Ochterski, J. W.; Martin, R. L.; Morokuma, K.; Zakrzewski, V. G.; Voth, G. A.; Salvador, P.; Dannenberg, J. J.; Dapprich, S.; Daniels, A. D.; Farkas, O.; Foresman, J. B.; Ortiz, J. V.; Cioslowski, J.; Fox, D. J. Gaussian, Inc., Wallingford CT, 2010.

^[2] Details including the references for the DFT method and basis set can be found online at the homepage of Gaussian, Inc.; <http://www.gaussian.com/>

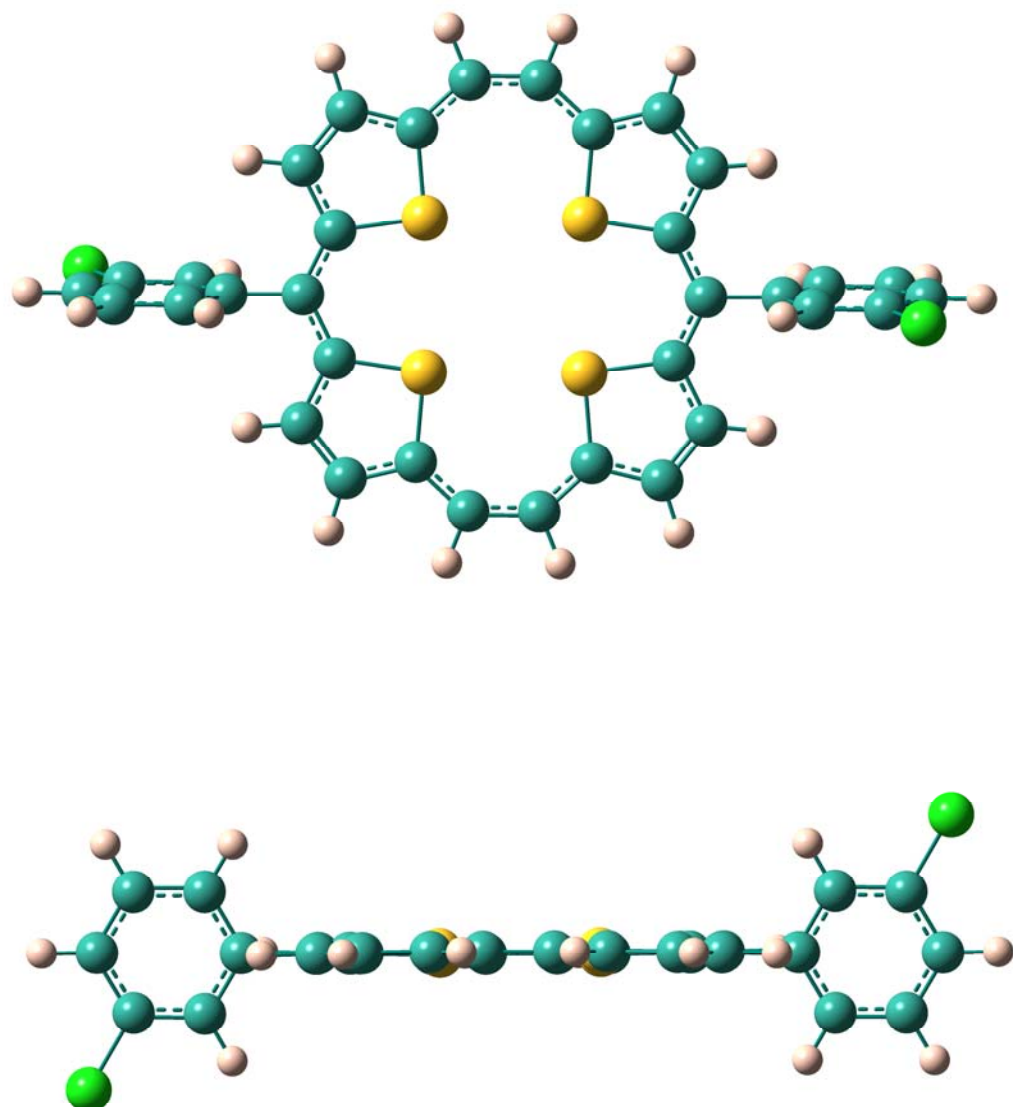


Figure S29: Energy minimized structure of **11a** by DFT method at B3LYP/6-311G(d) level using the Gaussian09 program (Top and side views shown above).

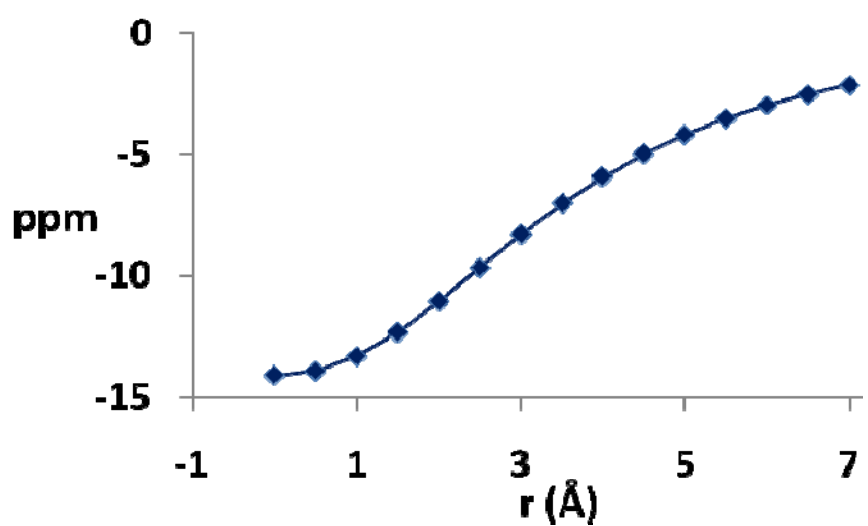
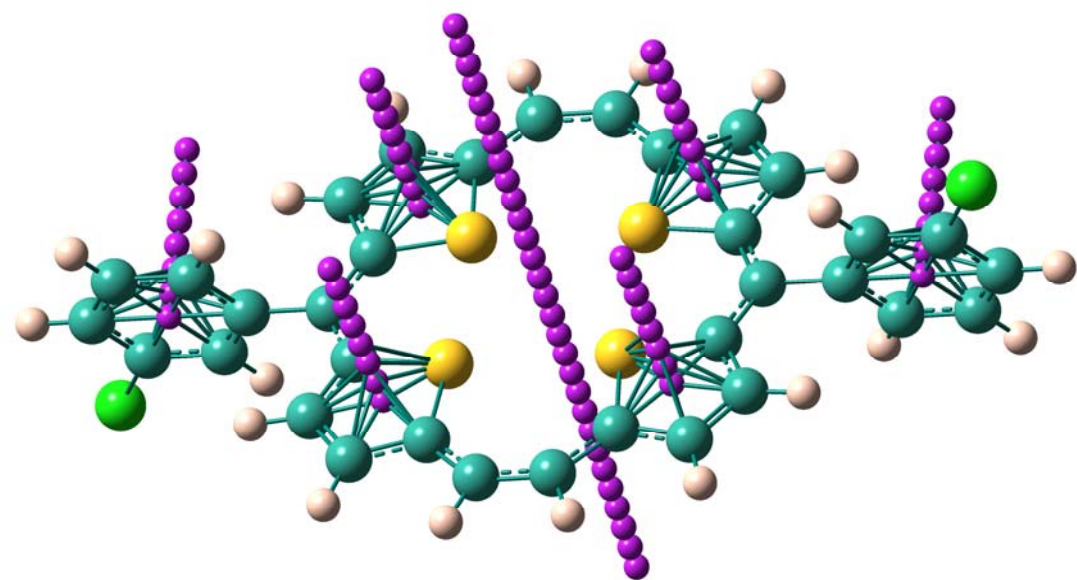


Figure S30: The ghost (Bq) atoms (in purple) were placed (0.5 Å interval) in the centre of the molecule. The -ve NICS values clearly indicate the aromaticity of **11a**. NICS is maximum at 0 Å and decreases as the distance of the ghost atom is increased in 0.5 Å intervals.

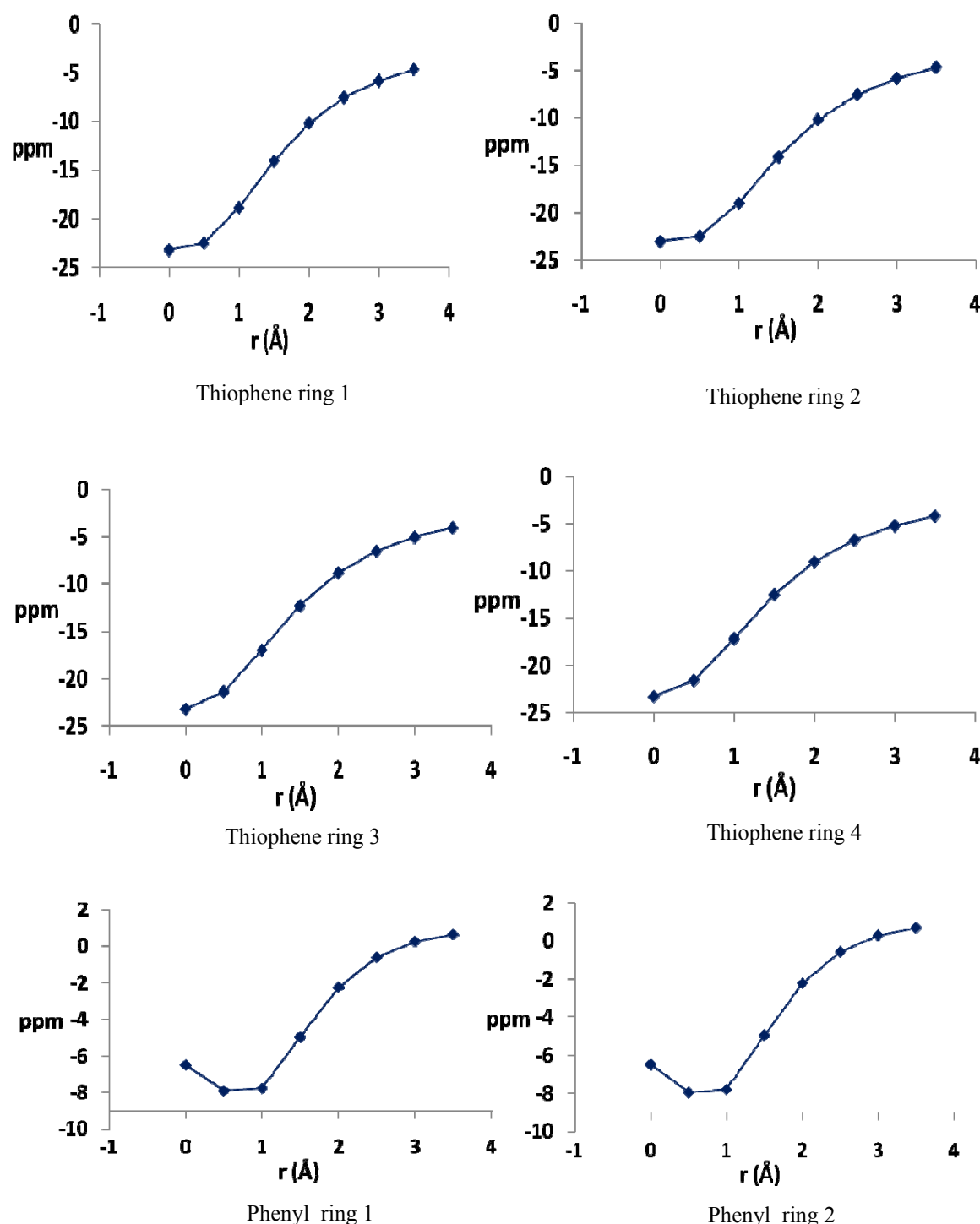


Figure S31: As shown above is the behaviour of the four thiophene rings of **11a**. The NICS are negative and maximum at their centres and decreases as we move farther. Further the NICS at the centre is far higher than the normal thiophene showing their increased aromatic character when they are part of the annulene ring. Phenyl rings are showing the normal behavior like benzene but with decreased NICS values.

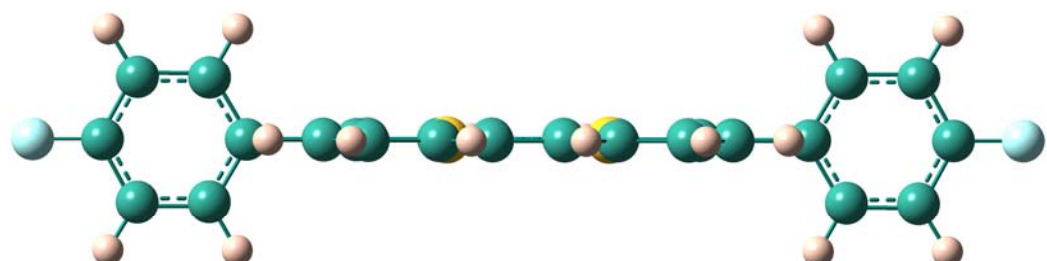
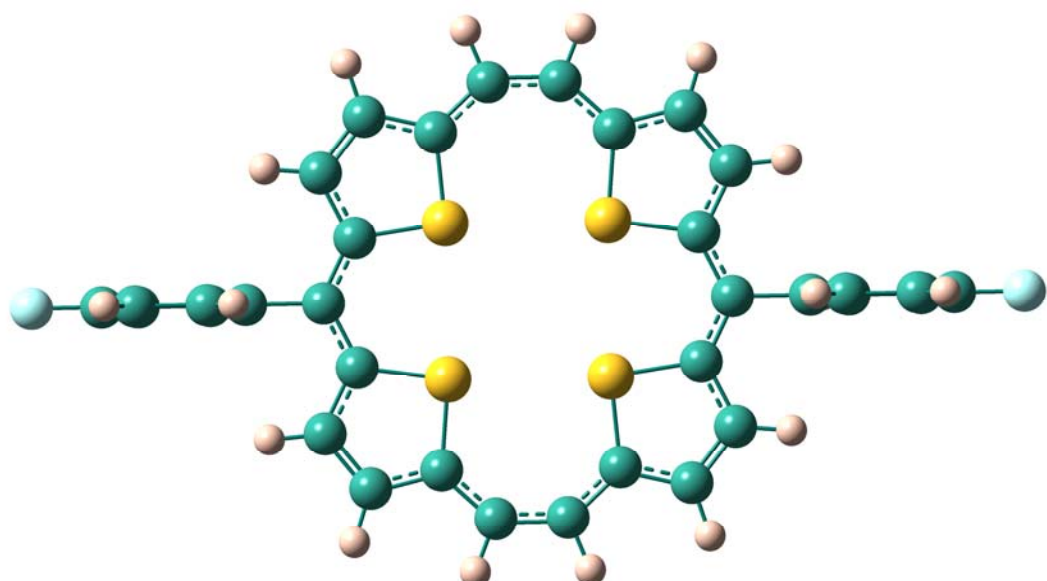


Figure S32: Energy minimized structure of **11b** by DFT method at B3LYP/6-311G(d) level using the Gaussian09 program (Top and side views shown above).

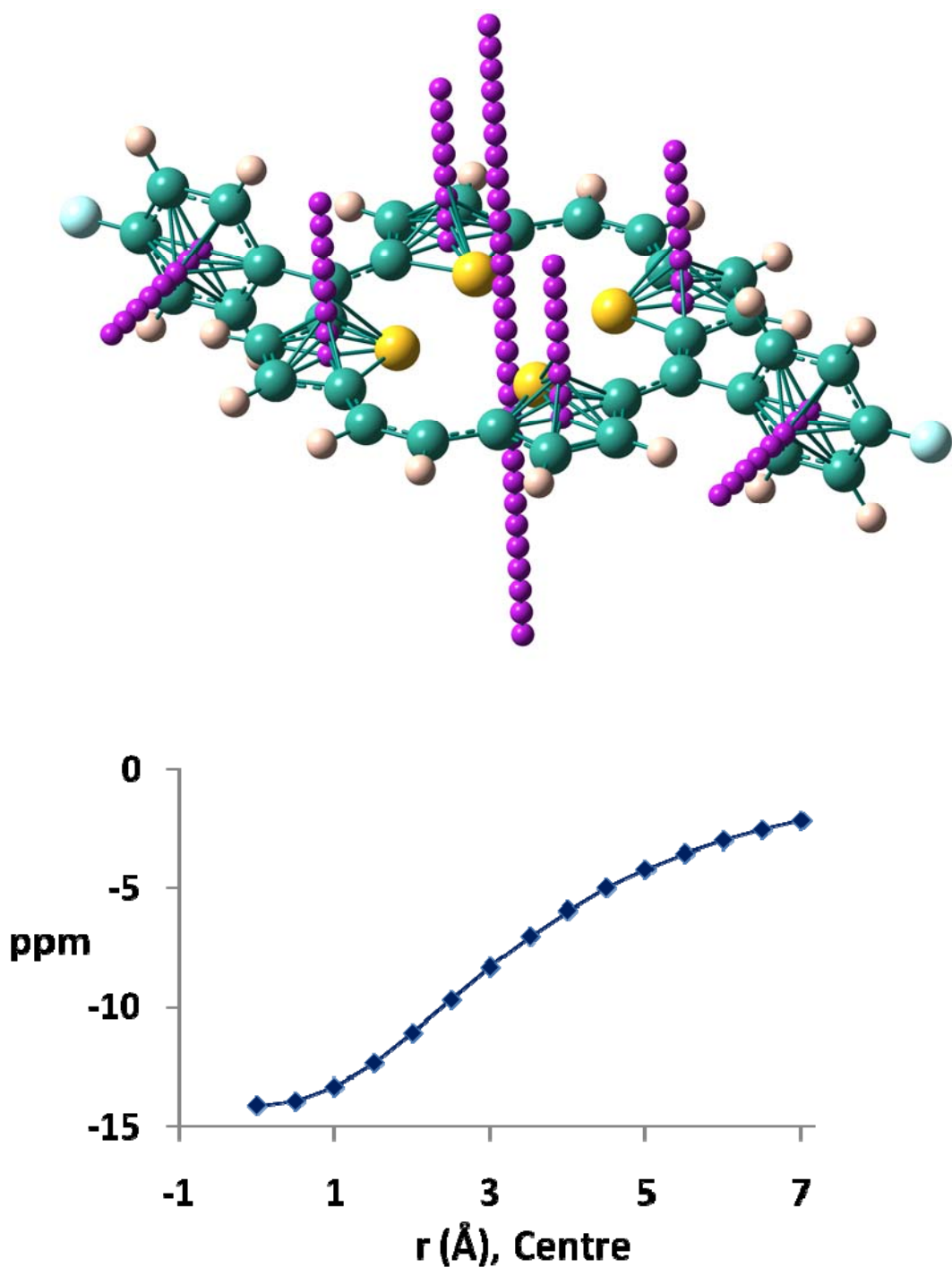


Figure S33: The ghost (Bq) atoms were placed (0.5 Å interval) in the centre of the molecule (in purple). The -ve NICS values clearly indicate the aromaticity of **11b**. NICS is maximum at 0 Å and decreases as the distance of the ghost atom is increased in 0.5 Å intervals.

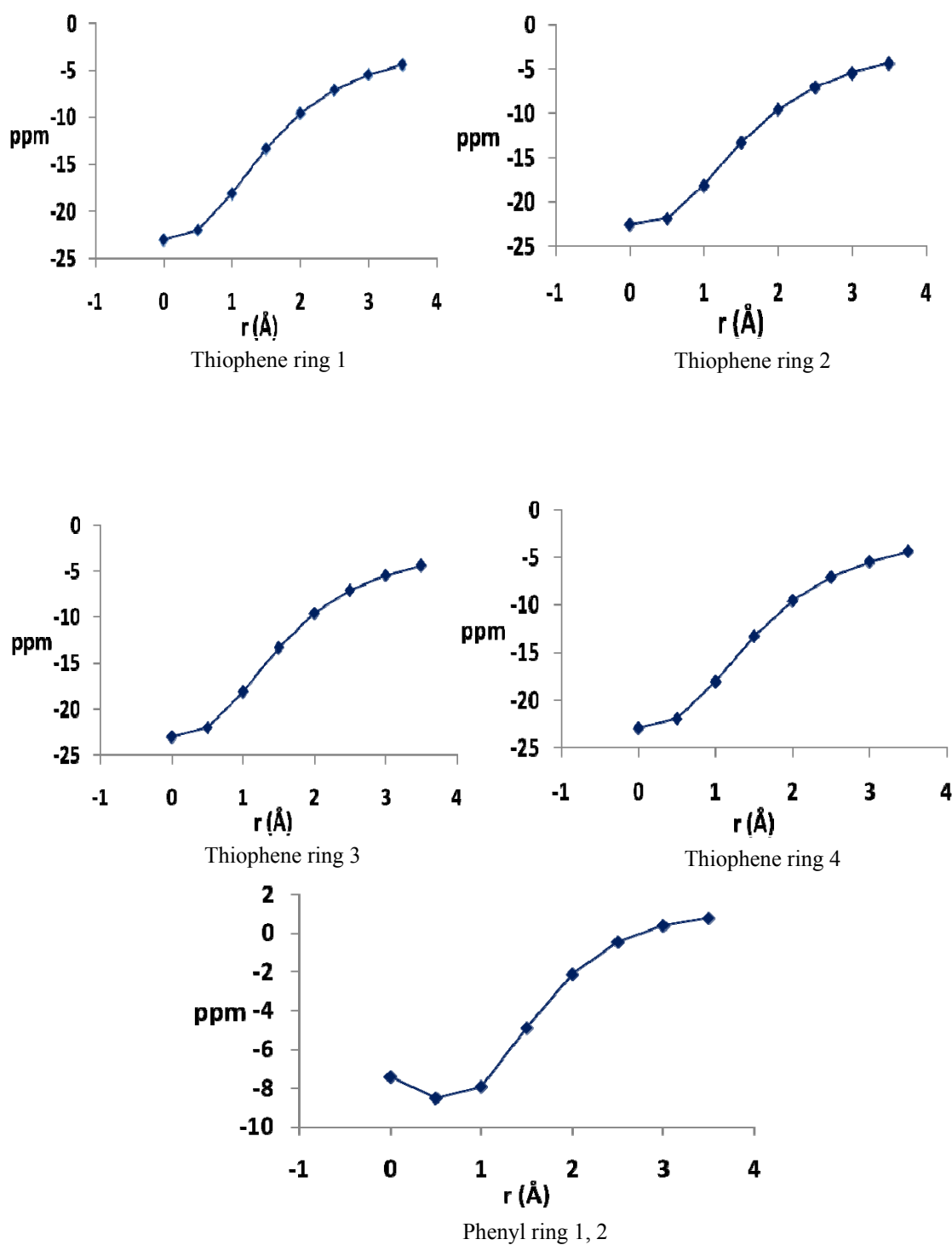


Figure S34: As shown above is the behaviour of the four thiophene rings of **11b**. The NICS are negative and maximum at their centres and decreases as we move farther. Further the NICS at the centre is far higher than the normal thiophene showing their increased aromatic character when they are part of the annulene ring. Phenyl rings are showing the normal behavior like benzene but with decreased NICS values.

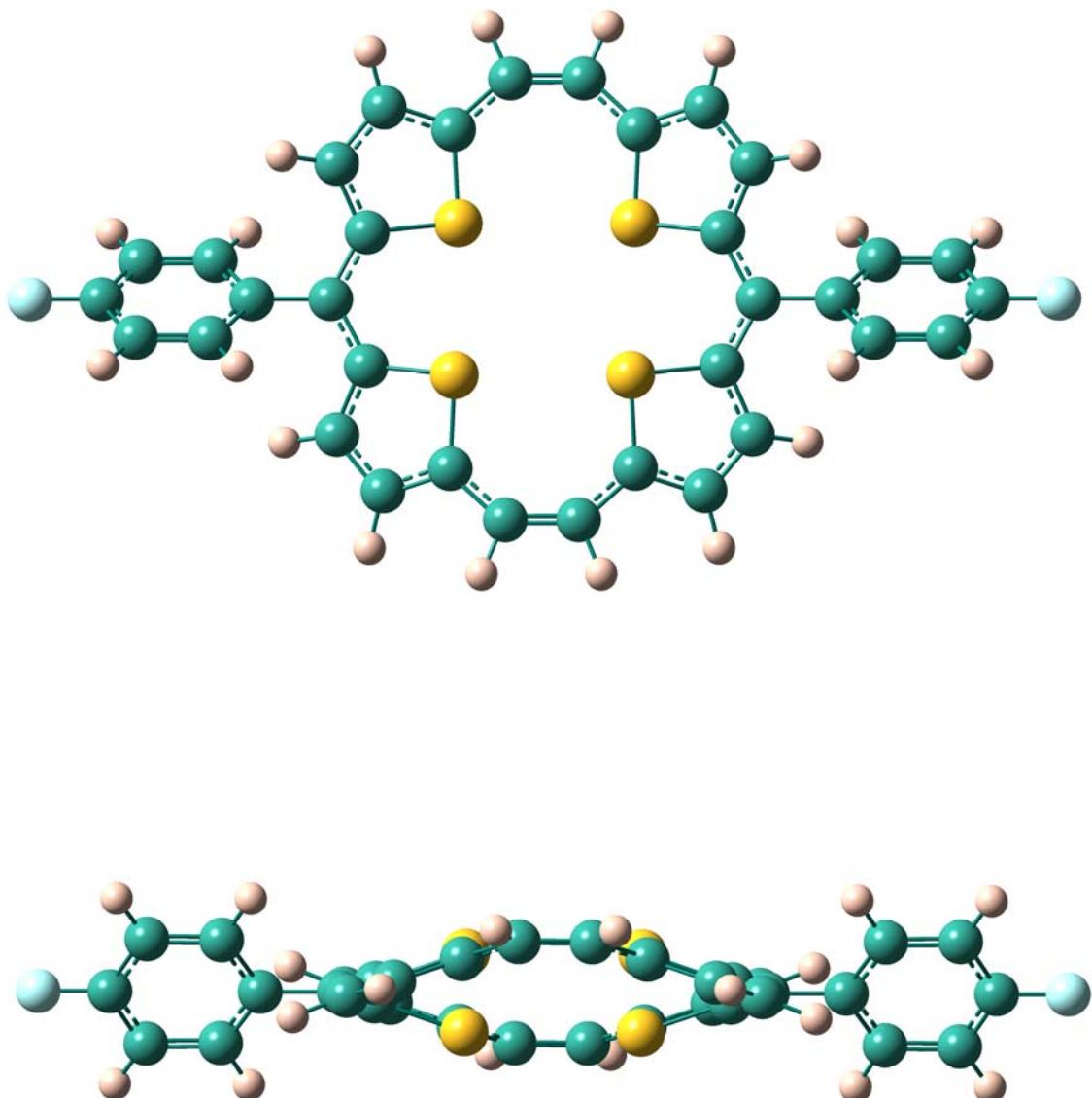


Figure S35: Energy minimized structure of antiaromatic dication **12b**. Upper (top view), lower (side view).

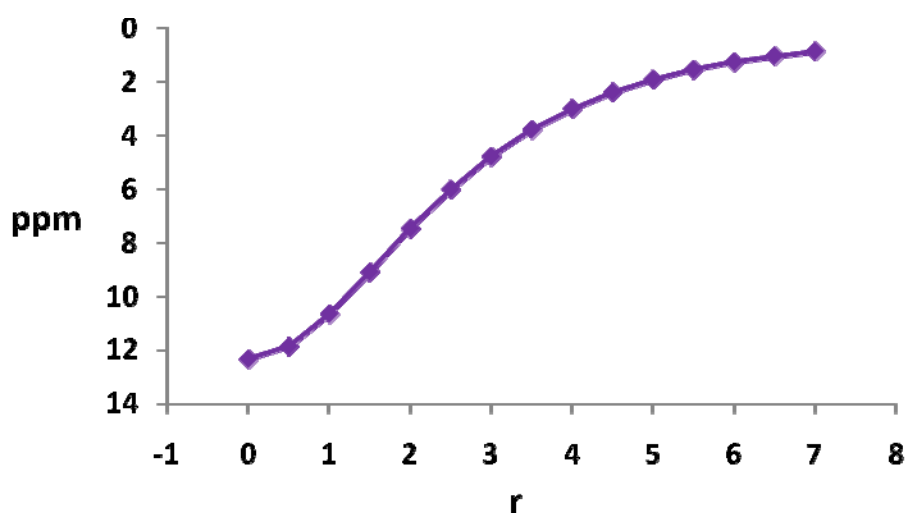
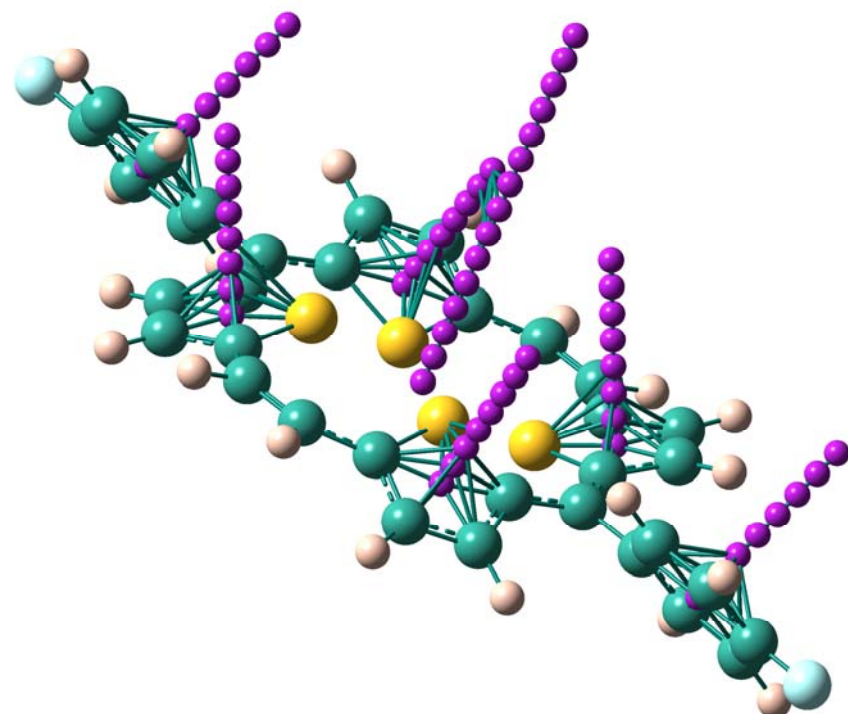
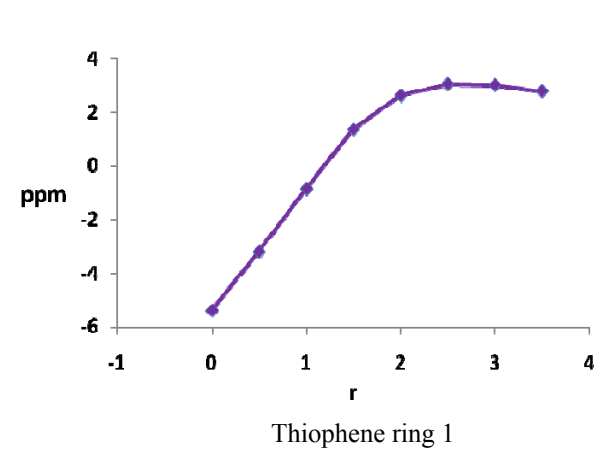
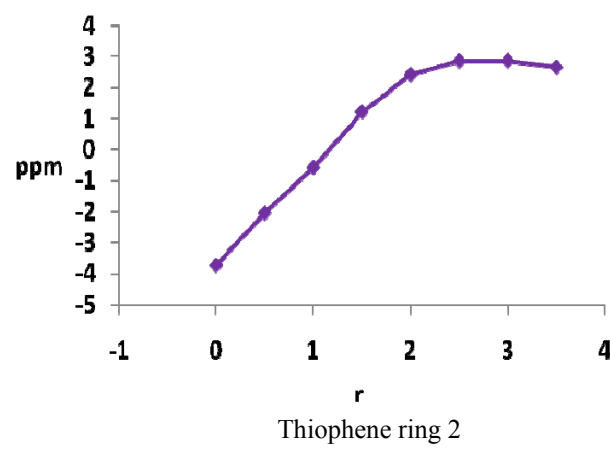


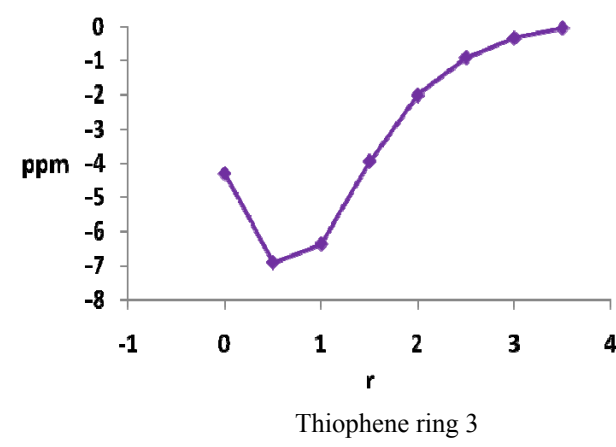
Figure S36: Placement of the ghost atoms (at 0.5 Å intervals) at the centre of all the individual rings as well as the main ring of **12b** (anti aromatic). The +ve NICS values (NICS 1 = 10.65) indicates the antiaromatic behaviour of the dication **12b**. The resulting NICS vs. r (distance from centre in Å) graph is also shown for the main centre of the **12b**. The graphs for the four thiophene rings are also shown (Figure S37).



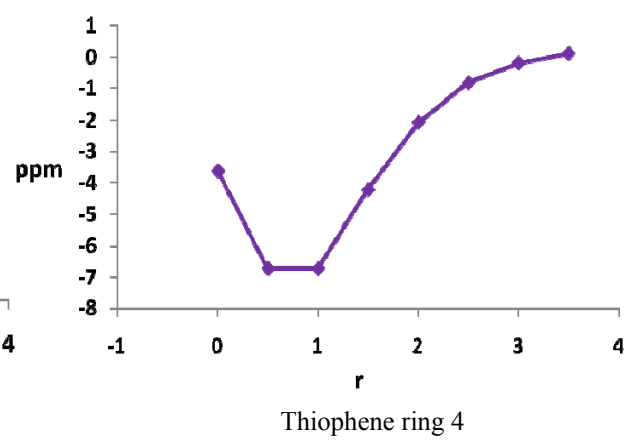
Thiophene ring 1



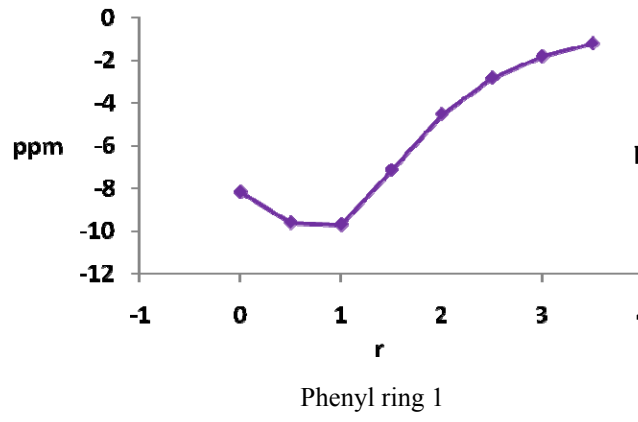
Thiophene ring 2



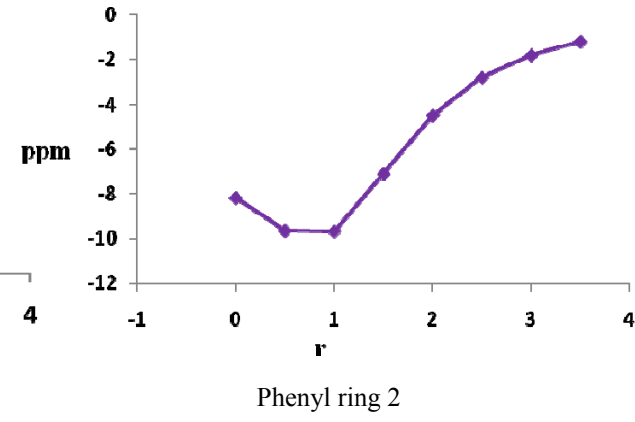
Thiophene ring 3



Thiophene ring 4



Phenyl ring 1



Phenyl ring 2

Figure S37: For **12b** As shown at the top, at the centre of a set of two thiophene rings aromaticity (-ve NICS) is lost at about 1 Å distance and antiaromatic ring current is then observed due to the impact of the main annulene ring. The other set of thiophenes maintain their aromaticity as they points outwards to the annulene core as shown in Fig. S36. They also show a dip at 1 Å which is not shown by a free thiophene ring. The *p*-florophenyl rings shows the normal aromaticity.

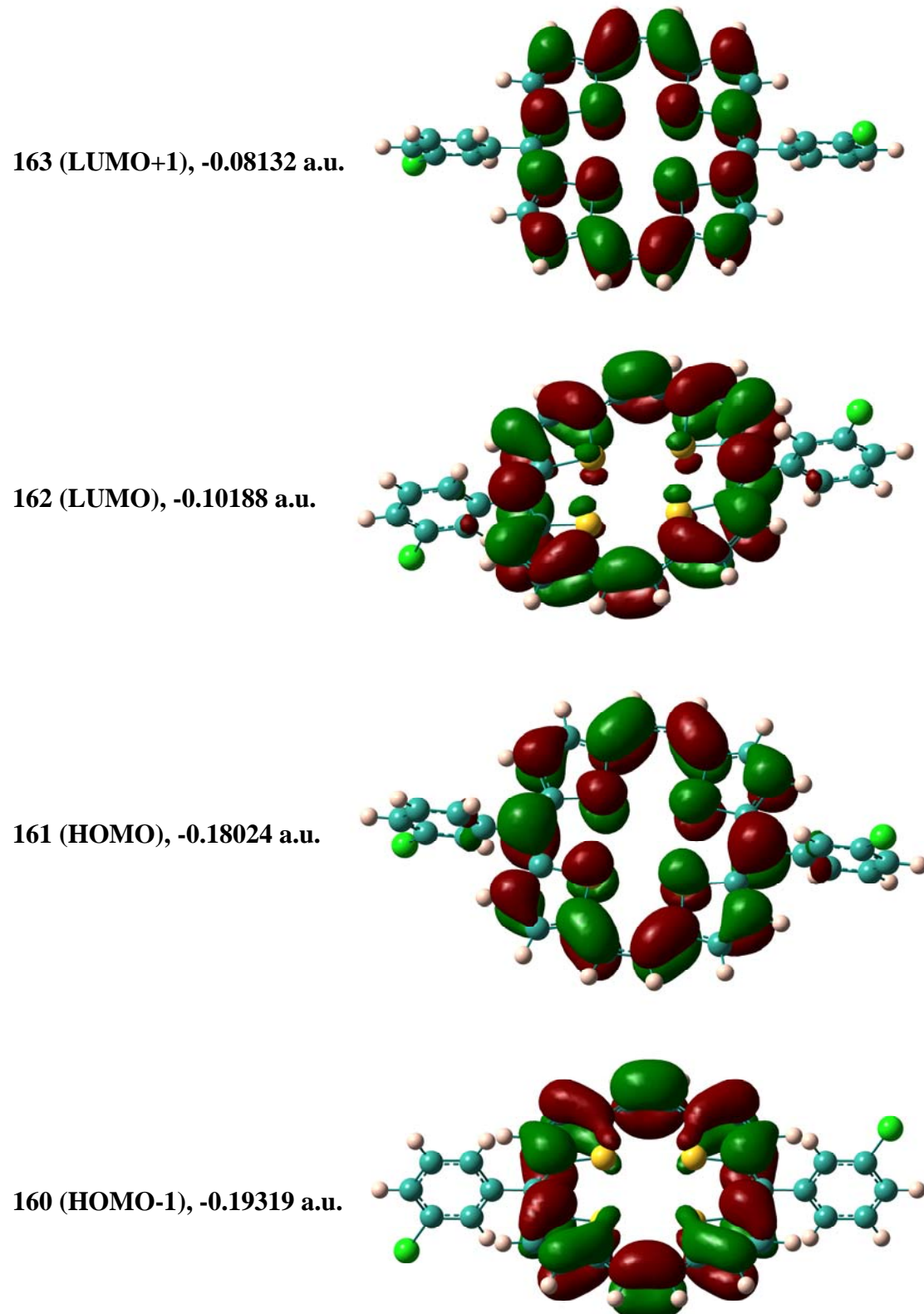


Figure S38: HOMO-LUMO and their neighbouring energy levels for **11a** are shown along with their energies (left) in a.u. HOMO - LUMO levels are showing high degree of delocalisation on the 22π annulene ring periphery. The energy of HOMO = -0.18024 a.u. and that of LUMO = -0.10188 a.u.

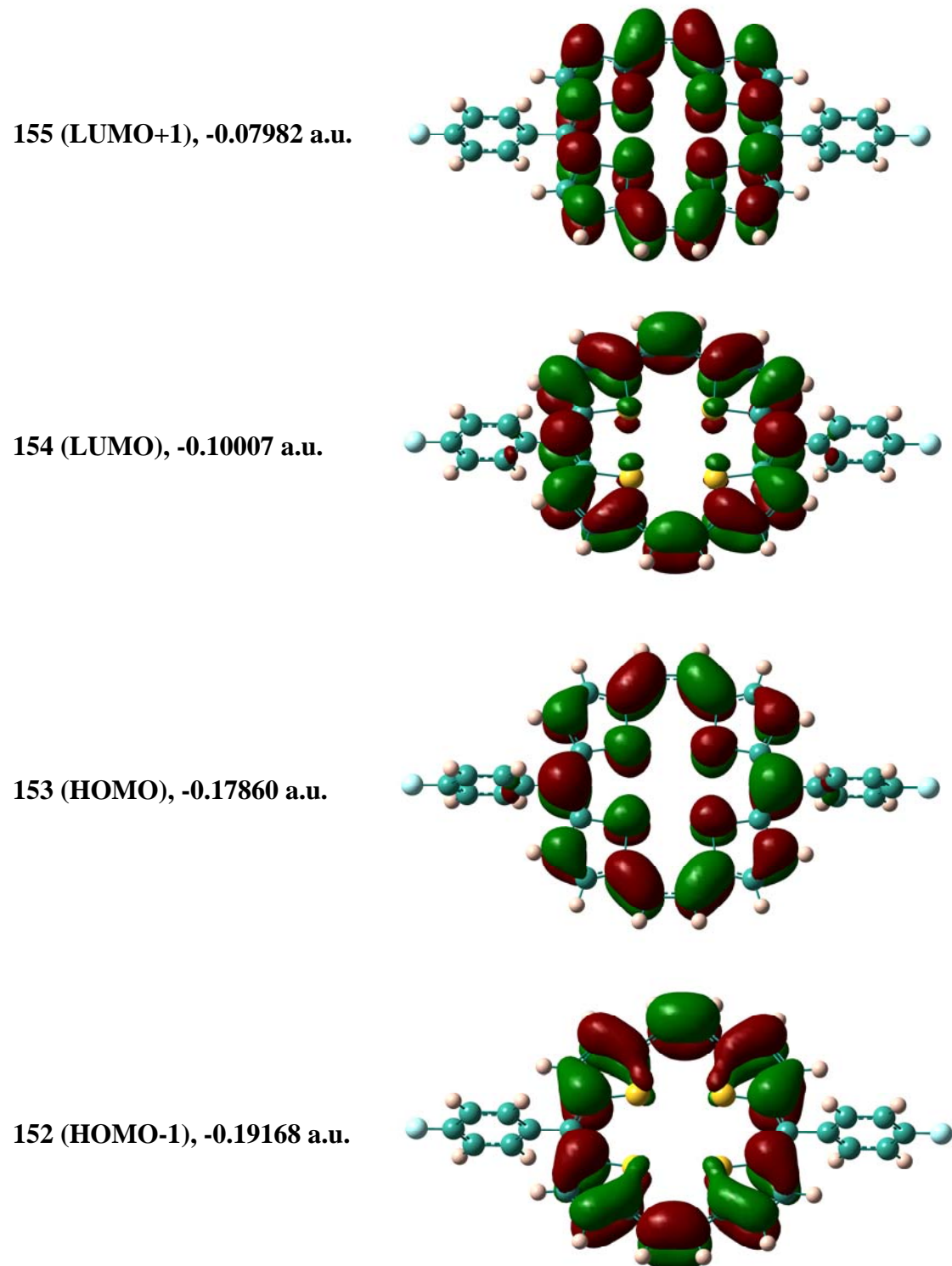


Figure S39: HOMO-LUMO and their neighbouring energy levels for **11b** are shown along with their energies (left) in a.u. HOMO - LUMO levels are showing high degree of delocalisation on the 22π annulene ring periphery. The energy of HOMO = -0.17860 a.u. and that of LUMO = -0.10007 a.u..

Cartesian coordinates

Table S1: Cartesian coordinates of **11a**

SCF Done: E (RB3LYP) = -3821.16360453 a.u..

Center Number	Atomic Number	Atomic Type	Coordinates (Angstroms)		
			X	Y	Z
1	16	0	1.531384	1.550566	-0.136219
2	6	0	0.616009	4.241159	0.058379
3	6	0	1.655553	3.304537	-0.070987
4	6	0	3.019430	3.663395	-0.166820
5	1	0	3.331399	4.701394	-0.145682
6	6	0	3.894801	2.605820	-0.278562
7	1	0	4.967675	2.721984	-0.352155
8	6	0	3.278349	1.330467	-0.282769
9	6	0	3.922479	0.082407	-0.377136
10	6	0	5.417280	0.114888	-0.530463
11	6	0	6.001194	0.338373	-1.781666
12	1	0	5.364074	0.488042	-2.646428
13	6	0	7.387040	0.365558	-1.917886
14	1	0	7.832552	0.537041	-2.892251
15	6	0	8.211885	0.171465	-0.812425
16	1	0	1.009752	5.255799	0.060949
17	16	0	1.593335	-1.485276	-0.161228
18	6	0	0.770346	-4.212211	-0.189886
19	6	0	1.775879	-3.232787	-0.254923
20	6	0	3.146930	-3.534363	-0.419886
21	1	0	3.492342	-4.558717	-0.500783
22	6	0	3.982748	-2.440916	-0.474073
23	1	0	5.054065	-2.512847	-0.604389
24	6	0	3.325642	-1.192153	-0.349837
25	6	0	6.241901	-0.079660	0.582697
26	1	0	5.806569	-0.250874	1.559851
27	6	0	7.623798	-0.049276	0.428309
28	1	0	1.198289	-5.209666	-0.270588
29	16	0	-1.531384	-1.550563	0.136208
30	6	0	-0.616009	-4.241156	-0.058386
31	6	0	-1.655553	-3.304534	0.070984
32	6	0	-3.019429	-3.663392	0.166826
33	1	0	-3.331398	-4.701391	0.145693
34	6	0	-3.894799	-2.605816	0.278569
35	1	0	-4.967673	-2.721981	0.352170
36	6	0	-3.278348	-1.330464	0.282768
37	6	0	-3.922478	-0.082405	0.377133
38	6	0	-5.417278	-0.114886	0.530466
39	6	0	-6.001185	-0.338356	1.781675
40	1	0	-5.364062	-0.488017	2.646436
41	6	0	-7.387030	-0.365540	1.917902

42	1	0	-7.832538	-0.537012	2.892271
43	6	0	-8.211881	-0.171459	0.812443
44	1	0	-1.009752	-5.255797	-0.060953
45	16	0	-1.593334	1.485278	0.161222
46	6	0	-0.770347	4.212213	0.189875
47	6	0	-1.775879	3.232789	0.254911
48	6	0	-3.146931	3.534365	0.419869
49	1	0	-3.492344	4.558719	0.500760
50	6	0	-3.982748	2.440918	0.474058
51	1	0	-5.054066	2.512849	0.604371
52	6	0	-3.325642	1.192155	0.349828
53	6	0	-6.241904	0.079649	-0.582691
54	1	0	-5.806577	0.250852	-1.559850
55	6	0	-7.623801	0.049267	-0.428296
56	1	0	-1.198290	5.209668	0.270573
57	1	0	9.290710	0.190275	-0.908948
58	1	0	-9.290705	-0.190267	0.908971
59	17	0	8.650456	-0.294641	1.837998
60	17	0	-8.650465	0.294616	-1.837983

Table S2: Cartesian coordinates of **11b**

SCF Done: E (RB3LYP) = -3100.44898875 a.u.

Center Numbe	Atomic Number	Atomic Type	Coordinates (Angstroms)		
			X	Y	Z
1	16	0	1.517613	0.000059	1.569273
2	6	0	4.229223	0.000182	0.696513
3	6	0	3.270420	0.000137	1.723818
4	6	0	3.601244	0.000139	3.098206
5	1	0	4.633765	0.000177	3.428694
6	6	0	2.524907	0.000086	3.957796
7	1	0	2.618636	0.000076	5.035369
8	6	0	1.261141	0.000042	3.317893
9	6	0	0.000000	0.000000	3.942829
10	6	0	0.000000	0.000000	5.445866
11	6	0	0.000000	-1.203883	6.159156
12	1	0	-0.000012	-2.143791	5.617619
13	6	0	0.000002	-1.212480	7.552237
14	1	0	-0.000004	-2.138853	8.115171

15	6	0	0.000000	0.000000	8.224963
16	1	0	5.236320	0.000224	1.109286
17	16	0	-1.517613	-0.000060	1.569273
18	6	0	-4.229223	-0.000182	0.696513
19	6	0	-3.270420	-0.000137	1.723818
20	6	0	-3.601244	-0.000139	3.098206
21	1	0	-4.633765	-0.000177	3.428694
22	6	0	-2.524907	-0.000086	3.957796
23	1	0	-2.618636	-0.000076	5.035369
24	6	0	-1.261141	-0.000042	3.317893
25	6	0	0.000000	1.203883	6.159156
26	1	0	0.000012	2.143791	5.617619
27	6	0	-0.000002	1.212481	7.552237
28	1	0	0.000004	2.138854	8.115170
29	1	0	-5.236320	-0.000225	1.109286
30	16	0	-1.517613	-0.000060	-1.569273
31	6	0	-4.229223	-0.000182	-0.696513
32	6	0	-3.270420	-0.000137	-1.723818
33	6	0	-3.601244	-0.000139	-3.098206
34	1	0	-4.633765	-0.000177	-3.428694
35	6	0	-2.524907	-0.000086	-3.957796
36	1	0	-2.618636	-0.000076	-5.035369
37	6	0	-1.261141	-0.000042	-3.317893
38	6	0	0.000000	0.000000	-3.942829
39	6	0	0.000000	0.000000	-5.445866
40	6	0	0.000000	1.203883	-6.159156
41	1	0	0.000012	2.143791	-5.617619
42	6	0	-0.000002	1.212481	-7.552237
43	1	0	0.000004	2.138854	-8.115170
44	6	0	0.000000	0.000000	-8.224963
45	1	0	-5.236320	-0.000225	-1.109286
46	16	0	1.517613	0.000059	-1.569273
47	6	0	4.229223	0.000182	-0.696513
48	6	0	3.270420	0.000137	-1.723818
49	6	0	3.601244	0.000139	-3.098206
50	1	0	4.633765	0.000177	-3.428694
51	6	0	2.524907	0.000086	-3.957796
52	1	0	2.618636	0.000076	-5.035369
53	6	0	1.261141	0.000042	-3.317893
54	6	0	0.000000	-1.203883	-6.159156
55	1	0	-0.000012	-2.143791	-5.617619
56	6	0	0.000002	-1.212480	-7.552237
57	1	0	-0.000004	-2.138853	-8.115171
58	1	0	5.236320	0.000224	-1.109286
59	9	0	0.000000	0.000000	9.576524
60	9	0	0.000000	0.000000	-9.576524

Table S3: Cartesian coordinates of **12b**

SCF Done: E (RB3LYP) = -3099.91380272 a.u.

Center Number	Atomic Number	Atomic Type	Coordinates (Angstroms)		
			X	Y	Z
1	16	0	-1.633314	-1.552067	0.436315
2	6	0	-0.679356	-4.224876	0.095413
3	6	0	-1.715469	-3.224541	-0.023758
4	6	0	-2.981453	-3.533913	-0.527206
5	1	0	-3.238239	-4.526589	-0.874831
6	6	0	-3.847072	-2.448196	-0.576672
7	1	0	-4.841726	-2.495129	-0.997932
8	6	0	-3.294427	-1.257893	-0.083724
9	6	0	-3.959290	0.000000	-0.000004
10	6	0	-5.421555	0.000000	0.000000
11	6	0	-6.144183	0.925401	-0.790573
12	1	0	-5.611147	1.612479	-1.436648
13	6	0	-7.526729	0.915908	-0.806892
14	1	0	-8.093450	1.592083	-1.435653
15	6	0	-8.200984	0.000000	0.000009
16	1	0	-1.108067	-5.223936	0.098060
17	16	0	-1.633316	1.552066	-0.436338
18	6	0	-0.679357	4.224876	-0.095447
19	6	0	-1.715469	3.224540	0.023734
20	6	0	-2.981449	3.533913	0.527189
21	1	0	-3.238234	4.526589	0.874815
22	6	0	-3.847068	2.448196	0.576663
23	1	0	-4.841719	2.495129	0.997930
24	6	0	-3.294426	1.257892	0.083712
25	6	0	-6.144178	-0.925401	0.790580
26	1	0	-5.611138	-1.612479	1.436650
27	6	0	-7.526724	-0.915908	0.806906
28	1	0	-8.093441	-1.592084	1.435670

29	1	0	-1.108068	5.223936	-0.098106
30	16	0	1.633317	1.552066	-0.436334
31	6	0	0.679356	4.224876	-0.095446
32	6	0	1.715468	3.224540	0.023738
33	6	0	2.981447	3.533914	0.527196
34	1	0	3.238230	4.526590	0.874822
35	6	0	3.847066	2.448197	0.576672
36	1	0	4.841716	2.495131	0.997941
37	6	0	3.294425	1.257893	0.083720
38	6	0	3.959290	0.000001	0.000006
39	6	0	5.421555	0.000001	0.000014
40	6	0	6.144176	-0.925401	0.790594
41	1	0	5.611134	-1.612478	1.436664
42	6	0	7.526722	-0.915908	0.806924
43	1	0	8.093437	-1.592084	1.435690
44	6	0	8.200984	0.000000	0.000029
45	1	0	1.108067	5.223936	-0.098103
46	16	0	1.633314	-1.552067	0.436320
47	6	0	0.679357	-4.224876	0.095414
48	6	0	1.715470	-3.224540	-0.023754
49	6	0	2.981455	-3.533912	-0.527200
50	1	0	3.238242	-4.526588	-0.874825
51	6	0	3.847074	-2.448195	-0.576664
52	1	0	4.841728	-2.495128	-0.997922
53	6	0	3.294427	-1.257892	-0.083716
54	6	0	6.144185	0.925402	-0.790559
55	1	0	5.611151	1.612480	-1.436634
56	6	0	7.526731	0.915908	-0.806874
57	1	0	8.093454	1.592083	-1.435633
58	1	0	1.108068	-5.223936	0.098062
59	9	0	-9.527029	0.000000	0.000013
60	9	0	9.527029	0.000000	0.000036

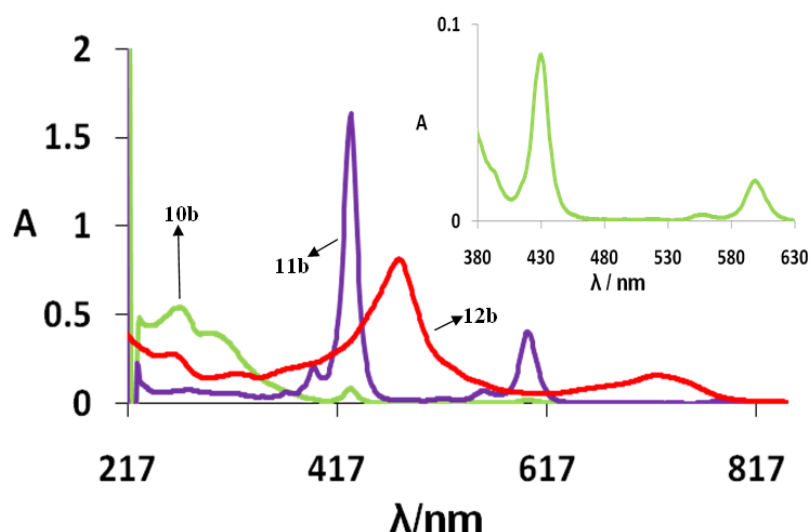


Figure S40: UV-Vis. spectra of **10b** (DCM), **11b** (DCM) and **12b** (H_2SO_4). (Inset shows the partial auto-oxidation of the **10b** into **11b**)

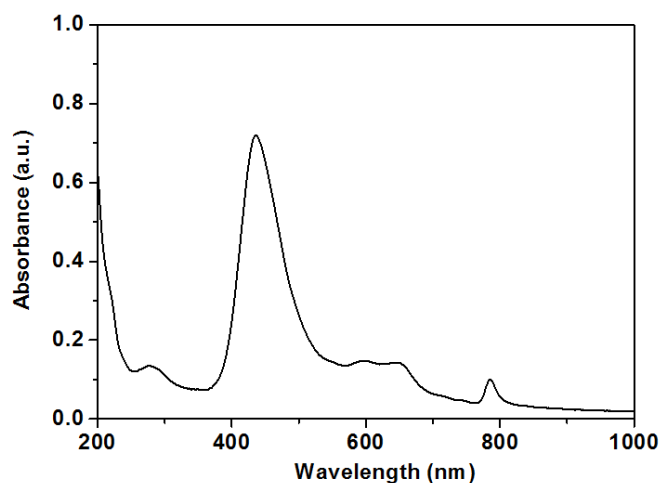


Figure S40a: UV-Vis. spectra of thin film of **11a**.

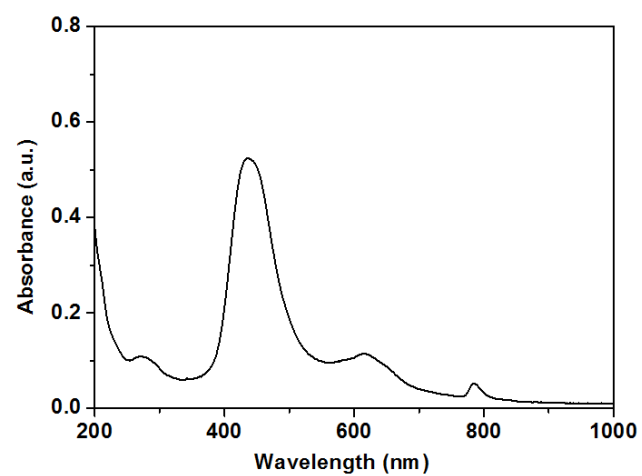


Figure S40b: UV-Vis. spectra of thin film of **11b**.

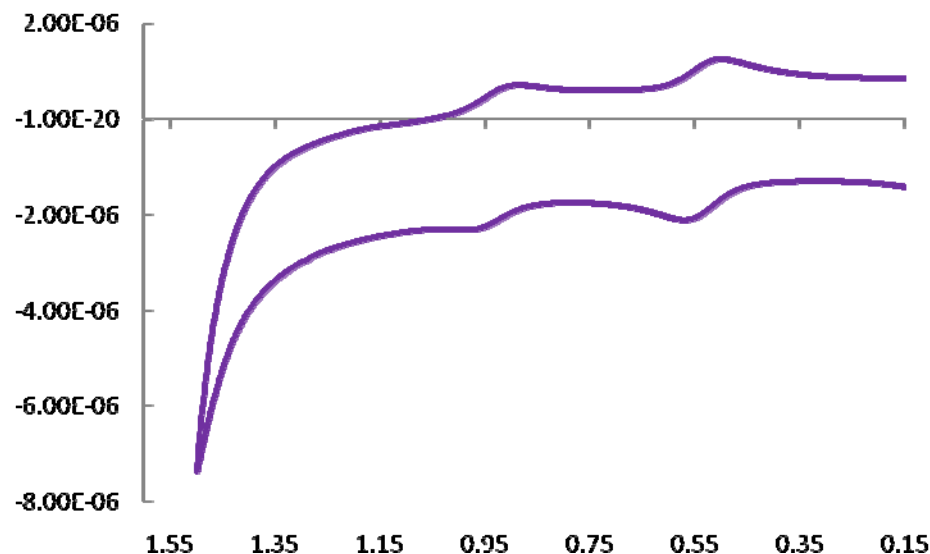


Figure S41: Cyclic voltammogram (CV) for **11b** (DCM, electrolyte TBAPF₆; working electrode: Pt; ref. electrode: Ag/AgCl; Scan rate 100 mV s⁻¹.

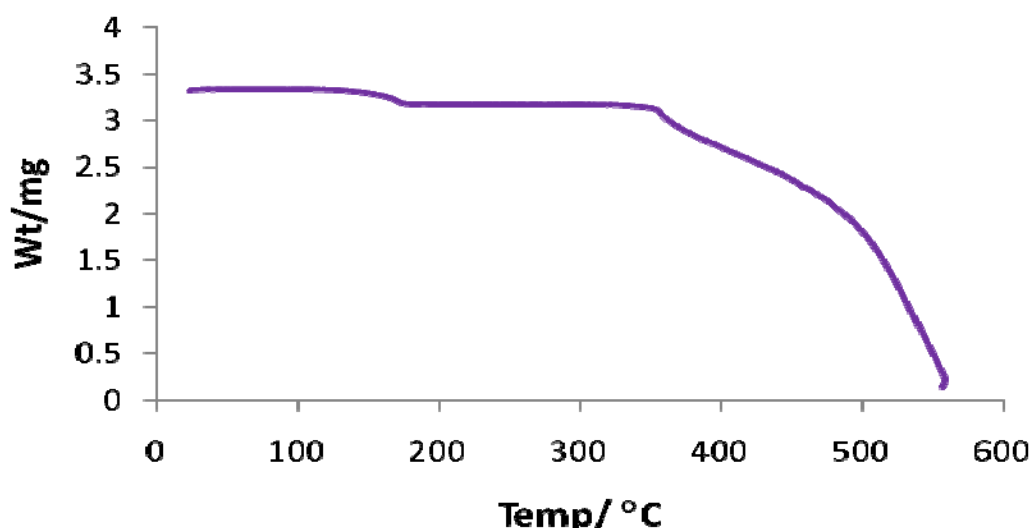


Figure S42: TGA Analysis of **11a** under N₂ with temperature rise of 10°C per minute. Thus**11a** is highly stable as it is having a high thermal decomposition temp. of about >355°C.

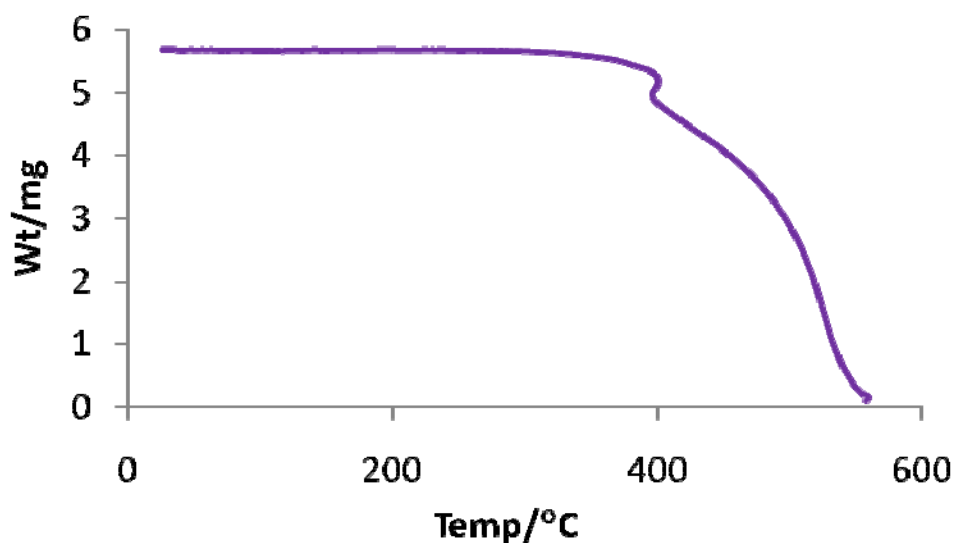


Figure S43: TGA Analysis of **11b** under N₂ with temperature rise of 10°C per minute. Thus**11b** is highly stable as it is having a high thermal decomposition temp. of about >355°C.

X-Ray Diffraction Analysis of 11a:

Single crystals of **11a** suitable for an X-Ray crystal structure determination were grown in a dark, quiet and undisturbed place from dry DCM with a toluene layer upon it (2 weeks).

Table S4: The crystallographic data for **11a**.

Empirical formula	C ₁₃₆ H ₈₀ Cl ₈ S ₁₆
Formula weight	2510.56
Temperature	150(2) K
Wavelength	1.54180 Å
Crystal system, space group	Orthorhombic, F d d 2
Unit cell dimensions	a = 60.299(6) Å alpha = 90 deg. b = 19.5214(15) Å beta = 90 deg. c = 9.5973(8) Å gamma = 90 deg.
Volume	11297.2(17) Å ³
Z, Calculated density	4, 1.476 Mg/m ³
Absorption coefficient	5.018 mm ⁻¹
F(000)	5152
Crystal size	0.23 x 0.18 x 0.14 mm
Theta range for data collection	2.93 to 72.40 deg.
Limiting indices	-72<=h<=73, -22<=k<=23, -9<=l<=11
Reflections collected / unique	19859 / 4940 [R(int) = 0.0462]
Completeness to theta = 72.40	99.3 %
Absorption correction	Semi-empirical from equivalents
Max. and min. transmission	0.5401 and 0.3915
Refinement method	Full-matrix least-squares on F ²
Data / restraints / parameters	4940 / 1 / 361
Goodness-of-fit on F ²	1.072
Final R indices [I>2sigma(I)]	R1 = 0.0503, wR2 = 0.1381

R indices (all data)

R1 = 0.0529, wR2 = 0.1411

Absolute structure parameter

0.00(2)

Largest diff. peak and hole

0.397 and -0.321 e.A^-3

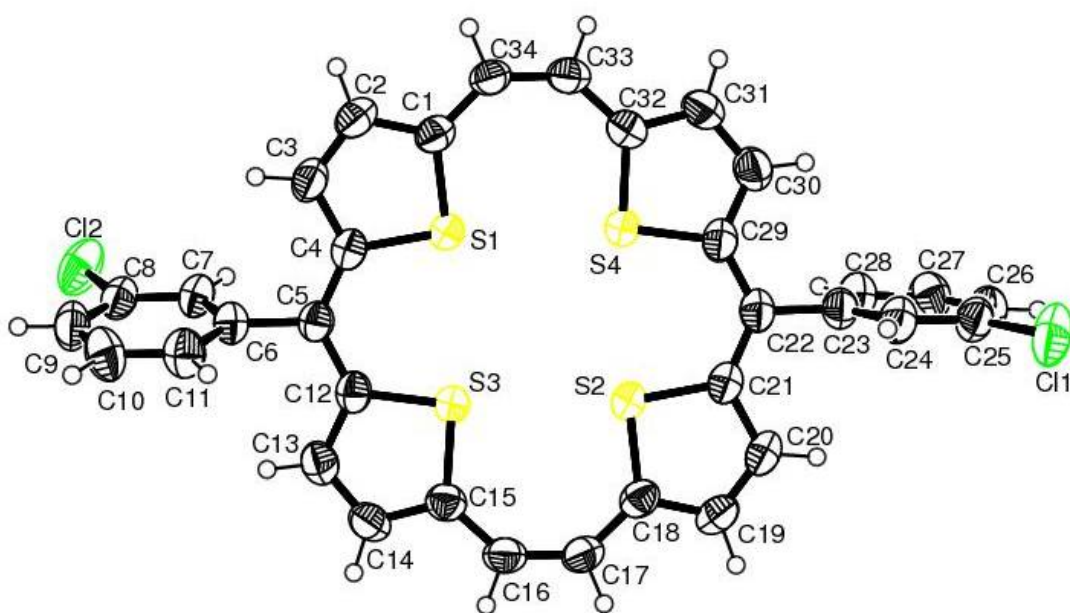


Table S5: Torsion angles [deg] for **11a**.

C(4)-S(1)-C(1)-C(34)	-176.7(4)
C(4)-S(1)-C(1)-C(2)	-0.2(3)
C(34)-C(1)-C(2)-C(3)	176.9(4)
S(1)-C(1)-C(2)-C(3)	0.1(5)
C(1)-C(2)-C(3)-C(4)	0.0(6)
C(2)-C(3)-C(4)-C(5)	179.3(4)
C(2)-C(3)-C(4)-S(1)	-0.1(5)
C(1)-S(1)-C(4)-C(5)	-179.3(3)
C(1)-S(1)-C(4)-C(3)	0.1(3)
C(3)-C(4)-C(5)-C(12)	-173.0(4)
S(1)-C(4)-C(5)-C(12)	6.3(6)
C(3)-C(4)-C(5)-C(6)	7.0(6)
S(1)-C(4)-C(5)-C(6)	-173.8(3)
C(4)-C(5)-C(6)-C(7)	69.9(5)
C(12)-C(5)-C(6)-C(7)	-110.1(5)
C(4)-C(5)-C(6)-C(11)	-110.1(5)
C(12)-C(5)-C(6)-C(11)	69.9(5)
C(11)-C(6)-C(7)-C(8)	0.0(7)
C(5)-C(6)-C(7)-C(8)	180.0(4)
C(6)-C(7)-C(8)-C(9)	0.6(7)
C(6)-C(7)-C(8)-Cl(2)	-178.5(4)
C(7)-C(8)-C(9)-C(10)	-0.5(8)
Cl(2)-C(8)-C(9)-C(10)	178.6(4)
C(8)-C(9)-C(10)-C(11)	-0.1(9)

C(9)-C(10)-C(11)-C(6)	0.7(9)
C(7)-C(6)-C(11)-C(10)	-0.6(8)
C(5)-C(6)-C(11)-C(10)	179.4(5)
C(4)-C(5)-C(12)-C(13)	-178.1(4)
C(6)-C(5)-C(12)-C(13)	1.9(6)
C(4)-C(5)-C(12)-S(3)	2.7(6)
C(6)-C(5)-C(12)-S(3)	-177.2(3)
C(15)-S(3)-C(12)-C(13)	-1.3(3)
C(15)-S(3)-C(12)-C(5)	178.1(3)
C(5)-C(12)-C(13)-C(14)	-178.0(4)
S(3)-C(12)-C(13)-C(14)	1.3(5)
C(12)-C(13)-C(14)-C(15)	-0.7(6)
C(13)-C(14)-C(15)-C(16)	-179.5(4)
C(13)-C(14)-C(15)-S(3)	-0.3(5)
C(12)-S(3)-C(15)-C(16)	-179.9(4)
C(12)-S(3)-C(15)-C(14)	0.9(3)
C(14)-C(15)-C(16)-C(17)	179.3(5)
S(3)-C(15)-C(16)-C(17)	0.3(8)
C(15)-C(16)-C(17)-C(18)	-0.1(10)
C(16)-C(17)-C(18)-C(19)	-173.0(5)
C(16)-C(17)-C(18)-S(2)	3.0(8)
C(21)-S(2)-C(18)-C(19)	4.1(3)
C(21)-S(2)-C(18)-C(17)	-172.3(4)
C(17)-C(18)-C(19)-C(20)	173.2(4)
S(2)-C(18)-C(19)-C(20)	-3.4(5)
C(18)-C(19)-C(20)-C(21)	0.6(6)
C(19)-C(20)-C(21)-C(22)	-173.1(4)
C(19)-C(20)-C(21)-S(2)	2.5(5)
C(18)-S(2)-C(21)-C(22)	171.9(4)
C(18)-S(2)-C(21)-C(20)	-3.8(3)
C(20)-C(21)-C(22)-C(29)	175.4(4)
S(2)-C(21)-C(22)-C(29)	0.5(6)
C(20)-C(21)-C(22)-C(23)	0.5(6)
S(2)-C(21)-C(22)-C(23)	-174.4(3)
C(21)-C(22)-C(23)-C(24)	-78.5(6)
C(29)-C(22)-C(23)-C(24)	105.9(5)
C(21)-C(22)-C(23)-C(28)	100.8(5)
C(29)-C(22)-C(23)-C(28)	-74.7(6)
C(28)-C(23)-C(24)-C(25)	-1.2(7)
C(22)-C(23)-C(24)-C(25)	178.2(4)
C(23)-C(24)-C(25)-C(26)	-0.9(8)
C(23)-C(24)-C(25)-Cl(1)	-179.9(4)
C(24)-C(25)-C(26)-C(27)	1.8(8)
Cl(1)-C(25)-C(26)-C(27)	-179.2(4)
C(25)-C(26)-C(27)-C(28)	-0.6(8)
C(26)-C(27)-C(28)-C(23)	-1.4(8)
C(24)-C(23)-C(28)-C(27)	2.3(8)
C(22)-C(23)-C(28)-C(27)	-177.0(5)
C(21)-C(22)-C(29)-C(30)	-177.7(4)
C(23)-C(22)-C(29)-C(30)	-2.8(7)
C(21)-C(22)-C(29)-S(4)	0.7(6)
C(23)-C(22)-C(29)-S(4)	175.6(3)
C(32)-S(4)-C(29)-C(22)	-178.0(4)
C(32)-S(4)-C(29)-C(30)	0.7(4)
C(22)-C(29)-C(30)-C(31)	178.4(4)
S(4)-C(29)-C(30)-C(31)	-0.2(5)
C(29)-C(30)-C(31)-C(32)	-0.4(7)
C(30)-C(31)-C(32)-C(33)	177.0(4)

C(30)-C(31)-C(32)-S(4)	0.9(6)
C(29)-S(4)-C(32)-C(33)	-176.7(4)
C(29)-S(4)-C(32)-C(31)	-0.9(4)
C(31)-C(32)-C(33)-C(34)	-179.4(5)
S(4)-C(32)-C(33)-C(34)	-4.2(8)
C(32)-C(33)-C(34)-C(1)	-7.9(10)
C(2)-C(1)-C(34)-C(33)	-177.8(5)
S(1)-C(1)-C(34)-C(33)	-1.7(8)

The crystal structure has been deposited at the Cambridge Crystallographic Data Centre (CCDC 900288). The data can be obtained free of charge via the Internet at www.ccdc.cam.ac.uk/data_request/cif.

Device Fabrication:

Experimental:

OFET devices were fabricated in the top-contact device configuration. The substrate was heavily doped, n-type Si gate electrode with a 500 nm thick SiO₂ layer as the gate dielectric. The gate dielectric was treated with octadecyltrichlorosilane (OTS) by vapor deposition method. Subsequently, organic semiconductors were deposited on the substrate by thermal evaporation under a pressure of 8×10^{-4} Pa at a deposition rate gradually increased from 0.1 Å s⁻¹ to 0.4 Å s⁻¹ at the first 20 nm and then maintained 0.5 Å s⁻¹ until the thickness of the film was 50 nm. The deposition rate and film thickness were monitored by a quartz crystal microbalance (ULVAC CRTM-6000). Finally, 20 nm thick gold source and drain electrode were deposited through a shadow mask. The channel length (*L*) and width (*W*) were 0.11 mm and 5.30 mm, respectively. The FET characteristics were measured at room temperature in air using Keithley 4200 SCS. Atomic force microscopy (AFM) measurements were carried out with a Nanoscope IIIa instrument (Digital Instruments) operating in tapping mode. UV-Vis spectra were recorded on a JASCO V-570 spectrometer.

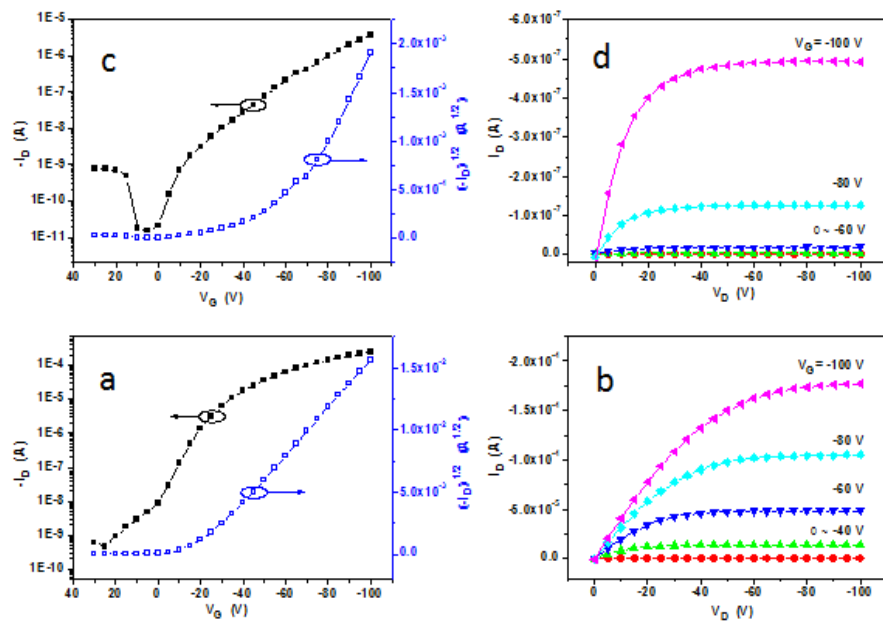


Figure S44: Typical transfer (a) and output (b) characteristics of FET devices based on **11a**, with OTS-treated SiO_2/Si substrate ($T_s = 100\text{ }^\circ\text{C}$). Typical transfer (c) and output (d) characteristics of FET devices based on **11b**, with OTS-treated SiO_2/Si substrate ($T_s = 100\text{ }^\circ\text{C}$).

CIF Files for **11a**:

```
data_gnu005

_audit_creation_method           SHELXL-97
_chemical_name_systematic;
;
?
;
_chemical_name_common           ?
_chemical_melting_point        ?
_chemical_formula_moiety       ?
_chemical_formula_sum          'C136 H80 Cl8 S16'
_chemical_formula_weight        2510.56

loop_
_atom_type_symbol
_atom_type_description
_atom_type_scat_dispersion_real
_atom_type_scat_dispersion_imag
_atom_type_scat_source
'C'   'C'   0.0181   0.0091
'International Tables Vol C Tables 4.2.6.8 and 6.1.1.4'
'H'   'H'   0.0000   0.0000
'International Tables Vol C Tables 4.2.6.8 and 6.1.1.4'
'Cl'   'Cl'   0.3639   0.7018
'International Tables Vol C Tables 4.2.6.8 and 6.1.1.4'
'S'   'S'   0.3331   0.5567
'International Tables Vol C Tables 4.2.6.8 and 6.1.1.4'

_symmetry_cell_setting         'Orthorhombic'
_symmetry_space_group_name_H-M  'F d d 2'

loop_
_symmetry_equiv_pos_as_xyz
'x, y, z'
'-x, -y, z'
'x+1/4, -y+1/4, z+1/4'
'-x+1/4, y+1/4, z+1/4'
'x, y+1/2, z+1/2'
'-x, -y+1/2, z+1/2'
'x+1/4, -y+3/4, z+3/4'
'-x+1/4, y+3/4, z+3/4'
'x+1/2, y, z+1/2'
'-x+1/2, -y, z+1/2'
'x+3/4, -y+1/4, z+3/4'
'-x+3/4, y+1/4, z+3/4'
'x+1/2, y+1/2, z'
'-x+1/2, -y+1/2, z'
'x+3/4, -y+3/4, z+1/4'
'-x+3/4, y+3/4, z+1/4'

_cell_length_a                 60.299(6)
_cell_length_b                 19.5214(15)
_cell_length_c                 9.5973(8)
_cell_angle_alpha              90.00
_cell_angle_beta               90.00
```

_cell_angle_gamma 90.00
_cell_volume 11297.2(17)
_cell_formula_units_Z 4
_cell_measurement_temperature 150(2)
_cell_measurement_reflns_used 8176
_cell_measurement_theta_min 2.9328
_cell_measurement_theta_max 72.2146

_exptl_crystal_description BLOCK
_exptl_crystal_colour BLACK
_exptl_crystal_size_max 0.23
_exptl_crystal_size_mid 0.18
_exptl_crystal_size_min 0.14
_exptl_crystal_density_meas ?
_exptl_crystal_density_diffrn 1.476
_exptl_crystal_density_method 'not measured'
_exptl_crystal_F_000 5152
_exptl_absorpt_coefficient_mu 5.018
_exptl_absorpt_correction_T_min 0.3915
_exptl_absorpt_correction_T_max 0.5401
_exptl_absorpt_correction_type multi-scan
_exptl_absorpt_process_details ;
(CrysAlis RED; Oxford Diffraction, 2009)
;

_diffrn_ambient_temperature 150(2)
_diffrn_radiation_wavelength 1.54180
_diffrn_radiation_type CuK\alpha
_diffrn_radiation_source 'Micro-Focus (Cu) X-ray Source'
_diffrn_radiation_monochromator graphite
_diffrn_measurement_device_type 'OXFORD DIFFRACTION SUPER NOVA'
_diffrn_measurement_method '\w/q-scan'
_diffrn_detector_area_resol_mean 15.9948
_diffrn_standards_number ?
_diffrn_standards_interval_count ?
_diffrn_standards_interval_time ?
_diffrn_standards_decay_% ?
_diffrn_reflns_number 19859
_diffrn_reflns_av_R_equivalents 0.0462
_diffrn_reflns_av_sigmaI/netI 0.0312
_diffrn_reflns_limit_h_min -72
_diffrn_reflns_limit_h_max 73
_diffrn_reflns_limit_k_min -22
_diffrn_reflns_limit_k_max 23
_diffrn_reflns_limit_l_min -9
_diffrn_reflns_limit_l_max 11
_diffrn_reflns_theta_min 2.93
_diffrn_reflns_theta_max 72.40
_reflns_number_total 4940
_reflns_number_gt 4655
_reflns_threshold_expression >2sigma(I)

_computing_data_collection 'CrysAlis CCD, Oxford Diffraction
Ltd.,'
_computing_cell_refinement 'CrysAlis RED, Oxford Diffraction
Ltd.,'

```
_computing_data_reduction      'CrysAlis RED, Oxford Diffraction
Ltd., '
_computing_structure_solution  'SHELXS-97 (Sheldrick, 1997)'
_computing_structure_refinement 'SHELXL-97 (Sheldrick, 1997)'
_computing_molecular_graphics   'Ortep3'
_computing_publication_material 'Shelx97'

_refine_special_details
;
    Refinement of F^2^ against ALL reflections. The weighted R-factor wR
and
    goodness of fit S are based on F^2^, conventional R-factors R are
based
    on F, with F set to zero for negative F^2^. The threshold expression
of
    F^2^ > 2sigma(F^2^) is used only for calculating R-factors(gt) etc.
and is
    not relevant to the choice of reflections for refinement. R-factors
based
    on F^2^ are statistically about twice as large as those based on F,
and R-
    factors based on ALL data will be even larger.
;

_refine_ls_structure_factor_coef  Fsqd
_refine_ls_matrix_type           full
_refine_ls_weighting_scheme      calc
_refine_ls_weighting_details
    'calc w=1/[s^2^(Fo^2^)+(0.0970P)^2^+9.1277P] where
P=(Fo^2^+2Fc^2^)/3'
_atom_sites_solution_primary     direct
_atom_sites_solution_secondary   difmap
_atom_sites_solution_hydrogens   geom
_refine_ls_hydrogen_treatment    riding
_refine_ls_extinction_method    none
_refine_ls_extinction_coef      ?
_refine_ls_abs_structure_details
    'Flack H D (1983), Acta Cryst. A39, 876-881'
_refine_ls_abs_structure_Flack   0.00(2)
_refine_ls_number_reflns         4940
_refine_ls_number_parameters    361
_refine_ls_number_restraints    1
_refine_ls_R_factor_all          0.0529
_refine_ls_R_factor_gt           0.0503
_refine_ls_wR_factor_ref         0.1411
_refine_ls_wR_factor_gt          0.1381
_refine_ls_goodness_of_fit_ref   1.072
_refine_ls_restrained_S_all     1.072
_refine_ls_shift/su_max          0.000
_refine_ls_shift/su_mean         0.000

loop_
_atom_site_label
_atom_site_type_symbol
_atom_site_fract_x
_atom_site_fract_y
_atom_site_fract_z
_atom_site_U_iso_or_equiv
```

_atom_site_adp_type
_atom_site_occupancy
_atom_site_symmetry_multiplicity
_atom_site_calc_flag
_atom_site_refinement_flags
_atom_site_disorder_assembly
_atom_site_disorder_group
S1 S 0.113642(14) 0.37324(5) 0.91723(11) 0.0467(2) Uani 1 1 d . . .
S2 S 0.184951(14) 0.33268(5) 0.90660(11) 0.0474(2) Uani 1 1 d . . .
S3 S 0.145561(15) 0.31985(5) 0.69777(11) 0.0487(2) Uani 1 1 d . . .
S4 S 0.152939(15) 0.39138(6) 1.12089(10) 0.0506(2) Uani 1 1 d . . .
C11 Cl 0.26458(2) 0.34249(9) 1.49820(19) 0.0886(5) Uani 1 1 d . . .
C12 Cl 0.03607(2) 0.42986(8) 0.35524(18) 0.0848(4) Uani 1 1 d . . .
C1 C 0.09336(6) 0.3904(2) 1.0407(5) 0.0477(9) Uani 1 1 d . . .
C2 C 0.07237(7) 0.3775(2) 0.9809(5) 0.0557(10) Uani 1 1 d . . .
H2 H 0.0589 0.3838 1.0307 0.067 Uiso 1 1 calc R . .
C3 C 0.07289(6) 0.3555(2) 0.8470(5) 0.0550(10) Uani 1 1 d . . .
H3 H 0.0599 0.3451 0.7954 0.066 Uiso 1 1 calc R . .
C4 C 0.09426(6) 0.34941(19) 0.7910(5) 0.0455(8) Uani 1 1 d . . .
C5 C 0.09968(6) 0.32730(18) 0.6566(5) 0.0448(8) Uani 1 1 d . . .
C6 C 0.08050(6) 0.3165(2) 0.5599(5) 0.0472(8) Uani 1 1 d . . .
C7 C 0.06835(6) 0.3715(2) 0.5097(5) 0.0505(9) Uani 1 1 d . . .
H7 H 0.0721 0.4169 0.5364 0.061 Uiso 1 1 calc R . .
C8 C 0.05068(6) 0.3599(2) 0.4202(5) 0.0537(9) Uani 1 1 d . . .
C9 C 0.04460(7) 0.2954(3) 0.3802(6) 0.0658(12) Uani 1 1 d . . .
H9 H 0.0324 0.2883 0.3195 0.079 Uiso 1 1 calc R . .
C10 C 0.05682(9) 0.2404(3) 0.4309(6) 0.0706(13) Uani 1 1 d . . .
H10 H 0.0529 0.1951 0.4045 0.085 Uiso 1 1 calc R . .
C11 C 0.07447(8) 0.2503(2) 0.5183(6) 0.0598(11) Uani 1 1 d . . .
H11 H 0.0827 0.2120 0.5509 0.072 Uiso 1 1 calc R . .
C12 C 0.12097(6) 0.31410(18) 0.6021(5) 0.0470(8) Uani 1 1 d . . .
C13 C 0.12608(7) 0.2938(2) 0.4658(5) 0.0548(9) Uani 1 1 d . . .
H13 H 0.1152 0.2883 0.3954 0.066 Uiso 1 1 calc R . .
C14 C 0.14810(7) 0.2825(2) 0.4432(5) 0.0560(9) Uani 1 1 d . . .
H14 H 0.1537 0.2680 0.3554 0.067 Uiso 1 1 calc R . .
C15 C 0.16194(7) 0.2936(2) 0.5582(5) 0.0501(9) Uani 1 1 d . . .
C16 C 0.18499(7) 0.2850(2) 0.5536(5) 0.0557(10) Uani 1 1 d . . .
H16 H 0.1898 0.2704 0.4642 0.067 Uiso 1 1 calc R . .
C17 C 0.20254(6) 0.2921(2) 0.6447(5) 0.0552(10) Uani 1 1 d . . .
H17 H 0.2163 0.2811 0.6019 0.066 Uiso 1 1 calc R . .
C18 C 0.20531(6) 0.31158(19) 0.7848(5) 0.0492(9) Uani 1 1 d . . .
C19 C 0.22626(6) 0.3210(2) 0.8462(6) 0.0570(10) Uani 1 1 d . . .
H19 H 0.2397 0.3100 0.7993 0.068 Uiso 1 1 calc R . .
C20 C 0.22593(6) 0.3468(2) 0.9773(5) 0.0566(11) Uani 1 1 d . . .
H20 H 0.2390 0.3558 1.0291 0.068 Uiso 1 1 calc R . .
C21 C 0.20435(6) 0.3593(2) 1.0305(5) 0.0486(9) Uani 1 1 d . . .
C22 C 0.19909(6) 0.3919(2) 1.1558(5) 0.0508(9) Uani 1 1 d . . .
C23 C 0.21852(6) 0.4165(2) 1.2416(5) 0.0523(9) Uani 1 1 d . . .
C24 C 0.23068(7) 0.3722(3) 1.3219(6) 0.0589(10) Uani 1 1 d . . .
H24 H 0.2268 0.3250 1.3275 0.071 Uiso 1 1 calc R . .
C25 C 0.24914(7) 0.3985(3) 1.3968(5) 0.0609(11) Uani 1 1 d . . .
C26 C 0.25502(7) 0.4655(3) 1.3886(6) 0.0672(12) Uani 1 1 d . . .
H26 H 0.2677 0.4819 1.4373 0.081 Uiso 1 1 calc R . .
C27 C 0.24256(8) 0.5091(3) 1.3097(6) 0.0700(13) Uani 1 1 d . . .
H27 H 0.2465 0.5561 1.3044 0.084 Uiso 1 1 calc R . .
C28 C 0.22424(7) 0.4857(2) 1.2373(5) 0.0611(11) Uani 1 1 d . . .
H28 H 0.2155 0.5168 1.1844 0.073 Uiso 1 1 calc R . .
C29 C 0.17796(6) 0.4090(2) 1.2067(5) 0.0511(9) Uani 1 1 d . . .

C30 C 0.17314(7) 0.4439(3) 1.3311(5) 0.0608(11) Uani 1 1 d . . .
H30 H 0.1843 0.4583 1.3944 0.073 Uiso 1 1 calc R . . .
C31 C 0.15105(8) 0.4553(3) 1.3535(5) 0.0621(11) Uani 1 1 d . . .
H31 H 0.1457 0.4781 1.4343 0.075 Uiso 1 1 calc R . . .
C32 C 0.13680(7) 0.4310(2) 1.2489(5) 0.0504(9) Uani 1 1 d . . .
C33 C 0.11373(7) 0.4355(2) 1.2577(5) 0.0535(9) Uani 1 1 d . . .
H33 H 0.1090 0.4571 1.3413 0.064 Uiso 1 1 calc R . . .
C34 C 0.09596(6) 0.4163(2) 1.1746(5) 0.0521(9) Uani 1 1 d . . .
H34 H 0.0821 0.4223 1.2206 0.062 Uiso 1 1 calc R . . .

loop_
_atom_site_aniso_label
_atom_site_aniso_U_11
_atom_site_aniso_U_22
_atom_site_aniso_U_33
_atom_site_aniso_U_23
_atom_site_aniso_U_13
_atom_site_aniso_U_12

S1 0.0368(4) 0.0591(5) 0.0443(5) -0.0034(4) -0.0015(3) 0.0022(3)
S2 0.0359(4) 0.0573(5) 0.0489(5) -0.0034(4) -0.0029(3) 0.0018(3)
S3 0.0405(4) 0.0598(5) 0.0458(5) -0.0069(4) -0.0033(4) 0.0031(4)
S4 0.0396(4) 0.0676(6) 0.0446(5) -0.0063(4) -0.0029(4) 0.0027(4)
C11 0.0624(7) 0.1088(10) 0.0947(11) 0.0262(9) -0.0300(7) -0.0010(7)
C12 0.0546(6) 0.0986(9) 0.1013(11) 0.0351(8) -0.0167(6) 0.0079(6)
C1 0.0414(18) 0.052(2) 0.049(2) 0.0067(17) 0.0050(16) 0.0029(15)
C2 0.0388(19) 0.066(2) 0.062(3) 0.010(2) 0.0058(17) 0.0032(17)
C3 0.0379(18) 0.069(2) 0.058(3) 0.007(2) -0.0051(17) -0.0058(17)
C4 0.0399(17) 0.0445(18) 0.052(2) 0.0041(16) -0.0057(15) -0.0010(14)
C5 0.0425(17) 0.0427(16) 0.049(2) 0.0029(15) -0.0053(16) 0.0002(13)
C6 0.0456(18) 0.0467(19) 0.049(2) 0.0016(16) -0.0070(17) -0.0059(14)
C7 0.0417(18) 0.052(2) 0.057(2) 0.0077(18) -0.0081(17) -0.0015(15)
C8 0.0412(18) 0.067(2) 0.053(2) 0.012(2) -0.0047(17) -0.0032(16)
C9 0.051(2) 0.087(3) 0.059(3) 0.003(2) -0.014(2) -0.016(2)
C10 0.078(3) 0.063(3) 0.071(3) -0.006(2) -0.016(3) -0.021(2)
C11 0.064(2) 0.045(2) 0.071(3) 0.002(2) -0.009(2) -0.0065(17)
C12 0.0457(18) 0.0442(18) 0.051(2) 0.0027(16) -0.0085(16) 0.0003(14)
C13 0.059(2) 0.055(2) 0.050(2) -0.0021(18) -0.0114(19) 0.0009(17)
C14 0.066(2) 0.058(2) 0.043(2) -0.0075(19) 0.0000(19) 0.0043(18)
C15 0.054(2) 0.0478(19) 0.049(2) -0.0034(17) 0.0015(17) 0.0048(15)
C16 0.055(2) 0.056(2) 0.056(3) -0.0109(19) 0.0095(18) 0.0044(17)
C17 0.0440(18) 0.060(2) 0.062(3) -0.008(2) 0.0066(18) 0.0063(16)
C18 0.0429(18) 0.0437(18) 0.061(3) -0.0024(17) 0.0017(17) 0.0049(14)
C19 0.0391(19) 0.060(2) 0.071(3) -0.002(2) 0.0065(19) 0.0049(15)
C20 0.0365(18) 0.066(2) 0.067(3) 0.005(2) -0.0071(18) 0.0007(16)
C21 0.0395(17) 0.053(2) 0.053(2) 0.0034(17) -0.0057(16) -0.0021(15)
C22 0.0457(19) 0.056(2) 0.051(2) 0.0020(18) -0.0093(17) -0.0067(15)
C23 0.0448(19) 0.064(2) 0.048(2) 0.0003(18) -0.0052(17) -0.0044(17)
C24 0.048(2) 0.068(3) 0.061(3) 0.006(2) -0.0088(19) -0.0056(18)
C25 0.0426(18) 0.083(3) 0.057(3) 0.005(2) -0.0049(19) -0.0047(19)
C26 0.052(2) 0.088(3) 0.062(3) -0.007(3) -0.008(2) -0.010(2)
C27 0.066(3) 0.069(3) 0.075(3) -0.006(3) -0.009(2) -0.015(2)
C28 0.057(2) 0.062(2) 0.065(3) 0.003(2) -0.009(2) -0.0064(19)
C29 0.0440(19) 0.059(2) 0.051(2) 0.0051(19) -0.0082(17) -0.0049(16)
C30 0.057(2) 0.073(3) 0.052(3) -0.007(2) -0.0046(19) -0.0119(19)
C31 0.064(2) 0.073(3) 0.050(3) -0.017(2) 0.0034(19) -0.004(2)
C32 0.056(2) 0.052(2) 0.044(2) -0.0017(17) 0.0014(17) 0.0006(16)
C33 0.056(2) 0.059(2) 0.045(2) -0.0010(18) 0.0091(18) 0.0060(17)
C34 0.0438(18) 0.066(2) 0.047(2) 0.0042(19) 0.0074(16) 0.0099(16)

```
_geom_special_details
;
All esds (except the esd in the dihedral angle between two l.s.
planes)
are estimated using the full covariance matrix. The cell esds are
taken
into account individually in the estimation of esds in distances,
angles
and torsion angles; correlations between esds in cell parameters are
only
used when they are defined by crystal symmetry. An approximate
(isotropic)
treatment of cell esds is used for estimating esds involving l.s.
planes.
;

loop_
_geom_bond_atom_site_label_1
_geom_bond_atom_site_label_2
_geom_bond_distance
_geom_bond_site_symmetry_2
_geom_bond_publ_flag
S1 C1 1.736(4) . ?
S1 C4 1.747(4) . ?
S2 C18 1.744(4) . ?
S2 C21 1.747(4) . ?
S3 C15 1.741(4) . ?
S3 C12 1.747(4) . ?
S4 C32 1.748(4) . ?
S4 C29 1.753(4) . ?
C11 C25 1.734(5) . ?
C12 C8 1.741(4) . ?
C1 C34 1.389(7) . ?
C1 C2 1.412(6) . ?
C2 C3 1.356(7) . ?
C2 H2 0.9500 . ?
C3 C4 1.401(5) . ?
C3 H3 0.9500 . ?
C4 C5 1.399(6) . ?
C5 C12 1.410(5) . ?
C5 C6 1.498(5) . ?
C6 C7 1.387(6) . ?
C6 C11 1.400(6) . ?
C7 C8 1.387(6) . ?
C7 H7 0.9500 . ?
C8 C9 1.368(7) . ?
C9 C10 1.390(7) . ?
C9 H9 0.9500 . ?
C10 C11 1.369(7) . ?
C10 H10 0.9500 . ?
C11 H11 0.9500 . ?
C12 C13 1.401(7) . ?
C13 C14 1.363(6) . ?
C13 H13 0.9500 . ?
C14 C15 1.401(6) . ?
C14 H14 0.9500 . ?
C15 C16 1.401(5) . ?
```

C16 C17 1.380(6) . ?
C16 H16 0.9500 . ?
C17 C18 1.407(7) . ?
C17 H17 0.9500 . ?
C18 C19 1.406(6) . ?
C19 C20 1.355(7) . ?
C19 H19 0.9500 . ?
C20 C21 1.419(6) . ?
C20 H20 0.9500 . ?
C21 C22 1.397(7) . ?
C22 C29 1.405(6) . ?
C22 C23 1.510(5) . ?
C23 C24 1.371(6) . ?
C23 C28 1.395(6) . ?
C24 C25 1.421(6) . ?
C24 H24 0.9500 . ?
C25 C26 1.358(7) . ?
C26 C27 1.364(7) . ?
C26 H26 0.9500 . ?
C27 C28 1.383(6) . ?
C27 H27 0.9500 . ?
C28 H28 0.9500 . ?
C29 C30 1.405(7) . ?
C30 C31 1.368(6) . ?
C30 H30 0.9500 . ?
C31 C32 1.405(6) . ?
C31 H31 0.9500 . ?
C32 C33 1.396(6) . ?
C33 C34 1.388(6) . ?
C33 H33 0.9500 . ?
C34 H34 0.9500 . ?

loop_
_geom_angle_atom_site_label_1
_geom_angle_atom_site_label_2
_geom_angle_atom_site_label_3
_geom_angle
_geom_angle_site_symmetry_1
_geom_angle_site_symmetry_3
_geom_angle_publ_flag
C1 S1 C4 93.07(19) . . ?
C18 S2 C21 93.2(2) . . ?
C15 S3 C12 93.3(2) . . ?
C32 S4 C29 93.6(2) . . ?
C34 C1 C2 122.8(4) . . ?
C34 C1 S1 128.5(3) . . ?
C2 C1 S1 108.6(3) . . ?
C3 C2 C1 114.9(4) . . ?
C3 C2 H2 122.5 . . ?
C1 C2 H2 122.5 . . ?
C2 C3 C4 114.3(4) . . ?
C2 C3 H3 122.8 . . ?
C4 C3 H3 122.8 . . ?
C5 C4 C3 126.5(4) . . ?
C5 C4 S1 124.4(3) . . ?
C3 C4 S1 109.1(3) . . ?
C4 C5 C12 127.7(4) . . ?
C4 C5 C6 115.7(3) . . ?

C12 C5 C6 116.6(4) . . ?
C7 C6 C11 118.6(4) . . ?
C7 C6 C5 120.9(3) . . ?
C11 C6 C5 120.5(4) . . ?
C8 C7 C6 119.7(4) . . ?
C8 C7 H7 120.2 . . ?
C6 C7 H7 120.2 . . ?
C9 C8 C7 122.0(4) . . ?
C9 C8 C12 119.1(3) . . ?
C7 C8 C12 118.9(3) . . ?
C8 C9 C10 118.1(4) . . ?
C8 C9 H9 120.9 . . ?
C10 C9 H9 120.9 . . ?
C11 C10 C9 121.2(4) . . ?
C11 C10 H10 119.4 . . ?
C9 C10 H10 119.4 . . ?
C10 C11 C6 120.5(4) . . ?
C10 C11 H11 119.8 . . ?
C6 C11 H11 119.8 . . ?
C13 C12 C5 126.7(4) . . ?
C13 C12 S3 108.8(3) . . ?
C5 C12 S3 124.5(3) . . ?
C14 C13 C12 114.1(4) . . ?
C14 C13 H13 122.9 . . ?
C12 C13 H13 122.9 . . ?
C13 C14 C15 115.4(4) . . ?
C13 C14 H14 122.3 . . ?
C15 C14 H14 122.3 . . ?
C16 C15 C14 123.2(4) . . ?
C16 C15 S3 128.5(4) . . ?
C14 C15 S3 108.3(3) . . ?
C17 C16 C15 136.8(4) . . ?
C17 C16 H16 111.6 . . ?
C15 C16 H16 111.6 . . ?
C16 C17 C18 136.4(4) . . ?
C16 C17 H17 111.8 . . ?
C18 C17 H17 111.8 . . ?
C19 C18 C17 122.8(4) . . ?
C19 C18 S2 108.7(3) . . ?
C17 C18 S2 128.4(3) . . ?
C20 C19 C18 115.1(4) . . ?
C20 C19 H19 122.4 . . ?
C18 C19 H19 122.4 . . ?
C19 C20 C21 114.3(4) . . ?
C19 C20 H20 122.8 . . ?
C21 C20 H20 122.8 . . ?
C22 C21 C20 126.6(4) . . ?
C22 C21 S2 124.7(3) . . ?
C20 C21 S2 108.5(3) . . ?
C21 C22 C29 127.8(4) . . ?
C21 C22 C23 116.0(4) . . ?
C29 C22 C23 116.0(4) . . ?
C24 C23 C28 119.7(4) . . ?
C24 C23 C22 121.4(4) . . ?
C28 C23 C22 118.9(4) . . ?
C23 C24 C25 118.4(4) . . ?
C23 C24 H24 120.8 . . ?
C25 C24 H24 120.8 . . ?

C26 C25 C24 121.5(4) . . ?
C26 C25 C11 120.0(4) . . ?
C24 C25 C11 118.5(4) . . ?
C25 C26 C27 119.3(4) . . ?
C25 C26 H26 120.4 . . ?
C27 C26 H26 120.4 . . ?
C26 C27 C28 120.9(5) . . ?
C26 C27 H27 119.6 . . ?
C28 C27 H27 119.6 . . ?
C27 C28 C23 120.2(5) . . ?
C27 C28 H28 119.9 . . ?
C23 C28 H28 119.9 . . ?
C22 C29 C30 126.7(4) . . ?
C22 C29 S4 124.8(4) . . ?
C30 C29 S4 108.4(3) . . ?
C31 C30 C29 114.5(4) . . ?
C31 C30 H30 122.8 . . ?
C29 C30 H30 122.8 . . ?
C30 C31 C32 115.4(4) . . ?
C30 C31 H31 122.3 . . ?
C32 C31 H31 122.3 . . ?
C33 C32 C31 123.0(4) . . ?
C33 C32 S4 128.7(3) . . ?
C31 C32 S4 108.1(3) . . ?
C34 C33 C32 135.8(4) . . ?
C34 C33 H33 112.1 . . ?
C32 C33 H33 112.1 . . ?
C33 C34 C1 135.8(4) . . ?
C33 C34 H34 112.1 . . ?
C1 C34 H34 112.1 . . ?

loop_
_geom_torsion_atom_site_label_1
_geom_torsion_atom_site_label_2
_geom_torsion_atom_site_label_3
_geom_torsion_atom_site_label_4
_geom_torsion
_geom_torsion_site_symmetry_1
_geom_torsion_site_symmetry_2
_geom_torsion_site_symmetry_3
_geom_torsion_site_symmetry_4
_geom_torsion_publ_flag

C4 S1 C1 C34 -176.7(4) ?
C4 S1 C1 C2 -0.2(3) ?
C34 C1 C2 C3 176.9(4) ?
S1 C1 C2 C3 0.1(5) ?
C1 C2 C3 C4 0.0(6) ?
C2 C3 C4 C5 179.3(4) ?
C2 C3 C4 S1 -0.1(5) ?
C1 S1 C4 C5 -179.3(3) ?
C1 S1 C4 C3 0.1(3) ?
C3 C4 C5 C12 -173.0(4) ?
S1 C4 C5 C12 6.3(6) ?
C3 C4 C5 C6 7.0(6) ?
S1 C4 C5 C6 -173.8(3) ?
C4 C5 C6 C7 69.9(5) ?
C12 C5 C6 C7 -110.1(5) ?
C4 C5 C6 C11 -110.1(5) ?

C12 C5 C6 C11 69.9(5) ?
C11 C6 C7 C8 0.0(7) ?
C5 C6 C7 C8 180.0(4) ?
C6 C7 C8 C9 0.6(7) ?
C6 C7 C8 C12 -178.5(4) ?
C7 C8 C9 C10 -0.5(8) ?
C12 C8 C9 C10 178.6(4) ?
C8 C9 C10 C11 -0.1(9) ?
C9 C10 C11 C6 0.7(9) ?
C7 C6 C11 C10 -0.6(8) ?
C5 C6 C11 C10 179.4(5) ?
C4 C5 C12 C13 -178.1(4) ?
C6 C5 C12 C13 1.9(6) ?
C4 C5 C12 S3 2.7(6) ?
C6 C5 C12 S3 -177.2(3) ?
C15 S3 C12 C13 -1.3(3) ?
C15 S3 C12 C5 178.1(3) ?
C5 C12 C13 C14 -178.0(4) ?
S3 C12 C13 C14 1.3(5) ?
C12 C13 C14 C15 -0.7(6) ?
C13 C14 C15 C16 -179.5(4) ?
C13 C14 C15 S3 -0.3(5) ?
C12 S3 C15 C16 -179.9(4) ?
C12 S3 C15 C14 0.9(3) ?
C14 C15 C16 C17 179.3(5) ?
S3 C15 C16 C17 0.3(8) ?
C15 C16 C17 C18 -0.1(10) ?
C16 C17 C18 C19 -173.0(5) ?
C16 C17 C18 S2 3.0(8) ?
C21 S2 C18 C19 4.1(3) ?
C21 S2 C18 C17 -172.3(4) ?
C17 C18 C19 C20 173.2(4) ?
S2 C18 C19 C20 -3.4(5) ?
C18 C19 C20 C21 0.6(6) ?
C19 C20 C21 C22 -173.1(4) ?
C19 C20 C21 S2 2.5(5) ?
C18 S2 C21 C22 171.9(4) ?
C18 S2 C21 C20 -3.8(3) ?
C20 C21 C22 C29 175.4(4) ?
S2 C21 C22 C29 0.5(6) ?
C20 C21 C22 C23 0.5(6) ?
S2 C21 C22 C23 -174.4(3) ?
C21 C22 C23 C24 -78.5(6) ?
C29 C22 C23 C24 105.9(5) ?
C21 C22 C23 C28 100.8(5) ?
C29 C22 C23 C28 -74.7(6) ?
C28 C23 C24 C25 -1.2(7) ?
C22 C23 C24 C25 178.2(4) ?
C23 C24 C25 C26 -0.9(8) ?
C23 C24 C25 C11 -179.9(4) ?
C24 C25 C26 C27 1.8(8) ?
C11 C25 C26 C27 -179.2(4) ?
C25 C26 C27 C28 -0.6(8) ?
C26 C27 C28 C23 -1.4(8) ?
C24 C23 C28 C27 2.3(8) ?
C22 C23 C28 C27 -177.0(5) ?
C21 C22 C29 C30 -177.7(4) ?
C23 C22 C29 C30 -2.8(7) ?

C21 C22 C29 S4 0.7(6) ?
C23 C22 C29 S4 175.6(3) ?
C32 S4 C29 C22 -178.0(4) ?
C32 S4 C29 C30 0.7(4) ?
C22 C29 C30 C31 178.4(4) ?
S4 C29 C30 C31 -0.2(5) ?
C29 C30 C31 C32 -0.4(7) ?
C30 C31 C32 C33 177.0(4) ?
C30 C31 C32 S4 0.9(6) ?
C29 S4 C32 C33 -176.7(4) ?
C29 S4 C32 C31 -0.9(4) ?
C31 C32 C33 C34 -179.4(5) ?
S4 C32 C33 C34 -4.2(8) ?
C32 C33 C34 C1 -7.9(10) ?
C2 C1 C34 C33 -177.8(5) ?
S1 C1 C34 C33 -1.7(8) ?

_diffrn_measured_fraction_theta_max 0.993
_diffrn_reflns_theta_full 72.40
_diffrn_measured_fraction_theta_full 0.993
_refine_diff_density_max 0.397
_refine_diff_density_min -0.321
_refine_diff_density_rms 0.065